

Daniel Kupelwieser

**Pion Cloud Effects in the
Electromagnetic Nucleon Structure
A Point-Form Approach**

Dissertation

zur Erlangung des Doktorgrades der Naturwissenschaften
an der Karl-Franzens-Universität Graz

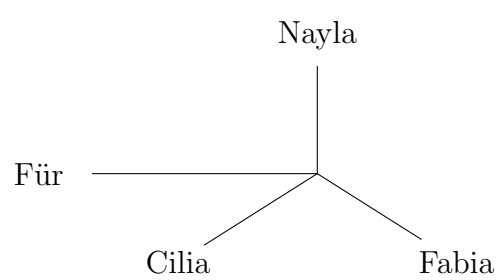
Eingereicht am Institut für Physik

Betreuer:
Ao. Univ.-Prof. Mag. Dr. Wolfgang Schweiger

Graz, im August 2016

Präambel

Ich, Daniel Kupelwieser, bestätige, dass es sich bei der hier vorgelegten Dissertation um eine Originalarbeit handelt, die von mir selbständig angefertigt und abgefasst wurde.



Abstract

The main objective of this thesis is to study the influence of the pion cloud on the electromagnetic structure of the nucleon. Our starting point is a hybrid constituent-quark model which contains, in addition to the valence quarks, also pions as elementary degrees of freedom. The quarks are subject to an instantaneous confining force and can emit and reabsorb the pions. The theoretical framework we use is relativistic quantum mechanics in its point-form realization. Electron–nucleon scattering is formulated as a multichannel problem for a Bakamjian–Thomas-type mass operator to account fully for the photon- and pion-exchange dynamics. We calculate the relativistically invariant one-photon-exchange amplitude for electron–nucleon scattering, from which the electromagnetic nucleon current and subsequently, the electromagnetic nucleon form factors are extracted. As it turns out, the basic ingredients to the one-photon-exchange amplitude are the electromagnetic γN and strong πN vertex form factors of the (confined) three-quark valence component of the nucleon (called the “bare nucleon”). The reason is that, due to instantaneous confinement, only eigenstates of the pure confinement problem, i.e bare baryons, can propagate in intermediate states. In order to calculate the strong and electromagnetic form factors of the bare nucleon we adopt the parametrization of the three-quark wave function proposed by Pasquini and Boffi who performed a similar calculation within the front form of relativistic dynamics. Our form factor results are comparable with those of Pasquini and Boffi and for momentum transfers $Q^2 \lesssim 5 \text{ GeV}^2$ in reasonable agreement with experiment. Pion loop effects turn out to be only significant below $Q^2 \lesssim 0.5 \text{ GeV}^2$. As a byproduct we also obtain a prediction for the strong πN coupling constant and the corresponding vertex form factor that is within the range of πN phenomenology.

Keywords: Electromagnetic nucleon form factors, pion cloud, pion–nucleon vertex, constituent-quark model, relativistic quantum mechanics, point-form dynamics.

Zusammenfassung

Das wesentliche Ziel dieser Dissertation ist das Studium des Einflusses der Pionwolke auf die elektromagnetische Struktur des Nukleons. Den Ausgangspunkt bildet ein hybrides Konstituentenquarkmodell, welches zusätzlich zu den Valenzquarks auch Pionen als elementare Freiheitsgrade aufweist. Die Quarks unterliegen einem instantanen Confinement und können Pionen emittieren und absorbieren. Als theoretisches Grundgerüst dient uns die relativistische Quantenmechanik in Punktform. Elektron–Nukleon-Streuung wird als Mehrkanalproblem mit einem Bakamjian–Thomas-Massenoperator formuliert. Wir berechnen die relativistisch invariante Amplitude für Ein-Photonen-Austausch, von welcher der elektromagnetische Strom sowie die elektromagnetischen Formfaktoren des Nukleons abgeleitet werden. Es ergibt sich, dass die Grundelemente der Amplitude für den Ein-Photonen-Austausch die elektromagnetischen γN - und starken πN -Formfaktoren der Drei-Quark Valenzkomponente des Nukleons (des „nackten“ Nukleons) sind. (Der Grund dafür ist, dass wegen des instantanen Confinements nur Eigenzustände des reinen Confinement-Problems, d.h. nackte Baryonen, in Zwischenzuständen propagieren können.) Um diese Größen zu berechnen, verwenden wir die Parametrisierung der Drei-Quark Wellenfunktion nach Pasquini und Boffi, welche eine ähnliche Berechnung in der Frontform der relativistischen Dynamik durchführten. Unsere Ergebnisse sind vergleichbar mit jenen von Pasquini und Boffi und stimmen für Impulsüberträge von $Q^2 \lesssim 5 \text{ GeV}^2$ angesessen mit experimentellen Werten überein. Die Auswirkungen des Pionenaustauschs erweisen sich nur unterhalb von $Q^2 \lesssim 0.5 \text{ GeV}^2$ als signifikant. Als Nebenprodukt erhalten wir auch eine Vorhersage für die starke πN -Kopplungskonstante und den zugehörigen Vertex-Formfaktor, welche sich im Rahmen der πN -Phänomenologie bewegt.

Contents

1	Introduction	4
1.1	Studying the electromagnetic structure of the nucleon	4
1.2	Structure of this document	6
2	Basic Concepts	8
2.1	Relativistic kinematics	8
2.2	Dirac and photon fields	8
2.3	The Poincaré group and $ISL(2,C)$	9
2.4	Relativistic quantum mechanics	10
2.4.1	The Poincaré algebra	10
2.4.2	Three forms of relativistic dynamics	11
2.4.3	Bakamjian–Thomas construction	13
2.4.4	Lorentz boosts and Wigner rotations	13
2.4.5	Velocity states	14
2.4.6	Coupled-channels approach and Feshbach reduction	16
2.5	Hadron properties and interactions	17
2.5.1	The constituent quark model of the nucleon	17
2.5.2	Electromagnetic current and form factors	18
2.5.3	The pion–quark/nucleon vertex	19
3	Electromagnetic Form Factors of the “Bare” Nucleon	21
3.1	Hadronic level	21
3.1.1	Basic setup	21
3.1.2	Eigenvalue equation and velocity states	22
3.1.3	Splitting of vertex operators	23
3.1.4	Insertion of completeness relations	23
3.1.5	Currents and spectator conditions	24
3.1.6	Analytic calculation of optical potential	25
3.2	Constituent level	27
3.2.1	Basic setup	27
3.2.2	Eigenvalue equation and Feshbach reduction	28
3.2.3	Vertex operators and completeness relations	28

3.2.4	Currents and spectator conditions	30
3.2.5	Wave functions	30
3.2.6	Analytic calculation of optical potential	31
3.3	Calculation of nucleon currents	34
3.3.1	Derivation	34
3.3.2	Three-quark wave function	34
3.3.3	Analytic Result	37
3.4	Extraction of form factors	38
3.5	Numerical implementation	41
3.5.1	Class structure	41
3.5.2	Kinematic quantities	42
3.5.3	Spin algebraics	44
3.5.4	Quark current	44
3.5.5	Integrand function	45
3.5.6	Integration	46
3.6	Results	48
4	Strong Form Factor	52
4.1	Hadronic level	52
4.1.1	Basic setup	52
4.1.2	Eigenvalue equation and Feshbach reduction	53
4.1.3	Insertion of completeness relations	53
4.1.4	The vertex operators	54
4.1.5	Analytic calculation of the optical potential	54
4.2	Constituent level	55
4.2.1	Basic setup	55
4.2.2	Eigenvalue equation and Feshbach reduction	55
4.2.3	Vertex operators and completeness relations	56
4.2.4	Currents and spectator condition	57
4.2.5	Wave functions	58
4.2.6	Analytic calculation of the optical potential	58
4.3	The microscopic expression for the pion–nucleon vertex	61
4.4	Extraction of the form factor	63
4.4.1	Kinematics	63
4.4.2	Pseudoscalar coupling	63
4.4.3	Pseudovector coupling	64
4.5	Numerical implementation	64
4.5.1	Kinematic quantities	64
4.5.2	Quark current and flavor function	65
4.5.3	Integrand function	66
4.6	Results	67

Contents	3
5 Overall Electromagnetic Form Factor	69
5.1 Basic setup	69
5.2 The nucleon–pion wave function	70
5.3 Eigenvalue equation and Feshbach reduction	73
5.4 Spectator conditions	75
5.5 Diagrams	76
5.5.1 Time-ordered diagrams	77
5.5.2 Covariant diagrams	84
5.6 Calculation of nucleon current	86
5.6.1 Kinematics	89
5.7 Numerical implementation	90
5.7.1 Form-factor input	90
5.7.2 Class structure in C++	93
5.7.3 Kinematic quantities	94
5.7.4 Currents and wave functions from form factors	96
5.7.5 Wigner rotations	98
5.7.6 Bare part	98
5.7.7 Integration	100
5.8 Results	102
5.8.1 Summary of results	102
5.8.2 Discussion of results	105
6 Summary and Outlook	107
A The nucleon with pion cloud	110
B Calculational details	114
B.1 Transformation of integration measures	114
B.2 Normalization of the three-quark wave function	115
B.3 Combination of time orderings	117
List of Figures	118
List of Tables	118
Acknowledgements	120
Bibliography	121

Chapter 1

Introduction

1.1 Studying the electromagnetic structure of the nucleon

Electron-nucleon scattering is the most important tool to learn about the electromagnetic structure of the nucleon [EW88]. In the present thesis we will concentrate on the nucleon properties that are probed in elastic electron–nucleon scattering. The quantities extracted from such scattering experiments are the nucleon form factors [Pun¹⁵]. They are scalar quantities that depend on the square of the four-momentum transferred from the electron to the nucleon. They encode the spatial structure of the photon–nucleon vertex and are thus also an important source of information on how the nucleon is composed of its charged constituents, the quarks.

Quantum chromodynamics (QCD) is nowadays considered to be the elementary quantum field theory of the strong interaction that tells us how quarks interact via gluon exchange and, in particular, how nucleons are built up from quarks (and also antiquarks and gluons). QCD is a gauge theory that is invariant under local $SU(3)_{\text{color}}$ transformations, i.e. both quarks and gluons carry a color charge and the Lagrangian of QCD is invariant under space-time dependent $SU(3)$ transformations in color space. In this sense, the color charge is the charge that is responsible for the strong interaction. One of the most prominent features of QCD is the observation that only colorless bound states of quarks, antiquarks and gluons are observed in nature in the form of hadrons (mesons and baryons). This is the phenomenon called “confinement”. As a consequence, colored objects (quarks, antiquarks and gluons) that form a colorless hadron can only be identified within a small spatial volume. What can happen, however, is that quark–antiquark fluctuations of the vacuum can form colorless mesons, which are then emitted and reabsorbed from the “core” of quarks, antiquarks and gluons. This “meson cloud” increases the spatial extension of the original hadron. The increase is maximal for the lightest meson, the pion. When the electromagnetic structure of the hadron is probed in electron–hadron

scattering, the photon exchanged between electron and hadron will “see” both, the core of the hadron and the surrounding meson cloud. Consequently, the electromagnetic hadron form factors extracted from elastic electron–hadron scattering data contain core- as well as meson-cloud contributions. A major goal of this thesis is to give an estimate for the size of the meson-cloud contribution to the electromagnetic nucleon form factors.

Since the solution of this problem within full QCD is still out of reach, we rather use an effective description of nucleons in terms of constituent quarks that are bound by an instantaneous confining potential and can also interact via the dynamical exchange of pions (which couple directly to the constituent quarks). This means that our meson cloud just consists of pions, which are supposed to provide the most important contribution to the cloud. This kind of model is in the spirit of so-called “chiral constituent quark models” [GR96], which assert that constituent quarks and (the lightest) pseudoscalar mesons are the effective particles and Goldstone bosons emerging from the spontaneous breakdown of chiral symmetry in QCD.

Within this constituent quark model, the nucleon consists of a three-quark core that is surrounded by a pion cloud. This is a problem with a finite number of degrees-of-freedom – as opposed to the full QCD bound-state problem – and can thus be treated within a quantum mechanical framework. Since we are exclusively dealing with light (constituent) quarks, it is mandatory to take relativity appropriately into account. We make use of the point-form of relativistic quantum mechanics (cf. Sec. 2.4.2, [Dir49, KP91, Kli98a]) in connection with the Bakamjian–Thomas construction (Sec. 2.4.3, [BT53, KP91]) to formulate electron–nucleon scattering in a Poincaré-invariant way. The same approach has already been adopted for the description of the electroweak properties of light mesons (π and ρ) [BSFK09, Bie11, GRS12] and for heavy–light mesons (D and B) [GRS12, GR13] as well as for determining the weak $B \rightarrow D^{(*)}$ decay form factors [GRS12].

In the present thesis we will extend this point-form approach for the calculation of electromagnetic form factors to the case of baryons that are, in particular, not only three-quark bound states, but contain also a three-quark–pion component. It should be mentioned that point-form calculations of electromagnetic form factors exist already [MBC⁺07, MCPW05, WB⁺01], but the authors did not account for extra pions and use an ansatz for the electromagnetic nucleon current on quark level (point-form spectator model) that differs slightly from the current which we extract from the invariant electron–nucleon scattering amplitude.

For the calculation of the pion-cloud contribution to the electromagnetic nucleon form factors we also need the structure of the pion–nucleon vertex, i.e. the pion–nucleon coupling and the pion–nucleon form factor. This will be obtained from considering the pion-loop contribution to the renormalization of the nucleon mass on the quark level. This means that our calculations will not only provide predictions for the electromagnetic structure of the nucleon, but at the same time also on its structure as seen by the pion via the strong interaction. Calculations of the strong pion–nucleon vertex form factor and coupling were also carried out within the point-form spectator model [MCP09], giving

again results that slightly differ from ours due to the same reason as in the electromagnetic case.

Pasquini and Boffi [PB07] already pursued a similar approach to meson-cloud effects, but they rather used the front-form of relativistic quantum mechanics and took a phenomenological ansatz for the pion–nucleon vertex. For comparison, we will take their three-quark wave function and use it to calculate both the strong and the electromagnetic form factors of the (bare) nucleon in a consistent way.

1.2 Structure of this document

Chapter 2 introduces the basic tools and concepts that are needed for this work. This includes relativistic kinematics, the Poincaré group, spin- $\frac{1}{2}$ and spin-1 fields, relativistic quantum mechanics and in particular its point-form realization, vertex operators, currents and the relativistic multichannel formulation that we are going to use.

In chapter 3 the electromagnetic form factors of a “bare” nucleon (which consists only of the 3-quark component) are determined. In Sec. 3.1 electron–nucleon scattering is first considered on the hadronic level to introduce the relativistic multichannel formalism, which we will use in the following. In this particular case only two channels are needed: One containing the electron and the nucleon and the other one containing the electron, the nucleon and the photon. Photon–electron and photon–nucleon vertex operators are responsible for the transition between these channels. After applying a Feshbach reduction to the mass-eigenvalue equation for this system to eliminate the channel containing the photon, one obtains an optical (energy-dependent) potential that describes the one-photon exchange between electron and nucleon. The one-photon-exchange amplitude – from which the electromagnetic nucleon current can then be separated – is obtained by taking matrix elements of this optical potential between states containing an electron and a nucleon. If one allows for spatially extended nucleons, the nucleon current will contain electromagnetic form factors. In order to find a microscopic expression for these form factors, the whole procedure is repeated in Sec. 3.2 on the quark level by considering electron scattering off a three-quark system that is confined by an instantaneous potential. The two channels now consist of three quarks and an electron and of three quarks, an electron and a photon, respectively. The photon channel is again eliminated to derive an optical potential. Matrix elements of this optical potential between states consisting of an electron and a three-quark bound state with nucleon quantum numbers finally yield the one-photon-exchange amplitude. Equating this amplitude with the one on hadronic level provides a microscopic expression for the electromagnetic nucleon current (Sec. 3.3), and in the sequel, also for the nucleon form factors (Sec. 3.4). The numerical implementation of the current- and form factor calculations is sketched in Sec. 3.5.

In chapter 4 an analogous procedure is applied to determine the strong πNN vertex form factor. The physical process that is analyzed in order obtain the pseudoscalar (or pseudovector) nucleon current is the mass eigenvalue problem for a nucleon that consists

of a three-quark valence component and a three-quark-plus-pion non-valence component. After eliminating the pionic channel, one ends up with an optical potential that describes the pion-loop contribution to the nucleon mass. Again equating this optical potential, as calculated on hadronic level, with the one obtained on constituent level, yields a microscopic expression for the pseudoscalar (or pseudovector) nucleon current and, in the sequel, also for the πNN vertex form factor. The interesting point to observe here is, that the optical potential on microscopic level can be reexpressed in terms of hadronic degrees-of-freedom with the quark substructure entering only through vertex form factors of “bare” baryons, i.e. eigenstates of the pure confinement problem.

This observation is used in chapter 5 to calculate the electromagnetic form factors of a physical nucleon N , consisting of a “bare” nucleon N_0 and an $N_0\pi$ component. In Sec. 5.1, the setup of the $Ne(\gamma)$ state as a two-channel compound of a bare $N_0e(\gamma)$ state and an $N_0\pi e(\gamma)$ state is laid out. The nucleon-pion wave function is first introduced here (Sec. 5.2). For this compound state, a coupled-channels eigenvalue equation for electron–nucleon scattering, analogous to the one in Sec. 3.1, is then formulated in Sec. 5.3. Again after a Feshbach reduction, a first expression for the optical potential for each in- and outgoing configuration (N_0 and $N_0\pi$) is obtained. In Sec. 5.4, spectator conditions are applied and the field theoretical vertex operators inserted. In Sec. 5.5, the expressions for the optical potential for the various possible time-ordered diagrams are obtained. These then add up to give a nice covariant expression for the overall optical one-photon-exchange potential. Finally, in Sec. 5.6, this result is compared to the expression for the optical potential we obtained on hadronic level in Sec. 3.1 to identify the nucleon current. After insertion of the nucleon-pion wave function, using the same kinematics as in Sec. 3.4, we then extract the overall form factor analogously. After having determined the microscopic form of the (bare) electromagnetic nucleon form factors in chapter 3 and of the strong $\pi N_0 N_0$ form factor in chapter 4, determination of the electromagnetic form factor of the physical nucleon is a purely hadronic problem. The numerical implementation of this program is sketched in Sec. 5.7; numerical form factor results are presented and discussed in Sec. 5.8.

Chapter 6 contains a short summary and an outlook.

In appendix A, the renormalization of the nucleon mass due to the pion loop is derived in some detail. The essential quantities to come out of this are the pion emission probability, the bare nucleon mass and the pion-nucleon wave function. Appendix B is devoted to further calculational details.

Chapter 2

Basic Concepts

We start out by introducing some basic concepts and tools that will be needed for this document. These can roughly be grouped into the fields of special relativity, quantum field theory, relativistic quantum mechanics as well as properties of hadrons and their interactions.

2.1 Relativistic kinematics

The metric signature we use is $(+ - - -)$, i.e. the (flat) metric is

$$\eta = \text{diag}(1, -1, -1, -1) \quad (2.1)$$

and the rest mass of a particle with relativistic energy ω and three-momentum \vec{p} is

$$m = \sqrt{\omega^2 - \vec{p}^2}. \quad (2.2)$$

Its four-momentum p is then

$$p = \begin{pmatrix} \omega \\ \vec{p} \end{pmatrix}. \quad (2.3)$$

We are using physical units, i.e.

$$c = \hbar = 1. \quad (2.4)$$

Whenever we are using three-velocities (denoted by \vec{v}), they are defined as the three-components of the corresponding four-velocities v , which in turn are defined as the four-momentum divided by the rest mass, i.e.

$$v := \frac{p}{m} = \begin{pmatrix} v^0 \\ \vec{v} \end{pmatrix} \quad \text{and} \quad v^0 = \sqrt{1 + \vec{v}^2}. \quad (2.5)$$

2.2 Dirac and photon fields

In quantum field theory fermions, i.e. spin- $\frac{1}{2}$ particles like the quark or the nucleon, are usually represented by the Dirac field ψ , which is a 4-spinor field fulfilling the Dirac

equation:

$$(i\gamma^\mu \partial_\mu - m)\psi = 0. \quad (2.6)$$

We use the Dirac representation of the Dirac algebra with the Dirac matrices γ^μ taking on the form [IZ80]

$$\gamma^0 = \begin{pmatrix} \mathbb{I}_2 & 0 \\ 0 & -\mathbb{I}_2 \end{pmatrix}, \quad \gamma^i = \begin{pmatrix} 0 & \sigma^i \\ -\sigma^i & 0 \end{pmatrix}. \quad (2.7)$$

The Fourier decomposition of the Dirac field reads [IZ80]

$$\psi(x) = \int \frac{d^3 p}{(2\pi)^3} \frac{1}{2\omega} \sum_{\alpha=\pm\frac{1}{2}} (c_\alpha(p) u_\alpha(p) e^{-ipx} + d_\alpha^*(p) v_\alpha(p) e^{ipx}). \quad (2.8)$$

The index α runs over the two independent spin orientations of the Dirac particle. After field quantization, the coefficients c_α and d_α^* become particle annihilation and creation operators, and u_α and v_α are the corresponding basis spinors which, in the representation (2.7), can be written as [IZ80]

$$u_{\frac{1}{2}}(\vec{p}) = \frac{p_\lambda \gamma^\lambda + m}{\sqrt{(m + \omega)}} \begin{pmatrix} 1 \\ 0 \\ 0 \\ 0 \end{pmatrix}, \quad u_{-\frac{1}{2}}(\vec{p}) = \frac{p_\lambda \gamma^\lambda + m}{\sqrt{(m + \omega)}} \begin{pmatrix} 0 \\ 1 \\ 0 \\ 0 \end{pmatrix}, \quad (2.9)$$

where the normalization is taken from [Bie11].

Similarly, the Fourier decomposition of the photon field reads [IZ80]

$$A^\nu(x) = \int \frac{d^3 p}{2\omega(2\pi)^3} \sum_{\mu\gamma=0}^3 (a_{\mu\gamma}(p) \epsilon_{\mu\gamma}^\nu(p) e^{-ipx} + a_{\mu\gamma}^\dagger(p) \epsilon_{\mu\gamma}^{*\nu}(p) e^{ipx}), \quad (2.10)$$

where the $\epsilon_{\mu\gamma}$ are four orthonormal polarization 4-vectors of the photon which, for fixed momentum, form a complete basis of Minkowski space:

$$\begin{aligned} g_{\nu\lambda} \epsilon_{\mu\gamma}^\nu(p) \epsilon_{\mu\gamma}^{*\lambda}(p) &= g_{\mu\gamma\mu\gamma} \\ \sum_{\mu\gamma=0}^3 g^{\mu\gamma\mu\gamma} \epsilon_{\mu\gamma}^\nu(p) \epsilon_{\mu\gamma}^{*\lambda}(p) &= g^{\nu\lambda} \end{aligned} \quad (2.11)$$

2.3 The Poincaré group and $ISL(2, \mathbb{C})$

The universal covering group of the restricted (i.e. proper orthochronous) Lorentz group \mathcal{L}_+^\uparrow is isomorphic to the Lie group $SL(2, \mathbb{C})$ [Tha92, SU00, KP91]. This can be seen by establishing an isomorphism between the space of hermitian 2×2 matrices and Minkowski space: If σ^μ is the four-vector of Pauli matrices with $\sigma^0 := \mathbb{I}_{2 \times 2}$, a general hermitian 2×2 matrix can be written as

$$X := S(x) = x^\mu \sigma_\mu. \quad (2.12)$$

The corresponding vector in Minkowski space is recovered via

$$x^\mu = \frac{1}{2} \operatorname{tr}(\sigma^\mu X) . \quad (2.13)$$

The restricted Poincaré group (i.e. the component of the identity) is the group of all restricted Lorentz transformations plus displacements in space-time, i.e. the group of all ordered pairs (Λ, a) with $\Lambda \in \mathcal{L}_+^\uparrow$ and a a vector in Minkowski space. In the space of hermitian 2×2 matrices, the effect of a Poincaré transformation (Λ, a) is

$$X' = S(\Lambda) X S(\Lambda)^\dagger + S(a) , \quad (2.14)$$

where $S(\Lambda) \in SL(2, \mathbb{C})$ (i.e. $\det S(\Lambda) = 1$) and $S(a)$ is a hermitian 2×2 matrix.

Poincaré transformations in Minkowski space are recovered via

$$\Lambda_\nu^\mu = \frac{1}{2} \operatorname{tr}(\sigma_\mu S(\Lambda) \sigma_\nu S(\Lambda)^\dagger) , \quad a^\mu = \frac{1}{2} \operatorname{tr}(\sigma_\mu S(a)) . \quad (2.15)$$

Note that $S(\Lambda)$ and $-S(\Lambda)$ give the same Λ , rendering $SL(2, \mathbb{C})$ a double covering of the restricted Lorentz group.

2.4 Relativistic quantum mechanics

2.4.1 The Poincaré algebra

Having discussed $ISL(2, \mathbb{C})$ as the universal covering group of the restricted Poincaré group, we can now turn to the representation of its algebra, the Poincaré algebra. The most general $SL(2, \mathbb{C})$ matrix can be written as [KP91]

$$S(\Lambda) = \exp \left(-\frac{i}{2} (\vec{\theta} + i \vec{\rho}) \vec{\sigma} \right) , \quad (2.16)$$

where the components of $\vec{\sigma}$ are the three Pauli matrices and $\vec{\theta}$, $\vec{\rho}$ are two sets of three parameters each, which parameterize a Lorentz transformation. Via a simple Taylor expansion, subsequent use of the multiplication relations of the Pauli matrices and finally, the representation properties from Sec. 2.3, it is easily shown that $\vec{\theta}$ encodes the angle and axis orientation of a rotation and $\vec{\rho}$ the rapidity, $|\vec{\rho}| = \operatorname{Arsinh} |\vec{v}|$, and the direction of a rotationless boost as defined in Eq. (2.35). According to Eq. (2.12), the displacement vector can be written as

$$S(a) = a^\mu \sigma_\mu . \quad (2.17)$$

With any nine of the ten parameters $\vec{\rho}$, $\vec{\theta}$ and a^μ set to zero, the subgroup generated by the remaining parameter constitutes an Abelian subgroup of $ISL(2, \mathbb{C})$. The representation of a (proper) Poincaré transformation can thus be written as

$$S(\Lambda, a) = \exp(-i P^\mu a_\mu) \exp(-i(\vec{J} \cdot \vec{\theta} + \vec{K} \cdot \vec{\rho})) , \quad (2.18)$$

where P^μ are now the four generators of space-time translations, \vec{J} the three generators of spatial rotations, and \vec{K} the three generators of rotationless Lorentz boosts.

In order for the group representation property (not explicitly mentioned here) of $S(\Lambda, a)$ to hold, the following canonical commutation relations (written in covariant form) have to be fulfilled [Dir49]:

$$\begin{aligned} [P^\mu, P^\nu] &= 0, \\ [K^{\mu\nu}, P^\lambda] &= i(g^{\nu\lambda}P^\mu - g^{\mu\lambda}P^\nu), \\ [K^{\mu\nu}, K^{\lambda\kappa}] &= -i(g^{\mu\lambda}K^{\nu\kappa} - g^{\nu\lambda}K^{\mu\kappa} + g^{\nu\kappa}K^{\mu\lambda} - g^{\mu\kappa}K^{\nu\lambda}), \end{aligned} \quad (2.19)$$

where we have used

$$K^{0i} := K^i, \quad K^{ij} := \epsilon^{ijk}J_k, \quad K^{\mu\nu} = -K^{\nu\mu}. \quad (2.20)$$

2.4.2 Three forms of relativistic dynamics

In physical terms, the generator(s) \vec{J} can be identified with the total angular momentum of the system which the Poincaré transformation is performed on. It is thus called the angular momentum operator. Likewise, P^μ corresponds to the total four-momentum and will be called the four-momentum operator. Its zero component $P^0 \equiv H$ is usually referred to as the Hamiltonian of the system. Total four-momentum and angular momentum are the conserved Noether charges of the respective space-time transformations [PS95]. For a local quantum-field theory they can be constructed from the energy-momentum tensor of the system under consideration, which includes contributions from the individual particles (the “free” part), as well as all interactions between the particles. For a set of Klein-Gordon fields ϕ_i , for example, we have

$$\Theta^{\mu\nu} = \frac{\partial \mathcal{L}}{\partial(\partial_\mu \phi_i)} \partial^\nu \phi_i - g^{\mu\nu} \mathcal{L}, \quad (2.21)$$

with $\mathcal{L} = \mathcal{L}_{\text{free}} + \mathcal{L}_{\text{int}}$. Demanding that interactions depend only on the fields but not on their derivatives, we have

$$\Theta_{\text{int}}^{\mu\nu} = -g^{\mu\nu} \mathcal{L}_{\text{int}}. \quad (2.22)$$

The four-momentum operator, for example, is then constructed via

$$P^\mu = \int_\sigma d\sigma_\nu \Theta^{\nu\mu}(x), \quad (2.23)$$

where σ is an oriented, spacelike hypersurface of Minkowski space-time which has to be specified. In classical relativistic dynamics the initial conditions of a given problem are defined on this surface. In quantizing the theory it serves as quantization surface.

Since the commutation relations (2.19) have to be fulfilled to guarantee Poincaré invariance, inclusion of interactions in any one of the 10 Poincaré generators has to result in other generators containing interactions accordingly. This happens automatically when quantizing a local (interacting) field theory, but becomes a non-trivial problem if one wants to stay within the framework of quantum mechanics and deal with only a finite number of degrees-of-freedom. In his 1949 article [Dir49] Dirac identified three special

forms of relativistic dynamics, which correspond to timelike foliations of space-time where the resulting hypersurfaces possess a high degree of symmetry under Poincaré transformations. For a particular form of dynamics, those Poincaré transformations that leave the corresponding hypersurfaces invariant are interaction-free. They are called “kinematic”, while transformations that shift or deform the hypersurfaces do contain interactions; they are called “dynamic”.

The instant form: In this most familiar picture, Minkowski space-time is foliated into hyperplanes of equal coordinate time (an “*instant*”),

$$x^0 = \text{const.} \quad (2.24)$$

These surfaces are related to each other via translations in the x^0 direction and are deformed by boosts. Spatial translations and rotations leave these surfaces invariant. Accordingly, the generators $P^0 \equiv H$ (the nonrelativistic Hamiltonian) and K_{0i} are dynamic while P^i and K_{ij} are kinematic.

The front form: A hyperplane tangent to the light cone is called a light *front*. In the corresponding form of dynamics, Minkowski space-time is foliated into light fronts parallel to each other. Their orientation is usually taken such that

$$x^0 + x^3 =: x^+ = \text{const.} \quad (2.25)$$

Let a new coordinate system be given by

$$\{A^0, A^1, A^2, A^3\} \mapsto \{A^+, A^1, A^2, A^-\} \quad (2.26)$$

$$\text{with } A^+ := A^0 + A^3, \quad A^- := A^0 - A^3 \quad (2.27)$$

for any 4-vector A^μ . There are only three dynamic generators in this approach: Translations generated by P^- that shift the light front in the x^+ direction, and the generators of the “front-form boosts”, K_{1+} and K_{2+} . The kinematic generators are those of translations within the light front, P^1 , P^2 and P^+ , of rotations around the propagation direction, K_{12} , and of the Lorentz transformations K_{+-} , K_{1-} and K_{2-} .

The point form: The initial surface in this approach is the space-time hyperboloid of equal proper time,

$$x^2 = (x^0)^2 - \vec{x}^2 = \tau^2 = \text{const.} \quad (2.28)$$

The four-momentum operator (2.23) is then

$$P^\mu = 2 \int_{\mathbb{R}^4} d^4x \delta(x^2 - \tau^2) \theta(x^0) x_\nu \Theta^{\nu\mu}(x), \quad (2.29)$$

and its interaction part, according to (2.22),

$$P_{\text{int}}^\mu = -2 \int_{\mathbb{R}^4} d^4x \delta(x^2 - \tau^2) \theta(x^0) x^\mu \mathcal{L}_{\text{int}}(x). \quad (2.30)$$

All translations shift the hyperboloid (2.28), while boosts and rotations (i.e. all transformations leaving the *point* $x = 0$ invariant) leave the hyperboloid (with $\tau = 0$) invariant. Thus, interactions only affect the 4 generators P^μ , i.e. the 4-momentum operator, but the full Lorentz group (6 independent generators $K_{\mu\nu}$) stays interaction-free. The greatest benefit of this approach is that boosts can be performed without having to worry about interactions, a feature that will be exploited heavily throughout this work.

2.4.3 Bakamjian–Thomas construction

The Bakamjian–Thomas construction [BT53] is a systematic procedure for adding interactions to a system of (a finite number of) free particles such that Poincaré invariance is preserved. In point form it leads to the factorization of the four-momentum operator,

$$P^\mu = M V_{\text{free}}^\mu \quad (2.31)$$

into a free 4-velocity operator,

$$V_{\text{free}}^\mu = M_{\text{free}}^{-1} P_{\text{free}}^\mu \quad (2.32)$$

and a mass operator

$$M = M_{\text{free}} + U \quad (2.33)$$

which contains all the interactions. The interaction-potential operator U has to be a Lorentz scalar that fulfills the commutation relations $[V_{\text{free}}^\mu, U] = 0$. These conditions satisfied, M commutes (like M_{free}) with all the Poincaré generators and represents the invariant mass of the system in the sense that

$$P^\mu P_\mu = M^2. \quad (2.34)$$

2.4.4 Lorentz boosts and Wigner rotations

A Lorentz boost (more precisely, a canonical boost) is a rotationless Lorentz transformation. We always use active boosts that act on particle velocities rather than frames of reference. In our notation (2.5) their action on a 4-vector is described by the matrix

$$B(\vec{v}) = \begin{pmatrix} v^0 & \vec{v}^\top \\ \vec{v} & \mathbb{I}_3 + \frac{v^0 - 1}{v^2} \vec{v} \vec{v}^\top \end{pmatrix}. \quad (2.35)$$

The inverse boost is defined by

$$B^{-1}(\vec{v}) = B(-\vec{v}). \quad (2.36)$$

The result of a boost with velocity \vec{v} , a general Lorentz transformation Λ and finally an inverse boost with the velocity $\vec{\Lambda}v$ is a pure rotation, called a “Wigner rotation” (or Thomas precession in the relativity literature [SU00]):

$$R_W(\Lambda, \vec{v}) := B^{-1}(\vec{\Lambda}v) \Lambda B(\vec{v}). \quad (2.37)$$

It is important to note that

$$R_W^{-1}(\Lambda, \vec{v}) = B^{-1}(\vec{v}) \Lambda^{-1} B(\vec{\Lambda v}) = R_W(\Lambda^{-1}, \vec{\Lambda v}). \quad (2.38)$$

We have already discussed the $SL(2, \mathbb{C})$ representation of the Lorentz algebra in Sec. 2.4.1. Via Eq. (2.16) and the following remarks, using the rapidity $\rho = \text{Arsinh} |\vec{v}|$, a canonical (rotationless) boost with velocity \vec{v} can be represented as

$$S(B(\vec{v})) = \cosh(\frac{\rho}{2}) \sigma_0 + \sinh(\frac{\rho}{2}) n^k \sigma_k \quad \text{with} \quad \vec{v} = \sinh \rho \vec{n}. \quad (2.39)$$

In our notation (2.5) this can equally be written as [Bie11]

$$S(B(\vec{v})) = \sqrt{\frac{v^0 + 1}{2}} \sigma^0 + \frac{\vec{\sigma} \cdot \vec{v}}{\sqrt{2(v^0 + 1)}}. \quad (2.40)$$

The spin- j representation of a rotation is accomplished by Wigner-D-functions. We need, in particular, the spin- $\frac{1}{2}$ representation of Wigner rotations,

$$D_{\mu'\mu}^{\frac{1}{2}}(R_W(\Lambda, \vec{v})) =: D_{\mu'\mu}(\Lambda, \vec{v}), \quad (2.41)$$

where $\mu, \mu' = \pm \frac{1}{2}$ are the spin polarization indices.

Since the Wigner-D-functions are the elements of a unitary representation of the rotation group, the following relations hold [Bie11]:

$$\begin{aligned} D_{\mu\mu'}^{\frac{1}{2}*}(R_W(\Lambda, \vec{v})) &= D_{\mu'\mu}^{\frac{1}{2}\dagger}(R_W(\Lambda, \vec{v})) = D_{\mu'\mu}^{\frac{1}{2}}(R_W^{-1}(\Lambda, \vec{v})), \\ \sum_{\mu''} D_{\mu\mu''}^{\frac{1}{2}}(R_W(\Lambda, \vec{v})) D_{\mu''\mu'}^{\frac{1}{2}}(R_W(\Lambda', \vec{v}')) &= D_{\mu\mu'}^{\frac{1}{2}}(R_W(\Lambda, \vec{v}) R_W(\Lambda', \vec{v}')), \\ D_{\mu\mu'}^{\frac{1}{2}}(\mathbb{I}) &= \delta_{\mu\mu'}, \end{aligned} \quad (2.42)$$

i.e. in our shorthand notation (2.41), via Eq. (2.38),

$$D_{\mu\mu'}^*(\Lambda, \vec{v}) = D_{\mu'\mu}^\dagger(\Lambda, \vec{v}) = D_{\mu'\mu}(\Lambda^{-1}, \vec{\Lambda v}). \quad (2.43)$$

2.4.5 Velocity states

The Bakamjian–Thomas construction in point form (2.31) is most easily carried out in a velocity-state representation. Since all interactions are contained in the mass operator and the free overall 4-velocity operator V_{free}^μ is factored out, it is most profitable to characterize the state of an n -particle system by its overall velocity \vec{V} , the constituents' momenta k_i^μ and their spin projections μ_i in the overall rest frame [Kli98b].

By means of Eq. (2.32), the eigenvalue of the free 4-velocity operator of an n -particle system is obtained from the particle masses m_i and the particle momenta p_i via

$$\vec{V} = \frac{\vec{P}_{\text{free}}}{M_{\text{free}}} = \frac{\sum \vec{p}_i}{\sqrt{(\sum p_i^0)^2 - (\sum \vec{p}_i)^2}} \quad \text{where} \quad p_i^0 = \sqrt{\vec{p}_i^2 + m_i^2}. \quad (2.44)$$

A velocity state is just a usual momentum state in the overall rest system that is boosted to the overall velocity \vec{V} by means of a rotationless boost (cf. Eq. (2.35)):

$$|\vec{V}, \vec{k}_1 \mu_1 \dots \vec{k}_n \mu_n\rangle := U_{B(\vec{V})} |\vec{k}_1 \mu_1 \dots \vec{k}_n \mu_n\rangle \quad (2.45)$$

with

$$\sum_i \vec{k}_i = 0 \quad \text{and thus} \quad M_{\text{free}} = \sum \omega_i \quad \text{where} \quad \omega_i := k_i^0 = \sqrt{\vec{k}_i^2 + m_i^2}. \quad (2.46)$$

The μ_i is the spin orientation of the i -th particle with respect to the canonical spin [KP91]. The physical momenta of the particles are

$$p_i = B(\vec{V}) k_i. \quad (2.47)$$

The behavior of a velocity state under a Lorentz transformation Λ is described as follows [Kli98b]:

$$U_\Lambda |\vec{V}, \{\vec{k}_i, \mu_i\}\rangle = \sum_{\{\mu'_i\}} |\vec{\Lambda V}, \{R_W(\Lambda, \vec{V}) \vec{k}_i, \mu'_i\}\rangle \prod_i D_{\mu'_i \mu_i}^{j_i}(R_W(\Lambda, \vec{V})), \quad (2.48)$$

(where $\vec{v}_i := \frac{\vec{k}_i}{m_i}$), i.e. spins and momenta for each particle i always transform with the *same* Wigner rotation (cf. Sec. 2.4.4) $R_W(\Lambda, \vec{V})$, so that orbital and spin angular momentum can be coupled as in the nonrelativistic case.

Orthogonality and completeness relations: The orthogonality relation for an n -particle velocity state reads [Kra01]

$$\begin{aligned} & \langle \vec{V}'; \{\vec{k}'_i, \mu'_i, \tau'_i\} | \vec{V}; \{\vec{k}_i, \mu_i, \tau_i\} \rangle \\ &= (2\pi)^3 V^0 \delta^3(\vec{V} - \vec{V}') \frac{2\omega_n}{\left(\sum_{j=1}^n \omega_j\right)^3} \prod_{j=1}^{n-1} \left((2\pi)^3 2\omega_j \delta^3(\vec{k}_j - \vec{k}'_j) \right) \prod_{j=1}^n \left(\delta_{\mu_j \mu'_j} \delta_{\tau_j \tau'_j} \right), \end{aligned} \quad (2.49)$$

where we have introduced (for later purposes) the isospin projection τ_i of the i -th particle. Note that, since the n -th particle's momentum is already determined by Eq. (2.46), there is no Dirac delta in $\vec{k}_n^{(\prime)}$! We take the momentum of particle n to be the *redundant* one. The Kronecker delta over $\mu_n^{(\prime)}, \tau_n^{(\prime)}$, however, remains. We introduce a shorthand notation by which Eq. (2.49) reads

$$\langle \vec{V}'; \{\vec{k}'_i, \mu'_i, \tau'_i\} | \vec{V}; \{\vec{k}_i, \mu_i, \tau_i\} \rangle = \Delta_{VV'} \frac{2\omega_n}{\left(\sum_{j=1}^n \omega_j\right)^3} \prod_{j=1}^{n-1} \Delta_{jj'}, \quad (2.50)$$

with $\Delta_{jj'}$ containing also $\delta_{\mu_j \mu'_j} \delta_{\tau_j \tau'_j}$ and the factor $\delta_{\mu_n \mu'_n} \delta_{\tau_n \tau'_n}$ being absorbed in $\Delta_{VV'}$.

Accordingly, the completeness relation, which defines the unity operator in the velocity-state representation, reads:

$$\mathbb{I}_n = \sum_{\{\mu_i, \tau_i\}} \int \frac{d^3 V}{(2\pi)^3 V^0} \prod_{j=1}^{n-1} \left(\frac{d^3 k_j}{(2\pi)^3 2\omega_j} \right) \frac{\left(\sum_{j=1}^n \omega_j \right)^3}{2\omega_n} |\vec{V}; \{\vec{k}_i, \mu_i, \tau_i\}\rangle \langle \vec{V}; \{\vec{k}_i, \mu_i, \tau_i\}|. \quad (2.51)$$

Note that since the n -th particle's momentum (the redundant one) is already determined by Eq. (2.46), there is no integration over \vec{k}_n (however the sums over μ_n, τ_n remain)! We again introduce a shorthand notation which reads

$$\mathbb{I}_n = \sum_{\vec{V}} \prod_{j=1}^{n-1} (Dk_j) \frac{\left(\sum_{j=1}^n \omega_j\right)^3}{2\omega_n} \left| \vec{V}; \{\vec{k}_i, \mu_i, \tau_i\} \right\rangle \left\langle \vec{V}; \{\vec{k}_i, \mu_i, \tau_i\} \right| \quad (2.52)$$

with the sum running over μ_i, τ_i , $i = 1, \dots, n$. For each occurring photon, a $\delta_{\mu_\gamma \mu'_\gamma}$ in Eq. (2.49) has to be replaced by the metric $(-g_{\mu_\gamma \mu'_\gamma})$ and the sum over photon polarizations in (2.51) by $\sum_{\mu_\gamma} (-g_{\mu_\gamma \mu_\gamma})$ [Kli03].

2.4.6 Coupled-channels approach and Feshbach reduction

One way to represent a multi-particle system with varying particle types and numbers is via a coupled-channels approach [KP91]. The Hilbert space corresponding to a multi-channel system is a (finite) direct sum of Hilbert spaces, each describing a particular channel that is characterized by certain types and numbers of particles. The mass operator of the whole system (the operator we are interested in) is then a matrix operator. On the main diagonal we find the mass operators that act solely on the channel Hilbert spaces, i.e., they keep the particle numbers fixed. Off-diagonal we find creation and annihilation operators, which are responsible for transitions between the different channels. The mass-eigenvalue equation for a system with particles A, B, C, \dots or combinations thereof, with channel mass operators M_{\dots} and overall eigenvalue \sqrt{s} would thus read, for example,

$$\begin{pmatrix} M_A & K_B & K_C & K_{BC} & \dots \\ K_B^\dagger & M_{AB} & 0 & K_C & \dots \\ K_C^\dagger & 0 & M_{AC} & K_B & \dots \\ K_{BC}^\dagger & K_C^\dagger & K_B^\dagger & M_{ABC} & \dots \\ \vdots & \vdots & \vdots & \vdots & \ddots \end{pmatrix} \begin{pmatrix} |A\rangle \\ |AB\rangle \\ |AC\rangle \\ |ABC\rangle \\ \vdots \end{pmatrix} = \sqrt{s} \begin{pmatrix} |A\rangle \\ |AB\rangle \\ |AC\rangle \\ |ABC\rangle \\ \vdots \end{pmatrix}. \quad (2.53)$$

The channel mass operators M_{\dots} may contain, in addition to the relativistic energies of the particles, also an instantaneous interaction term (like a confinement potential). Let us now adopt the velocity-state representation and assume that particles in a particular channel move freely. If they have masses m_i , momenta k_i with $\sum \vec{k}_i = 0$ and relativistic energies $\omega_i = \sqrt{\vec{k}_i^2 + m_i^2}$, where $i = A, B, \dots$, the eigenvalue of the channel mass operator $M_{AB\dots}$ is

$$m_{AB\dots} = \omega_A + \omega_B + \dots \quad (2.54)$$

The eigenvalue \sqrt{s} in Eq. (2.53), i.e. the square root of Mandelstam s , is the invariant mass of the complete, fully interacting multi-particle system, in which transitions between different channels may take place (we avoid using the symbol m here). The corresponding eigenstate is a superposition of states belonging to the different channels. Via straightforward manipulations, the system of equations (2.53) can be reduced to a single equation in one channel, which is the starting point for drawing diagrams. This is called a Feshbach reduction [Fes58, Fes62].

2.5 Hadron properties and interactions

2.5.1 The constituent quark model of the nucleon

In elementary particle physics one wants to describe the properties of hadrons, such as protons, neutrons and mesons, in terms of their elementary constituents, the quarks and gluons. Within a quantum field theory approach, quarks are the quanta of fields, which, in addition to the usual properties like mass, electric charge and spin (helicity), carry a so-called color charge. Forces between quarks are mediated by gluons, which are quanta of another field. Both quarks and gluons are dynamic degrees of freedom, i.e. quarks and gluons can be generated or destroyed following a certain set of rules. The quantum field theory that describes all this is called “quantum chromodynamics” (QCD). Experimentally, a single isolated quark can never be observed as a free state, a phenomenon called confinement. The rigorous proof of how this follows from the theory is still missing as of today, however.

A more phenomenological approach to hadron properties is provided by constituent-quark models. In the conventional constituent-quark models a hadron is considered a fixed multi-particle state, namely three quarks in the case of a baryon and a quark and an antiquark for a meson. The constituent quarks carry an effective mass which differs from the quark mass in QCD and acts as a free parameter of the model. The electric charge is $\frac{2}{3}$ (times the elementary charge $|e|$) for up (u), charm (c) and top (t) quarks, and $-\frac{1}{3}$ for down (d), strange (s) and bottom (b) quarks (like in QCD). Quarks are spin- $\frac{1}{2}$ particles. The quark content of the nucleon, which is the particle we will investigate, is uud for the proton and udd for the neutron.

Since we only work with nucleons and thus the light quarks u and d , we assume that these have the same mass. They are then assigned a further quantum number which is called isospin. It behaves just as regular spin does, but it is invariant under space-time transformations. Proton and neutron as well as up- and down-quark are considered an isospin-doublet, the positive isospin orientation being assigned to proton and up-quark, the negative to neutron and down-quark. If the masses of u and d quarks are neglected in the QCD Lagrangian, it exhibits an additional symmetry, the so-called “chiral symmetry”. This symmetry, however, is broken spontaneously in the quantized theory by the quark condensate. As a consequence, massless pions emerge as the Goldstone bosons of chiral symmetry breaking and quarks acquire an effective mass, thus becoming constituent quarks. However, since the constituent u and d quarks have slightly different masses and the pion is not massless albeit rather light, we say that chiral symmetry is only an approximate symmetry and call the pions the pseudo-Goldstone bosons of chiral symmetry breaking [GR96].

In order to be able to correctly describe the nucleon structure, a fully relativistic treatment is mandatory even at low momentum transfers and will also be employed here. The confinement of the quarks within the hadron is assumed to be caused by an instantaneous interaction, which gives rise to a purely discrete spectrum. Rather than solving the

bound-state problem for a particular confinement potential, we will use an appropriate ansatz for the three-quark wave function of the nucleon. Therein, both spin and isospin have to be taken into account when constructing a fully symmetric (fully antisymmetric when color is included) wave function.

For a model closer to the reality of a dynamic quark number, as described by field theory, one then introduces, in addition to the three-quark valence Fock component of the nucleon, a three-quark-plus-pion component and allows the pions to couple directly to the quarks. In this way one gets, in addition to the confinement potential, a hyperfine interaction. Such a model is in the spirit of the so-called “chiral constituent-quark model”, in which the lightest pseudoscalar mesons and constituent quarks emerge as effective degrees of freedom after spontaneous chiral symmetry breaking, with the pseudoscalar mesons representing the corresponding Goldstone bosons [GR96]. The resulting physical picture of a baryon is that of a quark core which is surrounded by a “cloud” of pseudoscalar mesons, which affects its mass eigenvalue as well as its electromagnetic structure. The only mesons that we will consider are the three pions (spin zero, electric charge and isospin +1, 0 and -1, quark content $u\bar{d}$ for the π^+ , $\bar{u}d$ for the π^- and a combination of $u\bar{u}$ and $d\bar{d}$ for the π^0).

2.5.2 Electromagnetic current and form factors

For the electromagnetic interaction of the photon with the nucleon, quark, or pion we use the standard field-theoretical vertices from quantum electrodynamics. The interaction part of the QED Lagrangian reads [IZ80]

$$\mathcal{L}_{\text{int}} = - \sum_i Q_i |e| \bar{\psi}_i \gamma^\mu \psi_i A_\mu =: -|e| \sum_i J_i^\mu A_\mu , \quad (2.55)$$

where A^μ is the electromagnetic 4-potential which arises from the photon field and J_i^μ is the electromagnetic current of (spin- $\frac{1}{2}$) particle i with electromagnetic charge Q_i (in units of $|e|$) and (matter) field ψ_i . Via (2.8) matrix elements of the current for a spin- $\frac{1}{2}$ particle i with ingoing and outgoing spin polarizations μ_i, μ'_i and momenta k_i, k'_i can be written as

$$J_{\mu_i, \mu'_i}^\mu(\vec{k}_i, \vec{k}'_i) = Q_i \bar{u}_{\mu'_i}(\vec{k}'_i) \gamma^\mu u_{\mu_i}(\vec{k}_i) . \quad (2.56)$$

In order to take into account the spatial extension of a particle (let's say the nucleon) as well as extra loops (higher-order terms) at the vertex, the electromagnetic current is expanded in terms of pertinent covariants as follows [GSS02, EW88, KM96, CDKM98]:

$$J_N^\mu = \bar{u}_{\mu'}(\vec{k}'_N) \left(F_1(q^2) \gamma^\mu - F_2(q^2) \frac{q_\nu}{4m_N} [\gamma^\mu, \gamma^\nu] \right) u_\mu(\vec{k}_N), \quad F_1(0) = 1 , \quad (2.57)$$

where $u_\mu(\vec{k}_N)$ and $u_{\mu'}(\vec{k}'_N)$ are the spinors (2.9) of ingoing and outgoing nucleon (with momentum $\vec{k}_N^{(\prime)}$ and (canonical) spin projection $\mu^{(\prime)}$), respectively, q^μ is the 4-momentum transfer and $F_1(q^2)$ and $F_2(q^2)$ are the *Dirac* and *Pauli form factors*.

Frequently, the electric and the magnetic *Sachs form factors* G_E and G_M are used equivalently. They are more intuitive in the sense that for $q^2 = 0$, they assume the values of the elementary charge and the magnetic moment μ_N ($= 2.79$ for the proton, -1.91 for the neutron), respectively:

$$\begin{aligned} G_E &= F_1 + \frac{q^2}{4m_N^2} F_2, \quad G_E(0) = Q_N \\ G_M &= F_1 + F_2, \quad G_M(0) = \mu_N . \end{aligned} \quad (2.58)$$

2.5.3 The pion–quark/nucleon vertex

The interaction between pion and nucleon can be described by *pseudoscalar* or *pseudovector* coupling with the interaction Lagrangians [EW88]

$$\mathcal{L}_{\text{int}}^{\text{ps}} = -i g_N \bar{\psi}_N \gamma^5 \vec{\tau} \psi_N \vec{\phi}_\pi \quad (2.59)$$

and

$$\mathcal{L}_{\text{int}}^{\text{pv}} = -\frac{f_N}{m_\pi} \bar{\psi}_N \gamma^\nu \gamma^5 \vec{\tau} \psi_N \partial_\nu \vec{\phi}_\pi , \quad (2.60)$$

respectively, where $\vec{\tau}$ is a vector consisting of the three Pauli matrices. Both $\vec{\tau}$ and $\vec{\phi}_\pi$ are vectors in isospin space. The strong π - N coupling constant has a value of $g_N \approx 13.4$ [EW88] or $g_N \approx 13.1$ [Bug04], depending on the literature one uses. Pseudoscalar and pseudovector coupling are equivalent for free nucleons.

Analogously, the (pointlike) interaction between pion and quark reads [EW88]

$$\mathcal{L}_{\text{int}}^{\text{ps}} = -i g \bar{\psi}_q \gamma^5 \vec{\tau} \psi_q \vec{\phi}_\pi \quad (2.61)$$

and

$$\mathcal{L}_{\text{int}}^{\text{pv}} = -\frac{f}{m_\pi} \bar{\psi}_q \gamma^\nu \gamma^5 \vec{\tau} \psi_q \partial_\nu \vec{\phi}_\pi , \quad (2.62)$$

respectively, where the pseudoscalar coupling constant has its value in the range [Wag98]

$$\frac{g^2}{4\pi} = 0.67 \dots 1.19 \quad (g = 2.90 \dots 3.87) . \quad (2.63)$$

For free quarks (nucleons), pseudoscalar and pseudovector coupling constants are related via [EW88]

$$\frac{f_{(N)}}{m_\pi} = \frac{g_{(N)}}{2m_{N/q}} . \quad (2.64)$$

Taking matrix elements of (2.59) and (2.60) between a nucleon-pion and a nucleon state, we end up with pseudoscalar and pseudovector currents

$$\begin{aligned} & -i g_N G_{\text{ps}}(Q^2 = -q^2) \bar{u}_{\mu'_N}(\vec{k}'_N) \gamma^5 u_{\mu_N}(\vec{k}_N) \chi_{\tau'_N}^\dagger \left(\vec{\tau} \cdot \vec{\phi}_\pi^* \right) \chi_{\tau_N} \\ & \equiv -i g_N J_N^5(\vec{k}_N, \mu_N, \vec{k}'_N, \mu'_N) \mathcal{F}(\tau_N, \tau'_N, \tau'_\pi) \end{aligned} \quad (2.65)$$

and

$$\begin{aligned} & i \frac{f_N}{m_\pi} G_{\text{pv}}(Q^2 = -q^2) \bar{u}_{\mu'_N}(\vec{k}'_N) \gamma^\nu \gamma^5 u_{\mu_N}(\vec{k}_N) k_{\pi\nu} \chi_{\tau'_N}^\dagger \left(\vec{\tau} \cdot \vec{\phi}_\pi^* \right) \chi_{\tau_N} \\ & \equiv i \frac{f_N}{m_\pi} J_N^{5\nu}(\vec{k}_N, \mu_N, \vec{k}'_N, \mu'_N) k_{\pi\nu} \mathcal{F}(\tau_N, \tau'_N, \tau'_\pi) , \end{aligned} \quad (2.66)$$

respectively. Here we have introduced vertex form factors $G_{\text{ps}}(Q^2)$ and $G_{\text{pv}}(Q^2)$ to account for the substructure of the nucleon (and potentially the pion). The quantities τ_N , τ'_N and τ_π denote the isospin orientations of the nucleons and the pion, respectively. The ingredients of the flavor function \mathcal{F} are defined as follows:

- The nucleon/quark isospinors are

$$|p\rangle = |u\rangle = \chi_{\tau=\frac{1}{2}} = \begin{pmatrix} 1 \\ 0 \end{pmatrix}, \quad |n\rangle = |d\rangle = \chi_{\tau=-\frac{1}{2}} = \begin{pmatrix} 0 \\ 1 \end{pmatrix}. \quad (2.67)$$

- The isospin wave functions of the pion are

$$\vec{\phi}_{\pi^+} = \frac{1}{\sqrt{2}} \begin{pmatrix} 1 \\ i \\ 0 \end{pmatrix}, \quad \vec{\phi}_{\pi^-} = \frac{1}{\sqrt{2}} \begin{pmatrix} 1 \\ -i \\ 0 \end{pmatrix}, \quad \vec{\phi}_{\pi^0} = \begin{pmatrix} 0 \\ 0 \\ 1 \end{pmatrix}, \quad (2.68)$$

where the isospin orientations are +1 for the π^+ , -1 for the π^- and 0 for the π^0 .

- Finally, $\vec{\tau}$ is a 3-vector of Pauli matrices.

The nonzero components of \mathcal{F} are

$$\begin{aligned} \mathcal{F}\left(\frac{1}{2}, \frac{1}{2}, 0\right) &= \begin{pmatrix} 1 & 0 \end{pmatrix} \sigma_3 \begin{pmatrix} 1 \\ 0 \end{pmatrix} = 1, \\ \mathcal{F}\left(-\frac{1}{2}, -\frac{1}{2}, 0\right) &= \begin{pmatrix} 0 & 1 \end{pmatrix} \sigma_3 \begin{pmatrix} 0 \\ 1 \end{pmatrix} = -1, \\ \mathcal{F}\left(\frac{1}{2}, -\frac{1}{2}, 1\right) &= \begin{pmatrix} 0 & 1 \end{pmatrix} \frac{1}{\sqrt{2}} (\sigma_1 - i \sigma_2) \begin{pmatrix} 1 \\ 0 \end{pmatrix} = \sqrt{2}, \\ \mathcal{F}\left(-\frac{1}{2}, \frac{1}{2}, -1\right) &= \begin{pmatrix} 1 & 0 \end{pmatrix} \frac{1}{\sqrt{2}} (\sigma_1 + i \sigma_2) \begin{pmatrix} 0 \\ 1 \end{pmatrix} = \sqrt{2}. \end{aligned} \quad (2.69)$$

Chapter 3

Electromagnetic Form Factors of the “Bare” Nucleon

In this chapter, we determine the electromagnetic properties of the nucleon without explicitly taking into account the (non-valence) three-quark-plus-pion component of the nucleon. However, its influence is implicitly accounted for by the choice of the model parameters, like the constituent-quark mass or the parameters of the three-quark bound-state wave function. With a slight adaption of these parameters and the replacement of the physical nucleon mass by a bare nucleon mass these results will later serve as input for the electromagnetic form factors of the bare nucleon.

The relevant quantities (i.e. optical one-photon exchange potential and nucleon current) are first derived in the hadronic picture, where the nucleon’s sub-structure is parametrized by means of phenomenological form factors, and then again in the quark picture, where the nucleon consists of three confined, pointlike quarks. By comparing these two results, one then obtains a microscopic (i.e., quark picture) expression for the nucleon current, from which one extracts the analytic expressions for the “bare” form factors.

3.1 Hadronic level

3.1.1 Basic setup

In order to demonstrate how our approach works and for later comparison, we first calculate the one-photon-exchange amplitude for elastic electron–nucleon scattering on the hadronic level. The electromagnetic interaction is mediated by the dynamic exchange of one single photon.

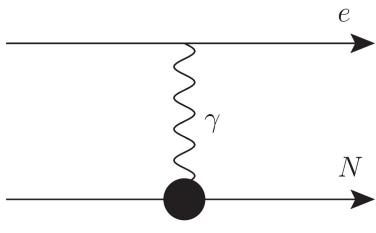


Figure 3.1: Diagram representing the one-photon-exchange amplitude $\mathcal{M}_{1\gamma}$ for electron–nucleon scattering. The blob at the photon–nucleon vertex indicates the possible occurrence of vertex form factors, which account for the (spatial) extension of the nucleon.

3.1.2 Eigenvalue equation and velocity states

We use a coupled-channels approach (cf. Sec. 2.4.6) with two channels: One contains the nucleon (N) and the electron (e) only and the other contains the exchanged photon (γ) in addition.

We work with velocity states (cf. Sec. 2.4.5) $|V; \vec{k}_N, \mu_N, \tau_N; \vec{k}_e, \mu_e\rangle$ and $|V; \vec{k}_N, \mu_N, \tau_N; \vec{k}_e, \mu_e; \vec{k}_\gamma, \mu_\gamma\rangle$ (where $\sum_i \vec{k}_i = 0$) and use the shorthand notation $|VNe\rangle$ and $|VN\gamma\rangle$, respectively. Since we employ the Bakamjian–Thomas construction (cf. Sec. 2.4.3), the overall 4-velocity V , which one obtains from the physical particles' momenta ($p_i = \Lambda_V k_i$) is conserved, i.e.

$$\vec{V} = \frac{\vec{p}_N + \vec{p}_e}{\sqrt{(p_N + p_e)^2}} = \frac{\vec{p}_N + \vec{p}_e + \vec{p}_\gamma}{\sqrt{(p_N + p_e + p_\gamma)^2}}. \quad (3.1)$$

The eigenvalue equation for the invariant mass operator then reads

$$\begin{pmatrix} M_{Ne} & K_\gamma \\ K_\gamma^\dagger & M_{Ne\gamma} \end{pmatrix} \begin{pmatrix} |VNe\rangle \\ |VN\gamma\rangle \end{pmatrix} = \sqrt{s} \begin{pmatrix} |VNe\rangle \\ |VN\gamma\rangle \end{pmatrix}, \quad (3.2)$$

where the diagonal matrix elements M_{Ne} and $M_{Ne\gamma}$ are the mass operators for non-interacting nucleon–electron and nucleon–electron–photon systems, respectively, with eigenvalues $m_{Ne} = \omega_N + \omega_e$ and $m_{Ne\gamma} = \omega_N + \omega_e + \omega_\gamma$ (see Eq. (2.46), $\omega_i = \sqrt{\vec{k}_i^2 + m_i^2}$). The off-diagonal elements K_γ and K_γ^\dagger , linking the two channels, are the annihilation resp. creation operators of the photon. \sqrt{s} (s being the Mandelstam variable) is the mass eigenvalue of the fully interacting two-channel system.

Via a **Feshbach reduction**, Eq. (3.2) can be reduced to the $N - e$ channel:

$$(\sqrt{s} - M_{Ne})|VNe\rangle =: P_{Ne}^{-1}|VNe\rangle = K_\gamma P_{Ne\gamma} K_\gamma^\dagger|VNe\rangle =: V_{\text{opt}}|VNe\rangle. \quad (3.3)$$

P_{Ne} is the *propagator* for the nucleon–electron state and $P_{Ne\gamma} := (\sqrt{s} - M_{Ne\gamma})^{-1}$ the propagator for the nucleon–electron–photon state. V_{opt} is called the optical potential. When the right hand side of Eq. (3.3) is read from right to left we see that, starting from the $|VNe\rangle$ state, a photon is created by K_γ^\dagger , then a $|VN\gamma\rangle$ state propagates and finally, the photon is destroyed again by K_γ . The optical potential thus describes the creation of the photon by either electron or nucleon, the propagation of the nucleon–electron–photon state, and the subsequent absorption of the photon by electron or nucleon.

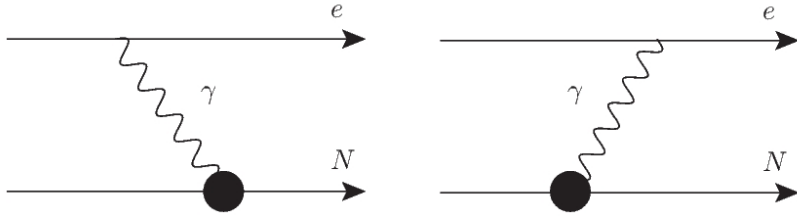


Figure 3.2: Time-ordered diagrams (contributing to $\mathcal{M}_{1\gamma}$) representing exchange of a photon between electron and nucleon on the hadronic level. The blob indicates that the nucleon-photon vertex is not point-like.

In this work, we restrict ourselves to the *perturbative* treatment of electron–nucleon scattering in leading order, i.e. one-photon exchange. This means that

$$\sqrt{s} \rightarrow m_{Ne} = \omega_N + \omega_e \quad (3.4)$$

and self-energy contributions due to photon emission and reabsorption (leading to loops) can be neglected.

3.1.3 Splitting of vertex operators

Due to the structure of the interaction Lagrangian (2.55), the photon creation and annihilation operators can each be split into a sum of photon–electron and photon–nucleon vertex operators [Bie11]:

$$\begin{aligned} K_\gamma^\dagger |VN e\rangle &= (K_{e\gamma}^\dagger + K_{N\gamma}^\dagger) |VN e\rangle, \\ K_\gamma |VN e \gamma\rangle &= (K_{e\gamma} + K_{N\gamma}) |VN e \gamma\rangle. \end{aligned} \quad (3.5)$$

Ignoring any photon loops (which only amount to radiative corrections to nucleon and electron masses), Eq. (3.3) takes the form

$$P_{Ne}^{-1} |VN e\rangle = \left(\underbrace{K_{e\gamma} P_{Ne\gamma} K_{N\gamma}^\dagger}_{V_{o1}} + \underbrace{K_{N\gamma} P_{Ne\gamma} K_{e\gamma}^\dagger}_{V_{o2}} \right) |VN e\rangle = V_{\text{opt}} |VN e\rangle. \quad (3.6)$$

This can be interpreted as a photon being emitted by the nucleon and then absorbed by the electron (left summand) or vice versa (right summand), represented by the two diagrams in Fig. 3.2. In what follows, we will only treat the first summand in some detail. The corresponding part of the optical potential we shall call V_{o1} .

3.1.4 Insertion of completeness relations

In order to calculate the invariant one-photon-exchange amplitude, we calculate matrix elements of the optical potential between nucleon–electron velocity states (cf. Sec. 2.4.5), $\langle V' N' e' | V_{\text{opt}} | V N e \rangle$. In order to end up with matrix elements of the vertex operators

$K_{\text{...}}^{(\dagger)}$ and the eigenvalue of the propagator $(m - M_{Ne\gamma})^{-1}$, we insert the appropriate unity operators (cf. Sec. 2.4.5) expressed in terms of velocity states (see Eqs. (2.51) and (2.52)):

$$\langle V' N' e' | V_{01} | V N e \rangle = \langle V' N' e' | K_{e\gamma} (m - M_{Ne\gamma})^{-1} \mathbb{I}_{Ne\gamma} K_{N\gamma}^\dagger | V N e \rangle. \quad (3.7)$$

Since the propagator is now acting on an eigenstate, it can be replaced by its eigenvalue $(\sqrt{s} - m_{Ne\gamma})^{-1}$. Note that, via Eq. (2.46), the eigenvalue of the free mass operator of the nucleon-electron-photon subsystem in the overall rest frame (velocity state) is just the sum over the relativistic energies of the particles:

$$m_{Ne\gamma} = \omega_N + \omega_e + \omega_\gamma. \quad (3.8)$$

The velocity-state unity element $\mathbb{I}_{Ne\gamma}$ is obtained from Eq. (2.51) resp. Eq. (2.52). In what follows, we will choose the momentum of the photon, \vec{k}_γ , as the redundant one:

$$\begin{aligned} \mathbb{I}_{Ne\gamma} &= \int \frac{d^3 V}{(2\pi)^3 V^0} \int \frac{d^3 k_N}{(2\pi)^3 2\omega_N} \int \frac{d^3 k_e}{(2\pi)^3 2\omega_e} \frac{(\omega_N + \omega_e + \omega_\gamma)^3}{2\omega_\gamma} \sum_{\mu_N, \mu_e, \mu_\gamma, \tau_N} (-g^{\mu_\gamma \mu_\gamma}) \\ &\quad \times \left| V; \vec{k}_N, \mu_N, \tau_N; \vec{k}_e, \mu_e; \vec{k}_\gamma, \mu_\gamma \right\rangle \left\langle V; \vec{k}_N, \mu_N, \tau_N; \vec{k}_e, \mu_e; \vec{k}_\gamma, \mu_\gamma \right| \quad (3.9) \\ &=: \sum_{\mu_\gamma} \sum_{\mu_N, \mu_e} DV Dk_N Dk_e \frac{(\omega_N + \omega_e + \omega_\gamma)^3}{2\omega_\gamma} (-g^{\mu_\gamma \mu_\gamma}) |V N e \gamma\rangle \langle V N e \gamma|. \end{aligned}$$

3.1.5 Currents and spectator conditions

Inserting Eq. (3.9) into the expression for the first summand of the optical potential, Eq. (3.7), we obtain velocity state matrix elements of the vertex operators. A further simplification arises when we demand that certain *spectator conditions* be met: They state that only those particles that hit each other at the vertex change their momentum, while the others remain unaffected. Furthermore, due to the Bakamjian–Thomas construction 2.4.3, the overall four-velocity V is conserved. The matrix elements of the vertex operators read [Bie11]:

$$\begin{aligned} \langle V' N' e' \gamma' | K_{N\gamma}^\dagger | V N e \rangle &= \langle V N e | K_{N\gamma} | V' N' e' \gamma' \rangle^* \\ &= \underbrace{(2\pi)^3 V^0 \delta^3(\vec{V} - \vec{V}')}_{\Delta_{VV'}} \underbrace{(2\pi)^3 \delta_{\mu_e \mu'_e} 2\omega_e \delta^3(\vec{k}_e - \vec{k}'_e)}_{\Delta_{ee'}} \frac{-1}{\sqrt{m_{Ne\gamma}^3 m_{Ne}^3}} \langle N' \gamma' | | K_{N\gamma}^\dagger | | N \rangle \\ &=: \Delta_{VV'} \Delta_{ee'} \frac{-1}{\sqrt{m_{Ne\gamma}^3 m_{Ne}^3}} \langle N' \gamma' | | K_{N\gamma}^\dagger | | N \rangle \quad (3.10) \end{aligned}$$

and

$$\begin{aligned} \langle V' N' e' \gamma' | K_{e\gamma}^\dagger | V N e \rangle &= \langle V N e | K_{e\gamma} | V' N' e' \gamma' \rangle^* \\ &= \Delta_{VV'} \Delta_{NN'} \frac{-1}{\sqrt{m_{Ne\gamma}^3 m_{Ne}^3}} \langle e' \gamma' | | K_{e\gamma}^\dagger | | e \rangle. \quad (3.11) \end{aligned}$$

For the reduced vertex matrix elements $\langle \dots | |K^{(\dagger)}| \dots \rangle$ we use the standard field-theoretical expressions, given by the interaction Lagrangian (2.55). This gives rise to the electromagnetic vector currents of the nucleon (J_N^μ) and the electron (J_e^μ) [Bie11]:

$$\begin{aligned} \langle N' \gamma' | |K_{N\gamma}^\dagger| |N \rangle &= |e| J_{N\nu}(\vec{k}_N, \mu_N, \tau_N; \vec{k}'_N, \mu'_N, \tau_N) \delta_{\tau_N \tau'_N} \epsilon_{\mu'_\gamma}^{\nu*}(\vec{k}'_\gamma) , \\ \langle e' \gamma' | |K_{e\gamma}^\dagger| |e \rangle &= |e| J_{e\nu}(\vec{k}_e, \mu_e; \vec{k}'_e, \mu'_e) \epsilon_{\mu'_\gamma}^{\nu*}(\vec{k}'_\gamma) = |e| Q_e \bar{u}_{\mu'_e}(\vec{k}'_e) \gamma_\nu u_{\mu_e}(\vec{k}_e) \epsilon_{\mu'_\gamma}^{\nu*}(\vec{k}'_\gamma) , \end{aligned} \quad (3.12)$$

where $\epsilon_{\mu_\gamma}^\nu(\vec{k}_\gamma)$ is the polarization 4-vector of the photon from Eq. (2.10). Note that for the electromagnetic interaction the isospin of the nucleon doesn't change, i.e. $\tau'_N = \tau_N$. Note also that the electron is a point particle, whence we have already inserted Eq. (2.56) to express its current. The nucleon current, on the other hand, is left as it is, since we are interested in the nucleon's spatial charge distribution.

At least for the electron, we can now easily observe that

$$J_{e\nu}(\vec{k}_e, \mu_e; \vec{k}'_e, \mu'_e) = J_{e\nu}(\vec{k}'_e, \mu'_e; \vec{k}_e, \mu_e)^* \quad (3.13)$$

(use $(\gamma^\mu)^\dagger = \gamma^0 \gamma^\mu \gamma^0$). Since by Eq. (2.10) the photon polarization vector in Eq. (3.12) has to be replaced by its complex conjugate if a photon is absorbed rather than emitted, this also implies

$$\langle e' \gamma' | |K_{e\gamma}^\dagger| |e \rangle = \langle e | |K_{e\gamma}| |e' \gamma' \rangle^*. \quad (3.14)$$

as already stated in Eq. (3.11).

For better readability, we introduce the following shorthand notations:

$$\begin{aligned} J^\nu(N, N') &:= J_N^\nu(\vec{k}_N, \mu_N, \tau_N; \vec{k}'_N, \mu'_N, \tau_N) , \\ J^\nu(e, e') &:= J_e^\nu(\vec{k}_e, \mu_e; \vec{k}'_e, \mu'_e) , \\ \epsilon^\nu(\gamma) &:= \epsilon_{\mu_\gamma}^\nu(\vec{k}_\gamma) . \end{aligned} \quad (3.15)$$

3.1.6 Analytic calculation of optical potential

With these tools at hand we can continue our analytic calculation of the first term of the optical potential, Eq. (3.7). We start by inserting the expression for the unity operator (3.9) in the $Ne\gamma$ -space, which allows us to replace the propagator by its eigenvalue:

$$\begin{aligned} &\langle V' N' e' | V_{01} | V N e \rangle \\ &= \langle V' N' e' | K_{e\gamma} P_{Ne\gamma} \mathbb{I}_{Ne\gamma} K_{N\gamma}^\dagger | V N e \rangle \\ &= \sum_{\mu''_\gamma} \sum_{\nu} \int DV'' Dk''_N Dk''_e \frac{m''_N m''_e}{2 \omega''_\gamma} \left(-g^{\mu''_\gamma \mu''_\gamma} \right) \langle V'' N'' e'' \gamma'' | K_{e\gamma}^\dagger | V' N' e' \rangle^* \\ &\quad \times (\sqrt{s} - m''_{Ne\gamma})^{-1} \langle V'' N'' e'' \gamma'' | K_{N\gamma}^\dagger | V N e \rangle . \end{aligned} \quad (3.16)$$

We continue by inserting the spectator conditions for the nucleon-photon and the electron-photon vertex, Eqs. (3.10) and (3.11):

$$\begin{aligned}
& \langle V' N' e' | V_{01} | V N e \rangle \\
&= \sum_{\mu''_\gamma} \sum_{\mu''_N} D V'' D k''_N D k''_e \frac{m''_N m''_{N e \gamma}}{2 \omega''_\gamma} \left(-g^{\mu''_\gamma \mu''_\gamma} \right) \\
&\quad \times \frac{\Delta_{V' V''} \Delta_{N' N''}}{\sqrt{m''_N m''_{N e \gamma}}} \langle e'' \gamma'' | | K_{e \gamma}^\dagger | | e' \rangle^* (\sqrt{s} - m''_{N e \gamma})^{-1} \frac{\Delta_{V V''} \Delta_{e e''}}{\sqrt{m''_N m''_{N e \gamma}}} \langle N'' \gamma'' | | K_{N \gamma}^\dagger | | N \rangle . \tag{3.17}
\end{aligned}$$

After elimination of the Delta functions and insertion of the nucleon and electron currents (3.12), keeping in mind (3.13), we get

$$\begin{aligned}
\langle V' N' e' | V_{01} | V N e \rangle &= |e|^2 \frac{\Delta_{V V'}}{2 \omega''_\gamma m''_{N e}} \sum_{\mu''_\gamma} \left(-g^{\mu''_\gamma \mu''_\gamma} \right) \\
&\quad \times J_\nu(e, e') \epsilon_{\mu''_\gamma}^\nu(\vec{k}'_\gamma) \frac{1}{\sqrt{s} - \omega'_N - \omega_e - \omega''_\gamma} J_\lambda(N, N') \epsilon_{\mu''_\gamma}^{\lambda*}(\vec{k}'_\gamma) \Big|_{\vec{k}'_\gamma = \vec{k}'_e - \vec{k}_e} . \tag{3.18}
\end{aligned}$$

We now make use of the completeness relation (2.11) for photon polarization vectors to obtain

$$\langle V' N' e' | V_{01} | V N e \rangle = - |e|^2 \frac{\Delta_{V V'}}{2 \omega''_\gamma} \frac{g_{\nu \lambda}}{m''_{N e}} \frac{J^\nu(N, N') J^\lambda(e, e')}{\sqrt{s} - \omega'_N - \omega_e - \omega''_\gamma} \Big|_{\vec{k}'_\gamma = \vec{k}'_e - \vec{k}_e} . \tag{3.19}$$

Remaining diagram: In the completely analogous way, we obtain for the reverse time ordering:

$$\langle V' N' e' | V_{02} | V N e \rangle = - |e|^2 \frac{\Delta_{V V'}}{2 \omega''_\gamma} \frac{g_{\nu \lambda}}{m''_{N e}} \frac{J^\nu(N, N') J^\lambda(e, e')}{\sqrt{s} - \omega_N - \omega'_e - \omega''_\gamma} \Big|_{\vec{k}'_\gamma = \vec{k}_e - \vec{k}'_e} . \tag{3.20}$$

Combination of the two time orderings: Finally, we combine the two time orderings as in Eq. (3.6) to obtain the matrix elements of $V_{\text{opt}} = V_{01} + V_{02}$. Since we are using

- elastic scattering (energy-momentum conservation) with
- a single exchange of a massless, i.e. light-like, photon in
- a perturbative treatment,

the following relations hold [Bie11]:

$$\begin{aligned}
\sqrt{s} &\longrightarrow m_{N e} = \omega_e + \omega_N = \omega'_e + \omega'_N \\
&\quad \text{and} \\
\omega''_\gamma^2 &= \vec{k}'_\gamma^2 = Q^2 := (\vec{k}_e - \vec{k}'_e)^2 = (\vec{k}_N - \vec{k}'_N)^2 . \tag{3.21}
\end{aligned}$$

For the invariant one-photon-exchange amplitude $\mathcal{M}_{1\gamma}$, we finally end up with (cf. App. B.3)

$$\boxed{\mathcal{M}_{1\gamma} := \langle V' N' e' | V_{\text{opt}} | V N e \rangle = |e|^2 \frac{\Delta_{VV'}}{m_{Ne}^3} J^\nu(N, N') \frac{g_{\nu\lambda}}{Q^2} J^\lambda(e, e')}, \quad (3.22)$$

where $Q^2 = -q^2$ is the inverse of the four-momentum transfer squared, $q^2 = (k_e - k'_e)^2$, i.e. with the metric (2.1), a positive quantity. We see that we have now indeed obtained a covariant expression as has already been suggested in Fig. 3.1.

3.2 Constituent level

Having obtained a macroscopic expression (i.e., an expression on the hadronic level) for the invariant one-photon-exchange electron–nucleon scattering amplitude, we now want to derive a microscopic (i.e. quark level) expression. By equating the two we will then obtain a microscopic description of the nucleon current J_N^ν . We proceed in a completely analogous way to Sec. 3.1.

3.2.1 Basic setup

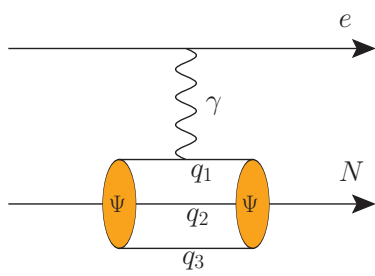


Figure 3.3: (One of three) quark-level diagram(s) (contributing to $\mathcal{M}_{1\gamma}$) for the calculation of the electromagnetic form factors of the “bare” nucleon. The electron exchanges a photon with one of the three quarks. The relation between the nucleon state (propagators) and the three-quark state is described by the wave function Ψ .

Instead of considering the nucleon as a quasi-elementary particle, we now model it as a bound state of three light constituent quarks (cf. Sec. 2.5.1) with masses of approx. 0.26 GeV each, independent of flavor (u or d). These are confined by an instantaneous potential, which enters the mass operator in Eq. (3.23). We will not specify the confinement potential, since it is mainly the three-quark bound-state wave function that enters the microscopic expression of the electromagnetic nucleon current. We will therefore rather choose an appropriate parametrization of the wave function. For our purposes it will also be important that confinement is instantaneous, since this implies that only hadrons (and not free quarks) can propagate in intermediate states.

Momentum is now transferred between the electron and one of the three quarks, where we use the symmetry properties of the three-quark wave function to make quark no. 1 the struck one. This will be exploited when we discuss the spectator condition in Sec. 3.2.4.

3.2.2 Eigenvalue equation and Feshbach reduction

The coupled-channels eigenvalue equation on quark level corresponding to Eq. (3.2) reads

$$\begin{pmatrix} M_{3qe}^{\text{conf}} & K_\gamma \\ K_\gamma^\dagger & M_{3qe\gamma}^{\text{conf}} \end{pmatrix} \begin{pmatrix} |\Psi_{3qe}\rangle \\ |\Psi_{3qe\gamma}\rangle \end{pmatrix} = \sqrt{s} \begin{pmatrix} |\Psi_{3qe}\rangle \\ |\Psi_{3qe\gamma}\rangle \end{pmatrix}, \quad (3.23)$$

where the diagonal mass operators M_{3qe}^{conf} and $M_{3qe\gamma}^{\text{conf}}$ include, beyond the relativistic energies of the three quarks, the electron and possibly a photon, an instantaneous confinement potential V^{conf} :

$$M_{3qe(\gamma)}^{\text{conf}} = M_{3qe(\gamma)} + V^{\text{conf}}. \quad (3.24)$$

Later on, we will need a complete set of velocity eigenstates of these mass operators. For $M_{3qe(\gamma)}$ these are just velocity states of free particles fulfilling the eigenvalue equation

$$M_{3qe(\gamma)} |V3qe(\gamma)\rangle = m_{3qe(\gamma)} |V3qe(\gamma)\rangle = \left(\sum_{i=1}^3 \omega_{q_i} + \omega_e (+\omega_\gamma) \right) |V3qe(\gamma)\rangle. \quad (3.25)$$

For $M_{3qe(\gamma)}^{\text{conf}}$ one rather has states consisting of a baryon, the electron and possibly the photon,

$$M_{3qe(\gamma)}^{\text{conf}} |VBe(\gamma)\rangle = m_{Be(\gamma)} |VBe(\gamma)\rangle = (\omega_B + \omega_e (+\omega_\gamma)) |VBe(\gamma)\rangle, \quad (3.26)$$

where $|B\rangle$ is an eigenstate of the confinement problem.

After a Feshbach reduction we get

$$(\sqrt{s} - M_{3qe}^{\text{conf}}) |\Psi_{3qe}\rangle =: (P_{3qe}^{\text{conf}})^{-1} |\Psi_{3qe}\rangle = \underbrace{K_\gamma P_{3qe\gamma}^{\text{conf}} K_\gamma^\dagger}_{V_{\text{opt}}} |\Psi_{3qe}\rangle \quad (3.27)$$

where the optical potential V_{opt} now contains all one-photon exchange contributions between the electron and the quarks. Since $P_{3qe\gamma}^{\text{conf}} = (\sqrt{s} - M_{3qe\gamma}^{\text{conf}})^{-1}$, we observe immediately that propagating intermediate states can only contain baryons, but not free quarks.

3.2.3 Vertex operators and completeness relations

In order to be able to compare the two expressions for the invariant one-photon-exchange amplitude on hadronic and on quark level, we again need the velocity-state matrix elements of V_{opt} between electron–nucleon states. Since we now have a photon-quark vertex instead of the photon-nucleon vertex, we need to sandwich the photon-quark vertex operator between free quark states. Furthermore, we have to insert a complete set of eigenstates of $M_{3qe\gamma}^{\text{conf}}$ in front of the propagator $P_{3qe\gamma}^{\text{conf}}$. Since we only have nucleons in the initial and final state, it suffices to insert the completeness relation (3.9).

The photon creation and annihilation operators are split into a sum of quark–photon and electron–photon vertex operators

$$K_\gamma^{(\dagger)} |3qe(\gamma)\rangle = (K_{q_1\gamma}^{(\dagger)} + K_{q_2\gamma}^{(\dagger)} + K_{q_3\gamma}^{(\dagger)} + K_{e\gamma}^{(\dagger)}) |3qe(\gamma)\rangle. \quad (3.28)$$

We again neglect self-energy photon loops (4 diagrams) and, in addition, photon exchange between the quarks (6 diagrams), which would lead to electromagnetic self-energy corrections of the electron and the nucleon masses. The matrix elements of the optical potential on quark level thus correspond to the following sum of 6 time-ordered diagrams, which describe the exchange of a photon between the electron and one of the three quarks (corresponds to Eq. (3.6) on the hadronic level):

$$\begin{aligned}
\langle V' N' e' | V_{\text{opt}} | V N e \rangle &= \langle V' N' e' | \underbrace{K_{e\gamma} P_{Ne\gamma}^{\text{conf}} \mathbb{I}_{Ne\gamma} \mathbb{I}_{3qe\gamma} K_{q_1\gamma}^\dagger \mathbb{I}_{3qe}}_{V_{01}} | V N e \rangle \\
&+ \langle V' N' e' | K_{e\gamma} P_{Ne\gamma}^{\text{conf}} \mathbb{I}_{Ne\gamma} \mathbb{I}_{3qe\gamma} K_{q_2\gamma}^\dagger \mathbb{I}_{3qe} | V N e \rangle \\
&+ \langle V' N' e' | K_{e\gamma} P_{Ne\gamma}^{\text{conf}} \mathbb{I}_{Ne\gamma} \mathbb{I}_{3qe\gamma} K_{q_3\gamma}^\dagger \mathbb{I}_{3qe} | V N e \rangle \\
&+ \langle V' N' e' | \mathbb{I}_{3qe} K_{q_1\gamma} \mathbb{I}_{3qe\gamma} \mathbb{I}_{Ne\gamma} P_{Ne\gamma}^{\text{conf}} K_{e\gamma}^\dagger | V N e \rangle \\
&+ \langle V' N' e' | \mathbb{I}_{3qe} K_{q_2\gamma} \mathbb{I}_{3qe\gamma} \mathbb{I}_{Ne\gamma} P_{Ne\gamma}^{\text{conf}} K_{e\gamma}^\dagger | V N e \rangle \\
&+ \langle V' N' e' | \mathbb{I}_{3qe} K_{q_3\gamma} \mathbb{I}_{3qe\gamma} \mathbb{I}_{Ne\gamma} P_{Ne\gamma}^{\text{conf}} K_{e\gamma}^\dagger | V N e \rangle. \tag{3.29}
\end{aligned}$$

Here we have already inserted pertinent completeness relations at the appropriate places. In what follows, we will concentrate on the treatment of the first line of Eq. (3.29), i.e. on the determination of the matrix elements $\langle V' N' e' | V_{01} | V N e \rangle$. The explicit expressions for the unity operators we need are (cf. Eq. (2.52)):

$$\begin{aligned}
\mathbb{I}_{Ne\gamma} &= \sum_{\mu_N, \tau_N} \sum_j D V D k_e D k_\gamma \frac{m_{Ne\gamma}^3}{2 \omega_N} (-g^{\mu_\gamma \mu_\gamma}) |V N e \gamma \rangle \langle V N e \gamma|, \\
\mathbb{I}_{3qe} &= \sum_{\mu_{q_1}, \tau_{q_1}} \sum_j D V D k_e D k_{q_2} D k_{q_3} \frac{m_{3qe}^3}{2 \omega_{q_1}} |V 3qe \rangle \langle V 3qe|, \\
\mathbb{I}_{3qe\gamma} &= \sum_{\mu_{q_1}, \tau_{q_1}} \sum_j D V D k_e D k_{q_2} D k_{q_3} D k_\gamma \frac{m_{3qe\gamma}^3}{2 \omega_{q_1}} (-g^{\mu_\gamma \mu_\gamma}) |V 3qe \gamma \rangle \langle V 3qe \gamma|,
\end{aligned} \tag{3.30}$$

where the invariant masses $m_{...}$ are defined via Eq. (2.46). Note that in $\mathbb{I}_{Ne\gamma}$, in contrast to Eq. (3.9), we have now chosen the nucleon momentum to be the redundant one. For quark-level quantities we always consider the momentum of quark 1 the redundant one.

Inserting these completeness relations into Eq. (3.29), we obtain velocity-state matrix elements of the vertex operators on quark level and, on the other hand, brackets of hadronic states with quark-level states, which will lead to three-quark wave functions. These two quantities will be treated in the next two sections.

3.2.4 Currents and spectator conditions

On quark level the spectator conditions for matrix elements of the vertex operators (cf. Sec. 3.1.5 for further details) read

$$\begin{aligned} \langle V' 3q' e' \gamma' | K_{q_1 \gamma}^\dagger | V 3qe \rangle &= \Delta_{VV'} \Delta_{ee'} \Delta_{q_2 q'_2} \Delta_{q_3 q'_3} \frac{(-1)}{\sqrt{m_{3qe\gamma}^3 m_{3qe}^3}} \langle q'_1 \gamma' | | K_{q_1 \gamma}^\dagger | | q_1 \rangle , \\ \langle V' N' e' \gamma' | K_{e\gamma}^\dagger | V Ne \rangle &= \Delta_{VV'} \Delta_{NN'} \frac{(-1)}{\sqrt{m_{Ne\gamma}^3 m_{Ne}^3}} \langle e' \gamma' | | K_{e\gamma}^\dagger | | e \rangle . \end{aligned} \quad (3.31)$$

We treat both quarks and the electron as point particles, whence, according to Sec. 2.5.2, their currents are

$$\begin{aligned} \langle q'_1 \gamma' | | K_{q_1 \gamma}^\dagger | | q_1 \rangle &= |e| J_\nu(q_1, q'_1) \delta_{\tau_{q_1} \tau'_{q_1}} \epsilon^{\nu *}(\gamma') \\ &= |e| Q_{q_1} \left(\bar{u}_{\mu'_{q_1}}(\vec{k}'_{q_1}) \gamma_\nu u_{\mu_{q_1}}(\vec{k}_{q_1}) \right) \delta_{\tau_{q_1} \tau'_{q_1}} \epsilon^{\nu *}_{\mu'_{q_1}}(\vec{k}'_\gamma) , \\ \langle e' \gamma' | | K_{e\gamma}^\dagger | | e \rangle &= |e| J_\nu(e, e') \epsilon^{\nu *}(\gamma') = |e| Q_e \left(\bar{u}_{\mu'_e}(\vec{k}'_e) \gamma_\nu u_{\mu_e}(\vec{k}_e) \right) \epsilon^{\nu *}_{\mu'_e}(\vec{k}'_\gamma) . \end{aligned} \quad (3.32)$$

Note that the electromagnetic interaction does not change the isospin of the quark!

3.2.5 Wave functions

In addition to the matrix elements of quark-level vertex operators, insertion of the completeness relations for free quarks also leads (via products $\mathbb{I}_{Ne} \mathbb{I}_{3qe}$, $\mathbb{I}_{Ne\gamma} \mathbb{I}_{3qe\gamma}$ etc.) to scalar products between nucleon states and quark states. These give rise to the three-quark bound-state wave function $\langle 3q | N \rangle$, which relates quark momenta, spins and isospins to the corresponding nucleon quantities and thus encodes quark confinement [Bie11]. We will later on use a phenomenological wave function that is defined in the center-of-momentum (c.o.m.) frame of the three quarks. We will have a closer look on it in Sec. 3.3.2. It arises in Eq. (3.29) via

$$\begin{aligned} \langle V' 3q' e' | V Ne \rangle &= \mathcal{N}_1 \Delta_{VV'} \Delta_{ee'} \langle 3q' | N \rangle , \\ \langle V' 3q' e' \gamma' | V Ne \gamma \rangle &= \mathcal{N}_2 \Delta_{VV'} \Delta_{ee'} \Delta_{\gamma\gamma'} \langle 3q' | N \rangle . \end{aligned} \quad (3.33)$$

\mathcal{N}_1 and \mathcal{N}_2 are normalization factors which are determined as follows:

Normalization of wave functions: We use the following condition from [Sen06]:

$$\sum_{\substack{\tilde{\mu}_{q_1}'' \tilde{\mu}_{q_2}'' \tilde{\mu}_{q_3}'' \\ \tau_{q_1}'' \tau_{q_2}'' \tau_{q_3}''}} \int d^3 \tilde{k}_{q_2}'' d^3 \tilde{k}_{q_3}'' \langle \tilde{N}' | \tilde{3q}'' \rangle \langle \tilde{3q}'' | \tilde{N} \rangle = \delta_{\tilde{\mu}_N \tilde{\mu}'_N} \delta_{\tau_N \tau'_N} . \quad (3.34)$$

The quantities with a “tilde” are defined in the c.o.m. frame of the three quarks that constitute the nucleon, *not* the overall c.o.m. frame of the electron-3-quark-system, i.e [SU00], in our shorthand notation (2.41):

$$U_{B(\vec{v}_{3q})} | \tilde{k}_{q_i} \tilde{\mu}_{q_i} \rangle = \sum_{\mu_{q_i} = \pm \frac{1}{2}} | k_{q_i} \mu_{q_i} \rangle D_{\mu_{q_i} \tilde{\mu}_{q_i}} \left(B(\vec{v}_{3q}), \frac{\vec{k}_{q_i}}{m_q} \right) \quad (3.35)$$

with

$$\begin{aligned}
 k_{q_i} &= B(\vec{v}_{3q}) \tilde{k}_{q_i} , \\
 \vec{v}_{3q} &= \frac{\vec{k}_{3q}}{m_{3q}} , \\
 \vec{k}_{3q} &= \vec{k}_{q_1} + \vec{k}_{q_2} + \vec{k}_{q_3} \equiv \vec{k}_N , \\
 m_{3q} &= \tilde{\omega}_{q_1} + \tilde{\omega}_{q_2} + \tilde{\omega}_{q_3} = \sqrt{(\omega_{q_1} + \omega_{q_2} + \omega_{q_3})^2 - \vec{k}_{3q}^2} .
 \end{aligned} \tag{3.36}$$

By $B(\vec{v})$ we mean a (canonical, i.e. rotationless) Lorentz boost with velocity \vec{v} . For the definition of the Wigner rotation R_W and its associated Wigner-D-function in Eq. (3.35), see Sec. 2.4.4. Note that \vec{v}_{3q} and m_{3q} depend on the actual momenta of the three quarks and not on the velocity and mass of the nucleon!

The Jacobian of the coordinate transformation *between velocity states* is derived in analogy to the quark–antiquark case [Fuc07] and runs along the lines of the derivation of the velocity-state integration measure given in [Kra01]. For details see App. B.1. The result is

$$d^3V \dots d^3k_{q_2} d^3k_{q_3} = d^3V \dots d^3\tilde{k}_{q_2} d^3\tilde{k}_{q_3} \frac{\omega_{q_1}}{\tilde{\omega}_{q_1}} \frac{\omega_{q_2}}{\tilde{\omega}_{q_2}} \frac{\omega_{q_3}}{\tilde{\omega}_{q_3}} \frac{\tilde{\omega}_{q_1} + \tilde{\omega}_{q_2} + \tilde{\omega}_{q_3}}{\omega_{q_1} + \omega_{q_2} + \omega_{q_3}} . \tag{3.37}$$

The normalization factors are derived in analogy to the quark–antiquark case [Bie11] as detailed in App. B.2. The result is

$$\begin{aligned}
 \mathcal{N}_1 &= 4(2\pi)^3 \frac{\sqrt{\omega_N \tilde{\omega}'_{q_1} \tilde{\omega}'_{q_2} \tilde{\omega}'_{q_3} (\sum \omega'_{q_i})}}{\sqrt{(\sum \tilde{\omega}'_{q_i}) (\omega_N + \omega_e)^3 (\sum \omega'_{q_i} + \omega_e)^3}} , \\
 \mathcal{N}_2 &= 4(2\pi)^3 \frac{\sqrt{\omega_N \tilde{\omega}'_{q_1} \tilde{\omega}'_{q_2} \tilde{\omega}'_{q_3} (\sum \omega'_{q_i})}}{\sqrt{(\sum \tilde{\omega}'_{q_i}) (\omega_N + \omega_e + \omega_\gamma)^3 (\sum \omega'_{q_i} + \omega_e + \omega_\gamma)^3}} .
 \end{aligned} \tag{3.38}$$

3.2.6 Analytic calculation of optical potential

We now continue the analytic calculations of the first term of the quark-level optical potential, i.e. V_{o1} , in Eq. (3.29). Letting the propagator act on its eigenfunction and after

some rearranging we obtain, via Eqs. (3.30),

$$\begin{aligned}
& \langle V' N' e' | V_{\text{o}1} | V N e \rangle \\
&= \langle V' N' e' | K_{e\gamma} P_{N e\gamma} \mathbb{I}_{N e\gamma} \mathbb{I}_{3qe\gamma} K_{q_1\gamma}^\dagger \mathbb{I}_{3qe} | V N e \rangle \\
&= \sum_{\mu_N^{(4)}, \tau_N^{(4)}} \sum_{\mu_{q_1}^{(3)}, \tau_{q_1}^{(3)}} \int DV^{(4)} Dk_e^{(4)} Dk_\gamma^{(4)} \frac{\left(m_{N e\gamma}^{(4)}\right)^3}{2\omega_N^{(4)}} \left(-g^{\mu_\gamma^{(4)} \mu_\gamma^{(4)}}\right) \\
&\quad \times \sum_{\mu_{q_1}^{(3)}, \tau_{q_1}^{(3)}} \int DV^{(3)} Dk_{q_2}^{(3)} Dk_{q_3}^{(3)} Dk_e^{(3)} Dk_\gamma^{(3)} \frac{\left(m_{3qe\gamma}^{(3)}\right)^3}{2\omega_{q_1}^{(3)}} \left(-g^{\mu_\gamma^{(3)} \mu_\gamma^{(3)}}\right) \\
&\quad \times \sum_{\mu_{q_1}^{\prime(3)}, \tau_{q_1}^{\prime(3)}} \int DV'' Dk_{q_2}^{\prime(3)} Dk_{q_3}^{\prime(3)} Dk_e^{\prime(3)} \frac{\left(m_{3qe}^{\prime(3)}\right)^3}{2\omega_{q_1}^{\prime(3)}} \frac{1}{\sqrt{s} - m_{N e\gamma}^{(4)}} \\
&\quad \times \langle V' N' e' | K_{e\gamma} | V^{(4)} N^{(4)} e^{(4)} \gamma^{(4)} \rangle \langle V^{(4)} N^{(4)} e^{(4)} \gamma^{(4)} | V^{(3)} 3q^{(3)} e^{(3)} \gamma^{(3)} \rangle \\
&\quad \times \langle V^{(3)} 3q^{(3)} e^{(3)} \gamma^{(3)} | K_{q_1\gamma}^\dagger | V'' 3q'' e'' \rangle \langle V'' 3q'' e'' | V N e \rangle, \tag{3.39}
\end{aligned}$$

where $x^{(3)}$, $x^{(4)}$ etc. is equivalent to x''' , x'''' etc. The invariant masses m_{\dots} are defined in Eq. (2.46).

After insertion of the spectator conditions (3.31) and the hadron wave functions (3.33) (with normalization factors (3.38)), the last two lines of (3.39) read

$$\begin{aligned}
& \Delta_V^{\prime(4)} \Delta_N^{\prime(4)} \frac{(-1)}{\sqrt{(m_{N e}^{\prime(4)})^3 (m_{N e\gamma}^{(4)})^3}} \langle e^{(4)} \gamma^{(4)} | | K_{e\gamma}^\dagger | | e' \rangle^* \\
& \times 4(2\pi)^3 \frac{\sqrt{\omega_N^{(4)} \tilde{\omega}_{q_1}^{(3)} \tilde{\omega}_{q_2}^{(3)} \tilde{\omega}_{q_3}^{(3)} (\sum \omega_{q_i}^{(3)})}}{\sqrt{(\sum \tilde{\omega}_{q_i}^{(3)}) (m_{N e\gamma}^{(4)})^3 (m_{3qe\gamma}^{(3)})^3}} \Delta_V^{(3)(4)} \Delta_e^{(3)(4)} \Delta_\gamma^{(3)(4)} \langle N^{(4)} | 3q^{(3)} \rangle \\
& \times \Delta_V^{\prime\prime(3)} \Delta_e^{\prime\prime(3)} \Delta_{q_2}^{\prime\prime(3)} \Delta_{q_3}^{\prime\prime(3)} \delta_{\tau_{q_1}^{\prime\prime} \tau_{q_1}^{(3)}} \frac{(-1)}{\sqrt{(m_{3qe\gamma}^{(3)})^3 (m_{3qe}^{\prime(3)})^3}} \langle q_1^{(3)} \gamma^{(3)} | | K_{q_1\gamma}^\dagger | | q_1'' \rangle \\
& \times 4(2\pi)^3 \frac{\sqrt{\omega_N \tilde{\omega}_{q_1}^{\prime\prime} \tilde{\omega}_{q_2}^{\prime\prime} \tilde{\omega}_{q_3}^{\prime\prime} (\sum \omega_{q_i}^{\prime\prime})}}{\sqrt{(\sum \tilde{\omega}_{q_i}^{\prime\prime}) (m_{N e}^{\prime(4)})^3 (m_{3qe}^{\prime(3)})^3}} \Delta_V^{(0)\prime\prime} \Delta_e^{(0)\prime\prime} \langle 3q'' | N \rangle, \tag{3.40}
\end{aligned}$$

where $\Delta_x^{(i)(j)}$ is shorthand for $\Delta_{x^{(i)} x^{(j)}}$. We now exploit the delta functions to perform most of the integrations in Eq. (3.39) and then cancel the resulting fractions as far as

possible. Insertion of the quark and electron currents (3.32) then yields

$$\begin{aligned}
& \langle V' N' e' | V_{01} | V N e \rangle \\
&= 2 (2\pi)^6 \Delta_{VV'} \sum_{\mu''_{q_1}, \mu_{q_1}^{(3)}, \tau''_{q_1}} \sum_{\substack{Dk''_{q_2} Dk''_{q_3} Dk''_{\gamma} \\ \mu_{q_2}^{(3)}, \mu_{q_3}^{(3)}, \tau_{q_2}^{(3)}, \tau_{q_3}^{(3)}}} g^{\mu_{q_2}^{(3)} \mu_{q_3}^{(3)}} \\
&\quad \times \frac{1}{\omega'_N} \frac{1}{\omega_{q_1}^{(3)}} \frac{1}{\omega_{q_1}''} \frac{\sqrt{\omega_N}}{\sqrt{(\omega_N + \omega_e)^3}} \frac{\sqrt{\omega'_N}}{\sqrt{(\omega'_N + \omega'_e)^3}} \frac{1}{(\sqrt{s} - \omega'_N - \omega_e - \omega_{\gamma}^{(3)})} \\
&\quad \times \Delta_N'^{(4)} J_{\nu}^{\dagger}(e', e^{(3)}) \epsilon_{\mu_{\gamma}^{(3)}}^* (\vec{k}_{\gamma}^{(3)}) \frac{\sqrt{\tilde{\omega}_{q_1}^{(3)} \tilde{\omega}_{q_2}^{(3)} \tilde{\omega}_{q_3}^{(3)} (\sum \omega_{q_i}^{(3)})}}{\sqrt{(\sum \tilde{\omega}_{q_i}^{(3)})}} \langle N' | q_1^{(3)} q_2'' q_3'' \rangle \\
&\quad \times J_{\lambda}(q_1'', q_1^{(3)}) \epsilon_{\mu_{\gamma}^{(3)}}^{\lambda} (\vec{k}_{\gamma}^{(3)}) \frac{\sqrt{\tilde{\omega}_{q_1}'' \tilde{\omega}_{q_2}'' \tilde{\omega}_{q_3}'' (\sum \omega_{q_i}'')}}{\sqrt{(\sum \tilde{\omega}_{q_i}'')}} \langle 3q'' | N \rangle,
\end{aligned} \tag{3.41}$$

where we have kept $\omega_{q_2,3}^{(3)}$ for readability. Next, we use the velocity-state conditions

$$\begin{aligned}
& \sum \vec{k}'_N + \vec{k}'_e = 0, \\
& \sum \vec{k}_N^{(4)} + \vec{k}_e + \vec{k}_{\gamma}^{(3)} = 0,
\end{aligned} \tag{3.42}$$

whence

$$\frac{1}{2(2\pi)^3 \omega'_N} \Delta_N'^{(4)} = \delta_{\mu'_N \mu_N^{(4)}} \delta_{\tau'_N \tau_N^{(4)}} \delta^3 (\vec{k}'_N - \vec{k}_N^{(4)}) = \delta_{\mu'_N \mu_N^{(4)}} \delta_{\tau'_N \tau_N^{(4)}} \delta^3 (\vec{k}_e + \vec{k}_{\gamma}^{(3)} - \vec{k}'_e), \tag{3.43}$$

where we have kept $\omega_{\gamma}^{(3)}$ for readability. We also employ the completeness relation (2.11) for the photon polarization vectors ϵ . We then denote all ingoing states with no prime and outgoing states with a single prime, and after some rearranging we obtain

$$\begin{aligned}
& \langle V' N' e' | V_{01} | V N e \rangle \\
&= \frac{1}{2} \Delta_{VV'} \sum_{\substack{\mu_{q_1} \mu'_{q_1} \mu_{q_2} \mu_{q_3} \\ \tau_{q_2} \tau_{q_3}}} \frac{d^3 k_{q_2}}{\omega_{q_2}} \frac{d^3 k_{q_3}}{\omega_{q_3}} \frac{1}{\omega_{\gamma} \omega'_{q_1} \omega_{q_1}} \frac{1}{(\sqrt{s} - \omega'_N - \omega_e - \omega_{\gamma})} \\
&\quad \times \frac{\sqrt{\omega'_N \omega_N}}{\sqrt{(\omega'_N + \omega'_e)^3 (\omega_N + \omega_e)^3}} \frac{\sqrt{\tilde{\omega}'_{q_1} \tilde{\omega}'_{q_2} \tilde{\omega}'_{q_3} (\sum \omega'_{q_i})}}{\sqrt{(\sum \tilde{\omega}'_{q_i})}} \frac{\sqrt{\tilde{\omega}_{q_1} \tilde{\omega}_{q_2} \tilde{\omega}_{q_3} (\sum \omega_{q_i})}}{\sqrt{(\sum \tilde{\omega}_{q_i})}} \\
&\quad \times \langle N' | q'_1 q_2 q_3 \rangle \langle q_1 q_2 q_3 | N \rangle J^{\nu}(e, e') | e | Q_{q_1}(\tau_{q_1}) \left(\bar{u}_{\mu'_{q_1}} (\vec{k}'_{q_1}) \gamma_{\nu} u_{\mu_{q_1}} (\vec{k}_{q_1}) \right),
\end{aligned} \tag{3.44}$$

with $\sum_i \vec{k}_{q_i}^{(\prime)} + \vec{k}_e^{(\prime)} = 0$, $\vec{k}_{\gamma} = \vec{k}'_e - \vec{k}_e$ and $\sum_i \tau_{q_i}^{(\prime)} = \tau_N^{(\prime)}$. At this point we have already inserted the full expression for the quark current (3.32) and finally abandoned our short-hand notation for the quark momenta.

Remaining diagrams: Derivation of V_{02} resp. V_{03} is completely analogous, with q_1 replaced by q_2 or q_3 , respectively. The reverse time ordering, $V_{04} - V_{06}$ is derived in a completely analogous way (see also Sec. 3.1.6), the net effect being that $(\sqrt{s} - \omega_N - \omega'_e - \omega_\gamma)^{-1}$ is replaced by $(\sqrt{s} - \omega'_N - \omega_e - \omega_\gamma)^{-1}$. Also the combination of the two time orderings is done as in App. B.3 by use of (3.21). The final result for the invariant one-photon-exchange amplitude on constituent level is

$$\begin{aligned} \mathcal{M}_{1\gamma} = & \langle V' N' e' | V_{\text{opt}} | V N e \rangle = \Delta_{VV'} \frac{\sqrt{\omega'_N \omega_N}}{m_{Ne}^3 Q^2} \sum_{i=1}^3 \sum_{\substack{\mu_{q_1}, \mu_{q_2}, \mu_{q_3} \\ \mu'_{q_i}, \tau_{q_2}, \tau_{q_3}}} \int \left(\prod \frac{d^3 k_{q_j \neq i}}{\omega_{q_j \neq i}} \right) \\ & \times \frac{1}{\omega'_{q_i} \omega_{q_i}} \frac{\sqrt{\tilde{\omega}'_{q_1} \tilde{\omega}'_{q_2} \tilde{\omega}'_{q_3} (\sum \omega'_{q_k})}}{\sqrt{(\sum \tilde{\omega}'_{q_k})}} \frac{\sqrt{\tilde{\omega}_{q_1} \tilde{\omega}_{q_2} \tilde{\omega}_{q_3} (\sum \omega_{q_k})}}{\sqrt{(\sum \tilde{\omega}_{q_k})}} \langle N' | q'_1 q'_2 q'_3 \rangle \langle q_1 q_2 q_3 | N \rangle \\ & \times J^\nu(e, e') |e| Q_{q_i}(\tau_{q_i}) \left(\bar{u}_{\mu'_{q_i}}(\vec{k}'_{q_i}) \gamma^\nu u_{\mu_{q_i}}(\vec{k}_{q_i}) \right). \end{aligned} \quad (3.45)$$

Due to the symmetry properties of the three-quark wave function, it can be assumed that the photon couples only to quark 1, implying an overall factor of 3 instead of the sum over i .

3.3 Calculation of nucleon currents

3.3.1 Derivation

Equating the expressions (3.22) and (3.45) for the invariant one-photon-exchange amplitude on hadronic and on quark level, respectively, we obtain a microscopic expression for the nucleon current:

$$\begin{aligned} & J_N^\nu(\vec{k}_N, \mu_N; \vec{k}'_N, \mu'_N; \tau_N) \\ & = 3 \sqrt{\omega'_N \omega_N} \sum_{\substack{\mu_1, \mu_2, \mu_3 \\ \mu_1, \tau_2, \tau_3}} \int \frac{d^3 k_2}{\omega_2} \frac{d^3 k_3}{\omega_3} \frac{1}{\omega'_1 \omega_1} \frac{\sqrt{\tilde{\omega}'_1 \tilde{\omega}'_2 \tilde{\omega}'_3 (\sum \omega'_k)}}{\sqrt{(\sum \tilde{\omega}'_k)}} \frac{\sqrt{\tilde{\omega}_1 \tilde{\omega}_2 \tilde{\omega}_3 (\sum \omega_k)}}{\sqrt{(\sum \tilde{\omega}_k)}} \\ & \times \langle N' | q'_1 q'_2 q'_3 \rangle \langle q_1 q_2 q_3 | N \rangle \left(|e| Q_1(\tau_1) \bar{u}_{\mu'_1}(\vec{k}'_1) \gamma^\nu u_{\mu_1}(\vec{k}_1) \right), \end{aligned} \quad (3.46)$$

where we have replaced the quark indices q_i simply by i and where the isospin of the nucleon is $\tau_N = +1/2$ for the proton and $-1/2$ for the neutron.

3.3.2 Three-quark wave function

Nucleon rest frame: Since the nucleon is a fermion, its three-quark wave function $\Phi := \langle \tilde{q}_1 \tilde{q}_2 \tilde{q}_3 | \tilde{N} \rangle$ (the “tilde” signifying that we are in the nucleon rest frame) has to be fully antisymmetric under exchange of any two quarks. It is a product of the space (or

momentum-) part Φ_X , a spin-flavor part Φ_{FS} and a color part Φ_C :

$$\Phi = \Phi_X \cdot \Phi_{FS} \cdot \Phi_C . \quad (3.47)$$

We assume the space part to be a pure s-wave. This means that Φ_X is completely symmetric. Since Φ_C is fully antisymmetric by construction (QCD), the spin-flavor part Φ_{FS} should also be completely symmetric, so that the full wave function Φ is completely antisymmetric.

But let us start with the flavor (isospin) part. It can be either a mixed symmetric or a mixed antisymmetric state (in quarks 2 and 3) [Sen06, Wag98]:

$$\begin{aligned} \Phi_F^{p,ma} &= \frac{1}{\sqrt{2}}(uud - udu) && \text{(proton, mixed antisymm.) ,} \\ \Phi_F^{p,ms} &= -\frac{1}{\sqrt{6}}(uud + udu - 2duu) && \text{(proton, mixed symm.) ,} \\ \Phi_F^{n,ma} &= \frac{1}{\sqrt{2}}(dud - ddu) && \text{(neutron, mixed antisymm.) ,} \\ \Phi_F^{n,ms} &= \frac{1}{\sqrt{6}}(dud + ddu - 2udd) && \text{(neutron, mixed symm.) .} \end{aligned} \quad (3.48)$$

This can also be expressed using Clebsch-Gordan coefficients for adding the isospins $\tau_i = \pm \frac{1}{2}$ of the quarks. We first couple the isospins of quarks 2 and 3 to an intermediate isospin $s \in \{0, 1\}$ with projection τ_s and then couple it with the isospin of quark 1:

$$\Phi_F = \sum_{\tau_1, \tau_2, \tau_3, \tau_s} C_{\frac{1}{2} \tau_2 \frac{1}{2} \tau_3}^{s \tau_s} C_{s \tau_s \frac{1}{2} \tau_1}^{\frac{1}{2} \tau_N} , \quad (3.49)$$

where $s = 0$ for the mixed antisymmetric state and $s = 1$ for the mixed symmetric state, and $\tau_N = +\frac{1}{2}$ for the proton and $-\frac{1}{2}$ for the neutron.

Analogously, we have for the spin part:

$$\begin{aligned} \Phi_S^{\uparrow,ma} &= \frac{1}{\sqrt{2}}(\uparrow\uparrow\downarrow - \uparrow\downarrow\uparrow) && (\mu_N = \frac{1}{2}, \text{ mixed antisymm.) ,} \\ \Phi_S^{\uparrow,ms} &= -\frac{1}{\sqrt{6}}(\uparrow\uparrow\downarrow + \uparrow\downarrow\uparrow - 2\downarrow\uparrow\uparrow) && (\mu_N = \frac{1}{2}, \text{ mixed symm.) ,} \\ \Phi_S^{\downarrow,ma} &= \frac{1}{\sqrt{2}}(\downarrow\uparrow\downarrow - \downarrow\downarrow\uparrow) && (\mu_N = -\frac{1}{2}, \text{ mixed antisymm.) ,} \\ \Phi_S^{\downarrow,ms} &= \frac{1}{\sqrt{6}}(\downarrow\uparrow\downarrow + \downarrow\downarrow\uparrow - 2\uparrow\downarrow\downarrow) && (\mu_N = -\frac{1}{2}, \text{ mixed symm.) ,} \end{aligned} \quad (3.50)$$

which, in the nucleon rest frame referred to by a “tilde”, corresponds to

$$\Phi_S^s = \sum_{\tilde{\mu}_1, \tilde{\mu}_2, \tilde{\mu}_3, \tilde{\mu}_s} C_{\frac{1}{2} \tilde{\mu}_2 \frac{1}{2} \tilde{\mu}_3}^{s \tilde{\mu}_s} C_{s \tilde{\mu}_s \frac{1}{2} \tilde{\mu}_1}^{\frac{1}{2} \tilde{\mu}_N} . \quad (3.51)$$

To obtain the fully symmetric spin-flavor part, we combine the product of mixed-symmetric states, $\Phi_F^{N,ms} \cdot \Phi_S^{\mu_N,ms}$, with the product of mixed-antisymmetric states, $\Phi_F^{N,ma} \cdot \Phi_S^{\mu_N,ma}$, which in terms of Clebsch-Gordan coefficients reads

$$\Phi_{FS} = \frac{1}{\sqrt{2}} \sum_s \sum_{\tilde{\mu}_1, \tilde{\mu}_2, \tilde{\mu}_3, \tilde{\mu}_s} C_{\frac{1}{2} \tilde{\mu}_2 \frac{1}{2} \tilde{\mu}_3}^{s \tilde{\mu}_s} C_{\frac{1}{2} \tau_2 \frac{1}{2} \tau_3}^{s \tau_s} C_{s \tilde{\mu}_s \frac{1}{2} \tilde{\mu}_1}^{\frac{1}{2} \tilde{\mu}_N} C_{s \tau_s \frac{1}{2} \tau_1}^{\frac{1}{2} \tau_N} . \quad (3.52)$$

Note that one has the same s in all four coefficients! It is then irrelevant which two of the three quarks are coupled first. Since necessarily, $\tilde{\mu}_s = \tilde{\mu}_2 + \tilde{\mu}_3$, $\tau_s = \tau_2 + \tau_3$, $\sum \tilde{\mu}_i = \tilde{\mu}_N$ and $\sum \tau_i = \tau_N$, Eq. (3.52) can equally be written in the form

$$\Phi_{\text{FS}} = \frac{1}{\sqrt{2}} \sum_s \sum_{\substack{\tilde{\mu}_2, \tilde{\mu}_3 \\ \tau_2, \tau_3}} C_{\frac{1}{2} \tilde{\mu}_2 \frac{1}{2} \tilde{\mu}_3}^{s(\tilde{\mu}_2 + \tilde{\mu}_3)} C_{\frac{1}{2} \tau_2 \frac{1}{2} \tau_3}^{s(\tau_2 + \tau_3)} C_{s(\tilde{\mu}_2 + \tilde{\mu}_3) \frac{1}{2} \tilde{\mu}_1}^{\frac{1}{2} \tilde{\mu}_N} C_{s(\tau_2 + \tau_3) \frac{1}{2} \tau_1}^{\frac{1}{2} \tau_N}, \quad (3.53)$$

where we have kept $\tilde{\mu}_1$ and τ_1 for better readability.

For the spatial (momentum-) part of the wave function, we take the model proposed by Schlumpf [Schl94, parameter set 3]. It was refitted by Pasquini and Boffi to accommodate a meson cloud in their front-form study of the electromagnetic nucleon form factors [PB07]. Accordingly, we will use the Schlumpf parametrization for calculating the electromagnetic nucleon form factors without the pion cloud and the Pasquini-Boffi parametrization for the “bare” electromagnetic nucleon form factors, which are needed for the calculation that includes pion-cloud effects. The momentum part of the Schlumpf wave function reads

$$\Phi_X = \frac{\mathcal{N}}{\left((\sum \tilde{\omega}_k)^2 + \beta^2 \right)^\gamma}. \quad (3.54)$$

The values of the parameters (m is the constituent quark mass) are given in table 3.1. The

parametrization	m	β	γ
Schlumpf	0.263	0.607	3.5
Pa.-Bo.	0.264	0.489	3.21

Table 3.1: Parameters for the Schlumpf wave function as given in [Schl94, parameter set 3] (first line) and as reparametrized by Pasquini and Boffi [PB07] (second line).

normalization constant \mathcal{N} is determined numerically to be $\mathcal{N} = \sqrt{459}$ for the Schlumpf parametrization and $\mathcal{N} = \sqrt{200}$ for Pasquini-Boffi parametrization, respectively.

Electron–nucleon rest frame: In order to use the spin-flavor wave function (3.52) for arbitrary velocity states of the electron–nucleon–photon system, we have to boost it from the nucleon rest frame to the overall rest frame of the 3-quark–electron–photon system using the Lorentz-transformation properties, Eq. (3.35). Each spin projection entering the Clebsch-Gordan coefficients thus has to be multiplied with a Wigner-D-function (cf. Sec. 2.4.4) corresponding to the Lorentz boost (3.35) and subsequently summed over all spin orientations (in the tilde frame). According to [Bie11] and taking into account that, via Eq. (2.43),

$$D_{\tilde{\mu}_N \mu_N} \left(B^{-1}(\vec{v}_{3q}), \frac{\vec{k}_N}{m_N} \right) = D_{\mu_N \tilde{\mu}_N}^* \left(B(\vec{v}_{3q}), \frac{\tilde{\vec{k}}_N}{m_N} \right) \quad (3.55)$$

and

$$\begin{aligned}
R_W(B(\vec{v}_{3q}), \frac{\vec{k}_N}{m_N}) &= R_W(B(\vec{v}_{3q}), \vec{0}) = B^{-1}(\overrightarrow{B(\vec{v}_{3q})\vec{0}}) B(\vec{v}_{3q}) B(\vec{0})_{3 \times 3} \\
&= B^{-1}(\vec{v}_{3q}) B(\vec{v}_{3q})_{3 \times 3} = \mathbb{I}_{3 \times 3} \\
\Rightarrow D_{\mu_N \tilde{\mu}_N}^*(\dots) &= \delta_{\mu_N \tilde{\mu}_N} ,
\end{aligned} \tag{3.56}$$

we obtain (shorthand notation)

$$\begin{aligned}
\langle q_1 q_2 q_3 | N \rangle &= \sum_{\{\tilde{\mu}_{q_i}\}} \prod_i D_{\tilde{\mu}_{q_i} \mu_{q_i}}^*(B^{-1}(\vec{v}_{3q}), \underbrace{\frac{\vec{k}_{q_i}}{m_q}}_{=: \vec{v}_{q_i}}) \langle \tilde{q}_1 \tilde{q}_2 \tilde{q}_3 | \tilde{N} \rangle \\
&\stackrel{(2.43)}{=} \sum_{\{\tilde{\mu}_{q_i}\}} \prod_i D_{\mu_{q_i} \tilde{\mu}_{q_i}}(B(\vec{v}_{3q}), \vec{v}_{q_i}) \langle \tilde{q}_1 \tilde{q}_2 \tilde{q}_3 | \tilde{N} \rangle , \\
\langle N' | q'_1 q'_2 q'_3 \rangle &= \sum_{\{\tilde{\mu}'_{q_i}\}} \prod_i D_{\tilde{\mu}'_{q_i} \tilde{\mu}_{q_i}}^*(B(\vec{v}'_{3q}), \vec{v}'_{q_i}) \langle \tilde{N}' | \tilde{q}'_1 \tilde{q}'_2 \tilde{q}'_3 \rangle .
\end{aligned} \tag{3.57}$$

We have thus succeeded in constructing $\Phi_X \cdot \Phi_{FS}$ such that it is fully symmetric under interchange of any two quarks. Multiplication by the color part Φ_C will then ensure full antisymmetry as required for a fermionic wave function. However, we don't have to care about Φ_C since the electromagnetic interaction does not change color and hence, the color matrix element just gives 1.

3.3.3 Analytic Result

Finally inserting Eqs. (3.52), (3.54) and (3.57) into (3.46) and performing the integrations in the rest frame of the three-quark subsystem using Eq. (3.37), we end up with

$$\begin{aligned}
&J_N^\nu(\vec{k}_N, \mu_N; \vec{k}'_N, \mu'_N; \tau_N) \\
&= \frac{3}{2} \sqrt{\omega'_N \omega_N} \sum Q_1(\tau_1) |e| \int d^3 \tilde{k}_2 d^3 \tilde{k}_3 \frac{1}{\omega'_1} \sqrt{\frac{\tilde{\omega}'_1 \tilde{\omega}'_2 \tilde{\omega}'_3}{\tilde{\omega}_1 \tilde{\omega}_2 \tilde{\omega}_3}} \sqrt{\frac{\sum \tilde{\omega}_k}{\sum \tilde{\omega}'_k}} \sqrt{\frac{\sum \omega'_k}{\sum \omega_k}} \\
&\times D_{\mu'_1 \tilde{\mu}_1}^*(B(\vec{v}'_{3q}), \vec{v}'_1) D_{\mu'_2 \tilde{\mu}'_2}^*(B(\vec{v}'_{3q}), \vec{v}'_2) D_{\mu'_3 \tilde{\mu}'_3}^*(B(\vec{v}'_{3q}), \vec{v}'_3) \\
&\times C_{\frac{1}{2} \tilde{\mu}'_2 \frac{1}{2} \tilde{\mu}'_3}^{s' \tilde{\mu}'_s} C_{\frac{1}{2} \tau_2 \frac{1}{2} \tau_3}^{s' \tau_s} C_{s' \tilde{\mu}'_s \frac{1}{2} \tilde{\mu}'_1}^{\frac{1}{2} \mu'_N} C_{s' \tau_s \frac{1}{2} \tau_1}^{\frac{1}{2} \tau_N} \\
&\times D_{\mu_1 \tilde{\mu}_1}(B(\vec{v}_{3q}), \vec{v}_1) D_{\mu_2 \tilde{\mu}_2}(B(\vec{v}_{3q}), \vec{v}_2) D_{\mu_3 \tilde{\mu}_3}(B(\vec{v}_{3q}), \vec{v}_3) \\
&\times C_{\frac{1}{2} \tilde{\mu}_2 \frac{1}{2} \tilde{\mu}_3}^{s \tilde{\mu}_s} C_{\frac{1}{2} \tau_2 \frac{1}{2} \tau_3}^{s \tau_s} C_{s \tilde{\mu}_s \frac{1}{2} \tilde{\mu}_1}^{\frac{1}{2} \mu_N} C_{s \tau_s \frac{1}{2} \tau_1}^{\frac{1}{2} \tau_N} \\
&\times \frac{\mathcal{N}}{\left((\sum \tilde{\omega}'_k)^2 + \beta^2\right)^\gamma} \frac{\mathcal{N}}{\left((\sum \tilde{\omega}_k)^2 + \beta^2\right)^\gamma} \bar{u}_{\mu'_1}(\vec{k}'_1) \gamma^\nu u_{\mu_1}(\vec{k}_1) ,
\end{aligned} \tag{3.58}$$

where the spectator conditions (3.31) as well as isospin invariance have fully been taken into account and hence, the sum runs over spins and isospins $\mu_1, \mu'_1, \mu_2, \mu_3, \tilde{\mu}_2, \tilde{\mu}'_3, \tilde{\mu}'_2$,

$\tilde{\mu}'_3, \tau_2, \tau_3$ ($= \pm \frac{1}{2}$), s, s' ($= 0, 1$), μ_s, μ'_s and τ_s ($= -s^{(\prime)} \dots s^{(\prime)}$), while

$$\begin{aligned} \mu_N^{(\prime)} &= \tilde{\mu}_1^{(\prime)} + \tilde{\mu}_2^{(\prime)} + \tilde{\mu}_3^{(\prime)}, \\ \tau_N &= \tau_1 + \tau_2 + \tau_3 \end{aligned} \quad (3.59)$$

always has to be satisfied. Recall that spins can be coupled the usual way only in the rest frame of the three-quark subsystem (“tilde”-frame) and via (3.56), $\tilde{\mu}_N^{(\prime)} \equiv \mu_N^{(\prime)}$!

3.4 Extraction of form factors

We now want to finally extract the electromagnetic form factors as defined in Sec. 2.5.2 from the microscopic expression we obtained for the nucleon current in Eq. (3.58). Since we have worked with velocity states ($\vec{k}_N^{(\prime)} + \vec{k}_e^{(\prime)} = 0$) so far, our microscopic current (3.58) still does not transform like a 4-vector; it is rather Wigner rotated when undergoing a Lorentz boost [Bie11]. If, however, the current is reexpressed in terms of *physical* momenta ($p_N^{(\prime)} = B(V) k_N^{(\prime)}$) and corresponding spin projections $\sigma_N^{(\prime)}$, the resulting current

$$\begin{aligned} J_N^\mu(\vec{p}_N, \sigma_N, \vec{p}'_N, \sigma'_N) \\ = B(V)_\nu^\mu \sum_{\mu_N, \mu'_N} J_N^\nu(\vec{k}_N, \mu_N, \vec{k}'_N, \mu'_N) D_{\mu'_N \sigma'_N}^*(B^{-1}(V), \frac{\vec{p}'_N}{m_N}) D_{\mu_N \sigma_N}(B^{-1}(V), \frac{\vec{p}_N}{m_N}) \end{aligned} \quad (3.60)$$

does indeed transform like a 4-vector. We can thus perform a decomposition into linearly independent 4-vectors, which can be built with the help of the nucleon spinors, γ -matrices and the particle momenta that occur in our electron–nucleon scattering process. Since we will later on extract our form factors in the rest frame of the electron–nucleon system where $\vec{V} = 0$ (and consequently, $p_N^{(\prime)} = k_N^{(\prime)}$), we will write down the general covariant decomposition of the microscopic current (3.58) already for this case [Bie11, CDKM98]:

$$J_N^\lambda(\vec{k}_N, \mu_N, \vec{k}'_N, \mu'_N) = \bar{u}_{\mu'_N}(\vec{k}'_N) \Gamma^\lambda u_{\mu_N}(\vec{k}_N), \quad (3.61)$$

where

$$\begin{aligned} \Gamma^\mu &= F'_1 \gamma^\mu + \frac{iF'_2}{2m_N} \sigma^{\mu\nu} q_\nu + B'_1 \left(\frac{\omega_\rho \gamma^\rho}{\omega_\rho k_N^\rho} - \frac{\mathbb{I}}{(1+\eta)m_N} \right) (k_N + k'_N)^\mu \\ &+ B'_2 \frac{m_N}{\omega_\rho k_N^\rho} \omega^\mu + B'_3 \frac{(m_N)^2}{(\omega_\rho k_N^\rho)^2} (\omega_\rho \gamma^\rho) \omega^\mu, \end{aligned} \quad (3.62)$$

$$\sigma^{\mu\nu} = \frac{i}{2} [\gamma^\mu, \gamma^\nu], \quad \eta = \frac{Q^2}{4m_N^2} \quad \text{and} \quad (3.63)$$

$$\omega^\mu = k_e^\mu + k_e'^\mu. \quad (3.64)$$

The coefficients F'_1 and F'_2 are the physical form factors of the nucleon we are looking for. The covariants they are multiplied with depend only on the nucleon momenta, whereas $B'_1 \dots B'_3$, are coefficients of covariants that contain also the electron momenta. These are called the unphysical, or spurious, form factors.

Actually, with the 4 components of the current and the 4 possibilities for incoming and outgoing orientations of the nucleon spin, one would get altogether 16 spin matrix elements (and accordingly, 16 possible covariants). But due to parity and time-reversal symmetry combined (8 conditions) and rotation invariance (4 conditions which are guaranteed by our approach, 2 of which are independent), not all of these are independent. With current conservation as an eleventh independent condition, we end up with 5 independent covariants and thus Eqs. (3.61) and (3.62) for the most general covariant decomposition of the microscopic current (3.58).

Even though the current is conserved, it can not be precluded that the unphysical part vanishes. The reason for this is that the Bakamjian–Thomas construction, on which our approach is based on, leads to wrong cluster properties (i.e., the violation of macroscopic causality). One consequence of this is that the form factors in front of the covariants may, in addition to the dependence on the 4-momentum transfer $Q^2 = -(k_N - k'_N)^2$, also exhibit a dependence on the invariant mass squared (i.e., Mandelstam s) of the electron–nucleon system. This dependence is still in accordance with relativistic invariance of the one-photon-exchange amplitude, but corresponds to a non-locality of the photon–nucleon vertex. Our studies reveal indeed that the microscopic current (3.58) contains an unphysical contribution and also the form factors exhibit an unwanted s -dependence. But as experience with electromagnetic meson form factors has shown [Bie11, BSFK09, GRS12, BS14], this s -dependence vanishes rather fast with increasing s . It is thus tempting to take $s \rightarrow \infty$, which has the advantage that (most of) the unphysical contributions vanish and one obtains manageable analytical expressions for the form factors. The s -dependence of the form factors may be interpreted as a dependence of the frame in which the $\gamma^* N \rightarrow N$ subprocess is considered. The $s \rightarrow \infty$ limit would then correspond to the infinite-momentum frame of the nucleon. It has the further advantage that we can easily compare our results with corresponding front-form calculations. In the cases of the pion [BSFK09], the ρ meson [BS14] and of heavy–light mesons [GRS12], this comparison has revealed the equivalence of the point-form results with corresponding front-form calculations.

We will proceed in the same way here: We first fix the electron–nucleon scattering kinematics, then let $s \rightarrow \infty$ (or equivalently, $|\vec{k}_N^{(\prime)}| \rightarrow \infty$) and look what happens in this

limit with the covariant decomposition (3.61) and (3.62). We use the following kinematics:

$$\begin{aligned}
k_N &= \begin{pmatrix} \sqrt{k^2 + m_N^2} \\ -\frac{Q}{2} \\ 0 \\ \sqrt{k^2 - \frac{Q^2}{4}} \end{pmatrix} \xrightarrow{k \rightarrow \infty} \begin{pmatrix} k \\ -\frac{Q}{2} \\ 0 \\ k \end{pmatrix}, \\
k'_N &= k_N + q = \begin{pmatrix} \sqrt{k^2 + m_N^2} \\ \frac{Q}{2} \\ 0 \\ \sqrt{k^2 - \frac{Q^2}{4}} \end{pmatrix} \xrightarrow{k \rightarrow \infty} \begin{pmatrix} k \\ \frac{Q}{2} \\ 0 \\ k \end{pmatrix}, \quad \text{where} \\
q &= (k'_N - k_N) = (k_e - k'_e) = \begin{pmatrix} 0 \\ Q \\ 0 \\ 0 \end{pmatrix}
\end{aligned} \tag{3.65}$$

is the transfer of four-momentum. It is then easily seen that contributions from B'_2 and B'_3 in (3.62) are of order k^{-1} resp. k^{-2} so that they can be safely neglected when $k \rightarrow \infty$.

Via a simple calculation performed in Mathematica®, we now obtain from Eqs. (3.61) and (3.62) a system of 16 equations, one for each of the four spacetime components of J^μ and the 4 spin orientations $\mu_N, \mu'_N = \pm \frac{1}{2}$. From these equations we want to determine the three form factors F'_1, F'_2, B'_1 . Neglecting contributions of $o(k^0)$ and using the 13 constraints (from parity, time-reversal, rotation invariance and current conservation)

$$\begin{aligned}
J_{-\frac{1}{2}-\frac{1}{2}}^1 &= J_{\frac{1}{2}\frac{1}{2}}^1 = J_{-\frac{1}{2}\frac{1}{2}}^1 = J_{\frac{1}{2}-\frac{1}{2}}^1 = J_{-\frac{1}{2}\frac{1}{2}}^2 = J_{\frac{1}{2}-\frac{1}{2}}^2 = 0, \\
J_{-\frac{1}{2}-\frac{1}{2}}^0 &= J_{\frac{1}{2}\frac{1}{2}}^0 = J_{-\frac{1}{2}-\frac{1}{2}}^3 = J_{\frac{1}{2}\frac{1}{2}}^3, \\
J_{-\frac{1}{2}\frac{1}{2}}^0 &= -J_{\frac{1}{2}-\frac{1}{2}}^0 = J_{-\frac{1}{2}\frac{1}{2}}^3 = -J_{\frac{1}{2}-\frac{1}{2}}^3, \\
J_{-\frac{1}{2}-\frac{1}{2}}^2 &= -J_{\frac{1}{2}\frac{1}{2}}^2,
\end{aligned} \tag{3.66}$$

(where $J_{\mu\mu'}^\nu$ is shorthand for $J_N^\nu(\vec{k}_N, \mu_N, \vec{k}'_N, \mu'_N)$), the system reduces to the three equations

$$\begin{aligned}
\left(\frac{4B'_1 Q^2}{4m_N^2 + Q^2} + 2F'_1 \right) k &= J_{\frac{1}{2}\frac{1}{2}}^0, \\
\left(\frac{F'_2 Q}{m_N} + \frac{8B'_1 m_N Q}{4m_N^2 + Q^2} \right) k &= J_{\frac{1}{2}-\frac{1}{2}}^0, \\
i(F'_1 Q + F'_2 Q) &= J_{\frac{1}{2}\frac{1}{2}}^2.
\end{aligned} \tag{3.67}$$

As one can see (assuming real form factors independent of k), $J_{\frac{1}{2}\frac{1}{2}}^0$ and $J_{-\frac{1}{2}\frac{1}{2}}^0$ have to be real and of order k^1 , while $J_{\frac{1}{2}\frac{1}{2}}^2$ has to be purely imaginary and of order k^0 .

Solving for the form factors (again by use of Mathematica[®]), we obtain:

$$\begin{aligned} F'_1 &= \frac{2m_N^2}{k(4m_N^2 + Q^2)} J_{\frac{1}{2}\frac{1}{2}}^0 - \frac{m_N Q}{k(4m_N^2 + Q^2)} J_{\frac{1}{2}-\frac{1}{2}}^0 - \frac{iQ}{4m_N^2 + Q^2} J_{\frac{1}{2}\frac{1}{2}}^2, \\ F'_2 &= -\frac{2m_N^2}{k(4m_N^2 + Q^2)} J_{\frac{1}{2}\frac{1}{2}}^0 + \frac{m_N Q}{k(4m_N^2 + Q^2)} J_{\frac{1}{2}-\frac{1}{2}}^0 + \frac{iQ}{4m_N^2 + Q^2} J_{\frac{1}{2}\frac{1}{2}}^2 - \frac{i}{Q} J_{\frac{1}{2}\frac{1}{2}}^2, \\ B'_1 &= \frac{1}{4k} J_{\frac{1}{2}\frac{1}{2}}^0 + \frac{m_N}{2kQ} J_{\frac{1}{2}-\frac{1}{2}}^0 + \frac{i}{2Q} J_{\frac{1}{2}\frac{1}{2}}^2. \end{aligned} \quad (3.68)$$

If we, however, demand agreement of our microscopic current (3.58) with the covariant decomposition (3.61) and (3.62) only in leading order $O(k^1)$, only the first two equations of (3.67) remain and there is no way to separate B'_1 . We thus have to redefine our physical form factors:

$$\begin{aligned} F'_1 &\longrightarrow F_1 := F'_1 + \frac{2B'_1 Q^2}{4m_N^2 + Q^2}, \\ F'_2 &\longrightarrow F_2 := F'_2 + \frac{8B'_1 m_N^2}{4m_N^2 + Q^2}, \end{aligned} \quad (3.69)$$

so that

$$\begin{aligned} F_1 &= \frac{1}{2k} J_{\frac{1}{2}\frac{1}{2}}^0, \\ F_2 &= \frac{m_N}{kQ} J_{\frac{1}{2}-\frac{1}{2}}^0 \end{aligned} \quad (3.70)$$

which is the result we would have obtained with the covariant expansion (2.57) right away. This means that all the unphysical contributions in the microscopic current (3.58) vanish in leading order if the limit $k \rightarrow \infty$ is taken. The Sachs form factors are then obtained via Eq. (2.58).

3.5 Numerical implementation

The starting point of our numerical analysis is Eq. (3.58). It is integrated using the Monte Carlo Miser integration routine of the GNU Scientific Library (GSL) under C++. For matrix and vector calculations we use the Eigen library, which defines the classes `Vector4d`, `Vector2cd`, `Matrix4d`, `Matrix2cd` for 4-dimensional real and 2-dimensional complex vectors and matrices (component type `double`), respectively. Components are in round brackets () .

3.5.1 Class structure

Functions for Pauli and Dirac (2.7) matrices of index `i`, `Matrix2cd pauli (int i)` and `Matrix4cd dirac (int i)`, are defined as global functions.

Any quantities that depend on the momenta \tilde{k}_{q_i} of the quarks are calculated in a class called `Mompart`. It is initialized again and again for each point of the Monte Carlo integration with the 6 independent momentum components of the quarks, `double karray [6]` (spherical coordinates) and a pointer to some other parameters, `InputParams * params`,

where `InputParams` is a structure containing parameters like the forward momentum of the nucleon `double k`, the momentum transfer `double Q`, double spin and isospin projections `int muNpr`, `tauN`, the desired number of Monte Carlo integration points `size_t inpoints` etc.

The public functions of the `Mompart` class are: The 6 Wigner rotations `Matrix2cd wigrotfactor1 () ...Matrix2cd wigrotfactor3pr ()`, the momentum parts of the 3-quark wave functions (3.54), `double spacepart ()` and `double spacepartpr ()`, the electromagnetic current of quark 1, `Matrix2cd quark1current ()`, as well as any other kinematic quantities explicitly appearing in Eq. (3.58), `double prefactor ()`.

The private functions are the Lorentz boost with 4-velocity `u` and its inverse in standard (2.35), (2.36) and $SL(2, \mathbb{C})$ (2.40) representation, `Matrix4d [inv]boost (Vector4d u)` and `Matrix2cd [inv]spinboost (Vector4d u)`.

In what follows, the class initialization and the more important or less obvious functions are discussed in detail.

3.5.2 Kinematic quantities

The initialization for the local variables reads

```
Mompart::Mompart (double karray[6] , InputParams * params):
    k2 (karray[0]), theta2 (karray[1]), phi2 (karray[2]),
    k3 (karray[3]), theta3 (karray[4]), phi3 (karray[5]),
    k (params->k), Q (params->Q)
```

We then (in curly brackets) start out by initializing the 4-momenta of the quarks in the “tilde” frame in spherical coordinates. Since $\sum \tilde{k}_{q_i} = 0$ and all particles are on their mass shells, we have

```
Vector4d ktild [4]; // in class declaration
ktild [2] << sqrt(pow(k2,2) + pow(m,2)),
    k2*sin(theta2)*cos(phi2),
    k2*sin(theta2)*sin(phi2),
    k2*cos(theta2);
// (analogously for ktild[3])

Vector3d k1tilde3d = -ktild[2].segment<3>(1)-ktild[3].segment<3>(1);
ktild[1](0) = sqrt(pow(m,2)+k1tilde3d.dot(k1tilde3d));
ktild[1].segment<3>(1) = k1tilde3d;
```

where `m` is the quark mass (globally defined) and `k2`, `phi2`, `theta2` the three integration variables for quark 2. We then introduce the invariant mass of the three quarks and the velocity according to Eq. (3.36) using the kinematics (3.65),

```
double mcl = ktild[e][1](0)+ktild[e][2](0)+ktild[e][3](0);

Vector4d vcl; // in class declaration
vcl << k/mcl , -Q/(2*mcl) , 0 , k/mcl;
```

where k is the modulus of the nucleon three-momentum that serves as an input parameter. The quark momenta in the electron–3-quark rest frame are obtained via a canonical boost as defined in (2.35) with velocity vcl :

```
Vector4d knaked [4]; // in class declaration
for (i=1; i<=3; i++){ knaked [i] = boost(vcl)*ktild[e][i]; }
```

where $boost(vcl)$ is the 4x4 boost matrix of boost velocity vcl , defined exactly as in Eq. (2.35).

In the boosted frame, the 3-momentum transfer to quark 1 is the same as to the nucleon in (3.65), while via the spectator conditions (3.31), quarks 2 and 3 remain unaffected:

```
Vector4d knakedpr [4]; // in class declaration

for (i=1; i<=3; i++){ knakedpr[i] = knaked[i]; }

knakedpr[1](1) = knaked[1](1) + Q;

knakedpr[1](0) =
sqrt(pow(m,2) + pow(knakedpr[1](1),2) + pow(knakedpr[1](2),2) + ... );
```

We then get the invariant mass and the velocity (3.36) for the outgoing (primed) 3-quark system via

```
double mclpr =
sqrt(pow((knakedpr[1]+knakedpr[2]+knakedpr[3])(0),2) - pow(k,2));

Vector4d vclpr; // in class declaration
vclpr << k/mclpr , Q/(2*mclpr) , 0 , k/mclpr;
```

Finally, the primed quark momenta in the rest frame of the 3-quark system are obtained via an inverse boost (2.36) with the primed 3-quark velocity:

```
for (i=1; i<=3; i++){ ktild[e][i] = invboost(vclpr)*knakedpr[i]; }
```

This completes the initialization of the class `Mompart`.

3.5.3 Spin algebraics

The Clebsch-Gordan coefficients in (3.58) are generated via the relations [NIST]

$$\begin{aligned}
 C_{j_1 m_1 j_2 m_2}^{j-m} &= (-1)^{j_1-j_2-m} \sqrt{2j+1} \begin{pmatrix} j_1 & j_2 & j \\ m_1 & m_2 & m \end{pmatrix} , \\
 \begin{pmatrix} j_1 & j_2 & j \\ m_1 & m_2 & m \end{pmatrix} &= (-1)^{j_1-j_2-m} \Delta(j_1 j_2 j) \\
 &\times \sum_s \frac{(-1)^s \sqrt{(j_1+m_1)!(j_1-m_1)!(j_2+m_2)!(j_2-m_2)!(j+m)!(j-m)!}}{s!(j_1+j_2-j-s)!(j_1-m_1-s)!(j_2+m_2-s)!(j-j_2+m_1+s)!(j-j_1-m_2+s)!} , \\
 \Delta(j_1 j_2 j) &= \left(\frac{(j_1+j_2-j)!(j_1-j_2+j)!(-j_1+j_2+j)!}{(j_1+j_2+j+1)!} \right)^{\frac{1}{2}} , \\
 z! &:= \Gamma(z+1), \quad \Gamma\left(\frac{1}{2}\right) = \sqrt{\pi}, \quad \Gamma(z+1) = z \Gamma(z) ,
 \end{aligned} \tag{3.71}$$

and are implemented as a 6-dimensional array of `doubles`. For simplicity, we have doubled all spin variables `mu1`, `mu1tilde`, `mu1pr`, `mu2tildepr`, ... that serve as function arguments, so they become integers. They are defined in a separate class `Clebschgordan` in a separate file.

The Wigner-D-functions are realized within the `Mompart` class as a sequence of boosts (2.37) in their spin representation (2.40), i.e.

```

Matrix2cd Mompart::wigrotfactor1 () { return
invspinbst(knaked[1]/m)*spinbst(vcl)*spinbst(ktilde[1]/m); }

Matrix2cd Mompart::wigrotfactor1pr () { return
invspinbst(ktildepr[1]/m)*invspinbst(vclpr)*spinbst(knakedpr[1]/m); }
// etc.

```

where we have used relations (2.43). With the call `Mompart mp`; the components of the Wigner-D-functions are then `mp.wigrotfactor1 () ((1-mu1)/2, (1-mu1tilde)/2)`, `mp.wigrotfactor1pr () ((1-mu1tildepr)/2, (1-mu1pr)/2)` etc.

3.5.4 Quark current

Similarly, the current of quark 1, `Matrix2cd Mompart::quark1current ()`, is realized as a complex 2×2 matrix within `Mompart` as well. The index number of the Lorentz component, `nu`, is an input parameter (only 0 is needed). Its construction is a little bit more complicated: First, the complex 4×4 “middle matrix” is built from Dirac matrices via the definitions of the current (3.32) and the basis spinors (2.9). Here the multiplication

with the rest-frame basis spinors, $(1, 0, 0, 0)^\top$ (which we call `u0plus`) and $(0, 1, 0, 0)^\top$ (`u0minus`), is not yet performed:

```
Matrix4cd middlematrix =
(dirac(0)*(knakedpr[1])(0) - dirac(1)*(knakedpr[1])(1) -
 dirac(2)*(knakedpr[1])(2) - dirac(3)*(knakedpr[1])(3) +
 Matrix4cd::Identity()*m).adjoint() / sqrt(m+(knakedpr[1])(0))
 * dirac(0) * dirac(nu) *
(dirac(0)*(knaked[1])(0) - dirac(1)*(knaked[1])(1) -
 dirac(2)*(knaked[1])(2) - dirac(3)*(knaked[1])(3) +
 Matrix4cd::Identity()*m) / sqrt(m+(knaked[1])(0));
```

Only then, a complex 2×2 matrix `q1c` in the spin polarizations of quark 1, i.e. with the components `q1c((1-mu1pr)/2, (1-mu1)/2)` is constructed by sandwiching it between the rest-frame basis spinors:

```
Matrix2cd q1c;
q1c << (u0plus.dot(middlematrix*u0plus) ,
           (u0plus.dot(middlematrix*u0minus) ,
           (u0minus.dot(middlematrix*u0plus) ,
           (u0minus.dot(middlematrix*u0minus);
return q1c;
```

3.5.5 Integrand function

The integrand is defined in a function `complex<double> integrand (double karray [6], InputParams * params)`. The first part is a prefactor (`double prefactor`) made up of the Jacobian of the spherical integration and the prefactor from the `Mompart` class. The second part is a factor that is made up of all the Clebsch-Gordan coefficients (initialized by external call `Clebschgordan cg`):

```
double cgfactor =
1/sqrt(2)*
cg.coeff(1,mu2tildepr,1,mu3tildepr,spr,muspr) *
cg.coeff(spr,muspr,1,mu1tildepr,Spr,params->muNpr) *
cg.coeff(1,tau2,1,tau3,spr,taus) *
cg.coeff(spr,taus,1,tau1,1,params->tauN) *
1/sqrt(2)*
cg.coeff(1,mu2tilde,1,mu3tilde,s,mus) *
cg.coeff(s,mus,1,mu1tilde,S,muN) *
cg.coeff(1,tau2,1,tau3,s,taus) *
cg.coeff(s,taus,1,tau1,1,params->tauN);
```

The full integrand finally reads

```
intgr +=  
prefactor *  
(tau1===-1 ? -0.33333 : tau1==1 ? 0.6666667 : 0) *  
cgfactor *  
wigrotnfactor1pr ((1-mu1tildepr)/2,(1-mu1pr)/2) *  
wigrotnfactor1 ((1-mu1)/2,(1-mu1tilde)/2) *  
wigrotnfactor2pr ((1-mu2tildepr)/2,(1-mu2)/2) *  
wigrotnfactor2 ((1-mu2)/2,(1-mu2tilde)/2) *  
wigrotnfactor3pr ((1-mu3tildepr)/2,(1-mu3)/2) *  
wigrotnfactor3 ((1-mu3)/2,(1-mu3tilde)/2) *  
spacepartpr *  
spacepart *  
quark1current ((1-mu1pr)/2,(1-mu1)/2);
```

where there is a sum (implemented by a lot of `for` loops, hence the `+=` in the first line) over spins and isospins `int mu1, mu1pr, mu2, mu3, mu2tilde, mu3tilde, mu2tildepr, mu3tildepr, tau2, tau3` ($= \pm 1$), `int s, spr` ($= 0, 2$) and `int mus, muspr, taus` ($= -s[pr] \dots s[pr]$). The dependent variables `int mu1tilde, mu1tildepr, tau1` are set accordingly (see Sec. 3.3.3) including a check whether they are in the range ± 1 .

The `Mompart` class is initialized by `Mompart mp`, and then we set `Matrix2cd wigrotnfactor1 = mp.wigrotnfactor1` etc. *before* the summation, so the initialization does not occur for every single summand, which would be very time-consuming. Note that the electric charge of quark 1 enters in the third line. After running all the `for` loops, the result of `complex<double> intgr` is returned. Note that since the form factors are real, only the real part of the integrand is needed via Eq. (3.70).

3.5.6 Integration

The function that is finally passed to the GSL Monte Carlo routine is constructed via

```
double intfunction (double karray[], size_t dim, void * p){  
    InputParams * fp = (InputParams *)p;  
    return real(integrand(karray, fp));    }
```

Integration is performed in the function

```

double integration (InputParams intpar) {

    double result, error; // variables where result is saved
    double kmin[] = {0,0,0,0,0,0}; // integration limits
    double kmax[] = {4.0,3.1416,6.2832,4,3.1416,6.2832};

    // This assigns the function for 6-dim. MC integration:
    gsl_monte_function INT = {&intfunction, 6, &intpar};

    const gsl_rng_type *T; // set up random number generator
    gsl_rng *r; T = gsl_rng_default; r = gsl_rng_alloc (T);

    // Now we allocate space for and perform the integration:
    gsl_monte_miser_state *s = gsl_monte_miser_alloc (6) ;
    gsl_monte_miser_integrate
    (&INT, kmin, kmax, 6, intpar.intpoints, r, s, &result, &error);

    return result; }

```

The integration was performed in parallel threads for various parameters using Pthreads, but this shall not be treated in detail here. A simple main function writing the results for various values of the momentum transfer Q and both outgoing nucleon spin polarizations μ_{Np} to an ASCII output file (CSV table) `out.csv` could look like this:

```

int main(){
    InputParams inpar;
    inpar.k = 1000000; // forward momentum of nucleon
    inpar.intpoints = 10000; // number of MC integration points
    inpar.tauN = 1 // for proton, -1 for neutron

    ofstream outfile; outfile.open("out.csv");
    outfile << "Q^2;;samespin;spinflip" << endl << endl;

    for (inpar.Q=0.0001; inpar.Q<2.0002; inpar.Q+=0.1){
        outfile << pow(inpar.Q,2) << ";" ;
        for (inpar.muNpr=1; inpar.muNpr>=-1; inpar.muNpr-=2){
            outfile << integration(inpar) << ";" ;
        }
        outfile << endl; }
    outfile.close(); return (0); }

```

The result yields the nucleon current (3.58); the form factors are then obtained via Eq. (3.70) using a tool of choice.

3.6 Results

For later purposes, we parametrize our numerical results in an appropriate way: The results we obtain for the electric and magnetic Sachs form factors of the proton and the magnetic Sachs form factor of the neutron are well described by a parametrization also used by Kelly [Kel04] to fit the available experimental data: With $\tau := \frac{Q^2}{4m_N^2}$, where $Q^2 = -q^2$ is the negative four-momentum transfer squared, a reasonably good parametrization of the electric proton and the magnetic proton and neutron Sachs form factors is achieved with

$$G_{E/M}^{p/n}(Q^2) = [\mu_N \cdot] \frac{1 + a_1 \tau}{1 + b_1 \tau + b_2 \tau^2 + b_3 \tau^3}. \quad (3.72)$$

μ_N is the magnetic moment of the respective nucleon. Our results are well approximated with the parameters given in Tab. 3.2. For comparison, the experimental values for the magnetic moments are $\mu_p = 2.79$ and $\mu_n = -1.91$ [PDG].

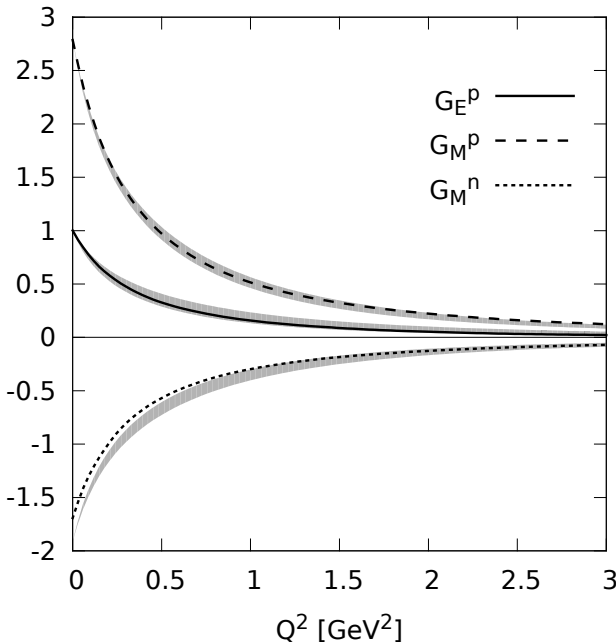


Figure 3.4: Electromagnetic Sachs form factors as functions of $Q^2 = -q^2$: G_E^p : electric form factor of the proton, G_M^p : magnetic form factor of the proton, G_M^n : magnetic form factor for neutron. Shaded areas: fit of experimental data (including errors) by Puckett et al. [Puc10] (proton) and Kelly [Kel04] (neutron).

	G_E^p	G_M^p	G_M^n
a_1	-0.60	-0.215	-0.31
b_1	10.3	10.6	11.0
b_2	15.6	14.1	15.1
b_3	3.24	-3.03	-5.51
μ_N		2.79	-1.69

Table 3.2: Parametrization of our form factor results according to Eq. (3.72).

For the electric neutron form factor a modified Galster fit [GKM⁺71] is used:

$$G_E^n(Q^2) = \frac{A\tau + B\tau^2}{1 + C\tau + D\tau^2} \cdot G_D(Q^2) \quad (3.73)$$

with the dipole form factor [DCC⁺66]

$$G_D(Q^2) = \frac{1}{\left(1 + \frac{Q^2}{0.71}\right)^2}. \quad (3.74)$$

Our numerical data are well represented with the fit parameters $A = 0.39$, $B = 1.54$, $C = 1.7$ and $D = 0.42$.

In Fig. 3.4, our results for the electric and the magnetic proton and magnetic neutron form factors are shown in comparison with parametrizations of a comprehensive set of experimental data by Puckett et al. [Puc10] (including recent JLab data) for the proton and Kelly [Kel04] for the neutron (shaded areas). Fig. 3.5 shows the electric neutron form factor as compared with the Kelly parametrization.

In Figs. 3.6, 3.7 and 3.8 we show the same comparison, however in these graphs, the form factors are divided by the dipole form factor G_D so that deviations and experimental errors become better visible. Also note the logarithmic scale on the abscissa. The results for both proton form factors are in reasonable agreement with the parametrization of the experimental data. Also, the neutron magnetic form factor is well reproduced with the absolute size of the neutron magnetic moment being a little bit too small. Only the reproduction of the neutron electric form factor seems to be less satisfactory. But here one has to keep in mind that it is a rather small quantity and that we have restricted our three-quark wave function to an s-wave, thus limiting our possibilities to treat such subtleties. Since we use the wave-function parameters of Schlumpf [Schl94], it is not surprising that our results strongly resemble those of Ref. [Schl94]. It is just a further indication for the equivalence of our point-form approach with corresponding front-form calculations in the $q^+ = 0$ frame, which has already been asserted in Ref. [BSFK09] and shown analytically for the electric pion form factor.

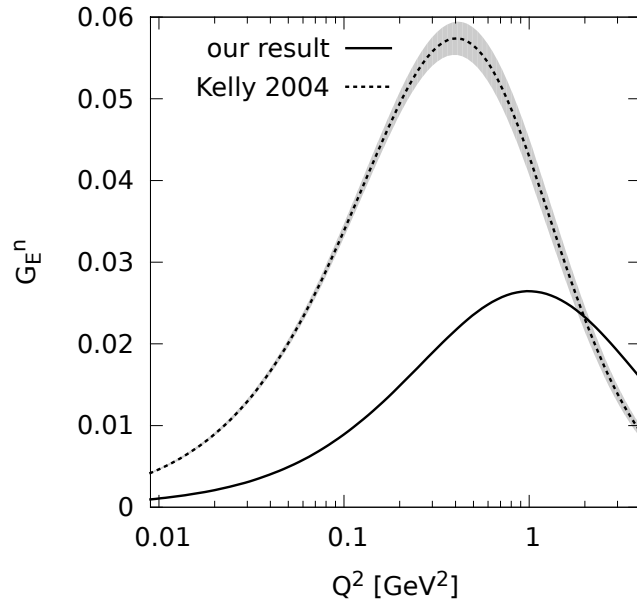


Figure 3.5: Electric neutron form factor G_E^n as function of $Q^2 = -q^2$.
 Shaded area: Fit of experimental data (including errors) by Kelly [Kel04].

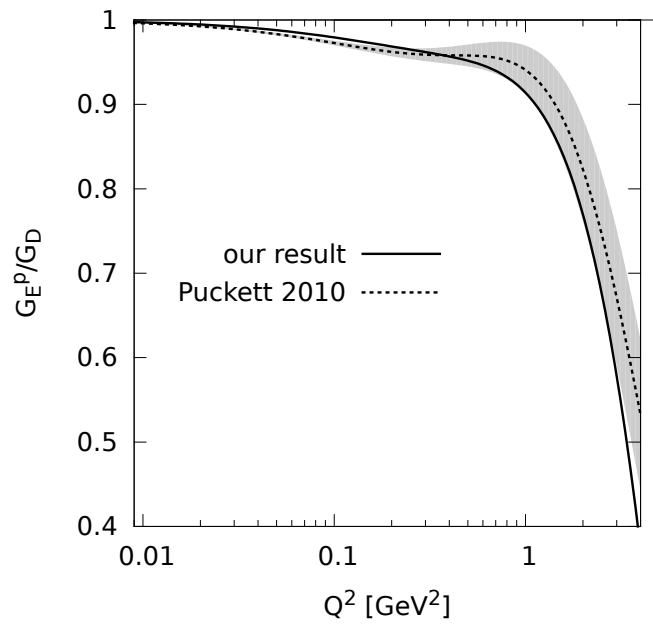


Figure 3.6: Electric proton form factor G_E^p/G_D as function of $Q^2 = -q^2$.
 Shaded area: Fit of experimental data (including errors) by Puckett et al. [Puc10].

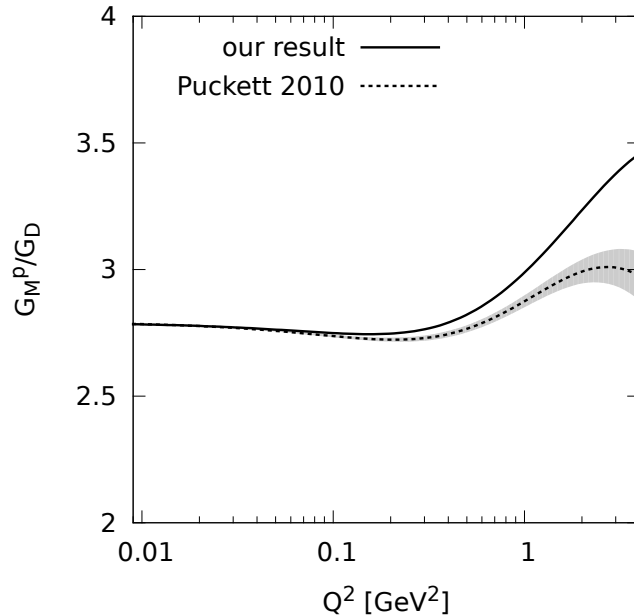


Figure 3.7: Magnetic proton form factor G_M^p/G_D as function of $Q^2 = -q^2$.
Shaded area: Fit of experimental data (including errors) by Puckett et al. [Puc10].

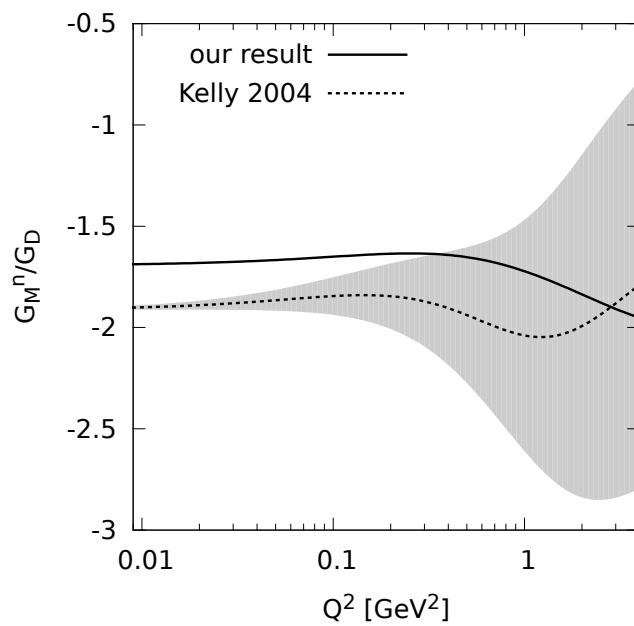


Figure 3.8: Magnetic neutron form factor G_M^n/G_D as function of $Q^2 = -q^2$.
Shaded area: Fit of experimental data (including errors) by Kelly [Kel04].

Chapter 4

Strong Form Factor

In this chapter we investigate the structure of the pion–nucleon vertex. The quantities we will obtain are the pion–nucleon coupling strength and the strong form factor, which encodes the nucleon structure as probed by the pion. To a large part, the derivation runs along the same lines as the one for the electromagnetic nucleon form factors in Chap. 3. Again, the nucleon is taken to be a confined 3-quark state. We start out by deriving the optical potential for pion emission and reabsorption by the nucleon on the hadronic level.

4.1 Hadronic level

4.1.1 Basic setup

We investigate a nucleon (N) that emits a pion (π) and absorbs it again. At the vertex, due to the nature of the strong interaction, total isospin is conserved, while due to the pseudoscalar nature of the pion, the spin of the emitting particle has to flip. In the intermediate state (N'') we restrict our investigation to nucleons, although a Δ baryon (spin and isospin $\frac{3}{2}$) or mass excitations of the nucleon could be created as well (but less likely).

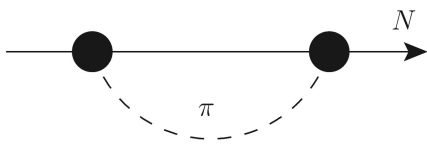


Figure 4.1: Self-energy contribution to the nucleon mass due to a pion loop. A pion is emitted and then absorbed again by the nucleon. A possible vertex form factor, accounting for a non-point-like vertex, is symbolized by the blob.

4.1.2 Eigenvalue equation and Feshbach reduction

We again use the coupled-channels approach (cf. Sec. 2.4.6). The Hilbert space for the problem at hand comprises two channels, one containing the nucleon (N) only, the other one containing, in addition, the pion (π). As mentioned before, transition of the nucleon to a Δ baryon is neglected.

We also use velocity states (cf. Sec. 2.4.5), $|VN\rangle$ and $|VN\pi\rangle$. Allowing for a pionic contribution to the nucleon, a physical nucleon state $|VN\rangle$ is now composed of a “bare” nucleon component $|V\tilde{N}\rangle$ and a “bare” nucleon + pion component $|\widetilde{VN\pi}\rangle$. In our multi-channel formulation, we write it in the form

$$|VN\rangle = \begin{pmatrix} |V\tilde{N}\rangle \\ |\widetilde{VN\pi}\rangle \end{pmatrix}. \quad (4.1)$$

The mass-eigenvalue equation for a physical nucleon is then:

$$\begin{pmatrix} M_{N_0} & K_\pi \\ K_\pi^\dagger & M_{N_0\pi} \end{pmatrix} \begin{pmatrix} |V\tilde{N}\rangle \\ |\widetilde{VN\pi}\rangle \end{pmatrix} = m \begin{pmatrix} |V\tilde{N}\rangle \\ |\widetilde{VN\pi}\rangle \end{pmatrix}. \quad (4.2)$$

The diagonal elements of the matrix mass operator, M_{N_0} and $M_{N_0\pi}$, are the free mass operators of the respective channels with eigenvalues m_{N_0} and $m_{N_0\pi} = \omega_{N_0} + \omega_\pi$ ($\omega_i = \sqrt{\vec{k}_i^2 + m_i^2}$), where m_{N_0} is the mass of the “bare” nucleon. The off-diagonal elements, K_π^\dagger and K_π , are the $(\pi N_0 N_0)$ -vertex operators. The (lowest) mass eigenvalue of Eq. (4.2) is the mass of the physical nucleon, $m = m_N$.

After a Feshbach reduction (cf. Sec. 3.1.2), Eq. (4.2) becomes

$$P_{N_0}^{-1}|V\tilde{N}\rangle := (m - M_{N_0})|V\tilde{N}\rangle = K_\pi P_{N_0\pi} K_\pi^\dagger |V\tilde{N}\rangle =: V_{\text{opt}}|V\tilde{N}\rangle \quad (4.3)$$

with the propagator $P_{N_0\pi} := (m - M_{N_0\pi})^{-1}$.

In App. A we show in some detail how the eigenvalue problem (4.2) is solved. In what follows, however, we are rather interested in the $(\pi N_0 N_0)$ -vertex of the *free* pion–nucleon system.

4.1.3 Insertion of completeness relations

As in Sec. 3.1.4 we now want to calculate velocity-state matrix elements of the optical potential. To this end, we insert the completeness relations for free nucleon–pion states in front of the propagator to obtain its eigenvalue and the vertex matrix elements:

$$\langle V'N'_0|V_{\text{opt}}|VN_0\rangle = \langle V'N'_0|K_\pi (m - M_{N_0\pi})^{-1} \mathbb{I}_{N_0\pi} K_\pi^\dagger|VN_0\rangle. \quad (4.4)$$

We again take the velocity-state completeness relations from Sec. 2.4.5 and use the short-hand notation (2.52) right away:

$$\mathbb{I}_{N_0\pi} = \sum D V D k_{N_0} \frac{m_{N_0\pi}^3}{2\omega_\pi} |VN_0\pi\rangle\langle VN_0\pi|, \quad (4.5)$$

where we have rendered the pion momentum redundant (whence a sum over pion isospins is implied).

4.1.4 The vertex operators

Upon insertion of expression (4.5) into equation (4.4) we obtain velocity-state matrix elements of the vertex operators. Since, due to the Bakamjian–Thomas construction in Sec. 2.4.3, the overall four-velocity V is conserved at the vertices, they read

$$\langle V' N_0' \pi' | K_\pi^\dagger | V N_0 \rangle = \langle V N_0 | K_\pi | V' N_0' \pi' \rangle^* = \Delta_{VV'} \frac{1}{\sqrt{m_{N_0 \pi}^3 m_{N_0}^3}} \langle N_0' \pi' | | K_\pi^\dagger | | N_0 \rangle. \quad (4.6)$$

The reduced vertex matrix element in Eq. (4.6) agrees with the pseudoscalar current of the nucleon:

$$\langle N_0' \pi' | | K_\pi^\dagger | | N_0 \rangle = -i g_{N_0} J_{N_0}^5(\vec{k}_{N_0}, \mu_{N_0}; \vec{k}'_{N_0}, \mu'_{N_0}) \cdot \mathcal{F}(\tau_{N_0}, \tau'_{N_0}, \tau'_\pi) \quad (4.7)$$

for the pseudoscalar coupling and with

$$\langle N_0' \pi' | | K_\pi^\dagger | | N_0 \rangle = +i \frac{f_{N_0}}{m_\pi} J_{N_0}^{5\nu}(\vec{k}_{N_0}, \mu_{N_0}; \vec{k}'_{N_0}, \mu'_{N_0}) k_{\pi\nu} \cdot \mathcal{F}(\tau_{N_0}, \tau'_{N_0}, \tau'_\pi) \quad (4.8)$$

for the pseudovector coupling, where \mathcal{F} is the flavor function as treated in Sec. 2.5.3.

4.1.5 Analytic calculation of the optical potential

With the above ingredients, the matrix elements of the optical potential, Eq. (4.4), become

$$\begin{aligned} & \langle V' N_0' | V_{\text{opt}} | V N_0 \rangle \\ &= \sum_{\pi''} D V'' D k''_{N_0} \frac{(m''_{N_0 \pi})^3}{2 \omega''_\pi} \langle V' N_0' | K_\pi | V'' N_0'' \pi'' \rangle (m_N - m''_{N_0 \pi})^{-1} \langle V'' N_0'' \pi'' | K_\pi^\dagger | V N_0 \rangle. \end{aligned} \quad (4.9)$$

Upon insertion of expression (4.6) for the vertices, we obtain

$$\begin{aligned} & \langle V' N_0' | V_{\text{opt}} | V N_0 \rangle \\ &= \sum_{\pi''} D V'' D k''_{N_0} \frac{(m''_{N_0 \pi})^3}{2 \omega''_\pi} \Delta_{V' V''} \frac{1}{\sqrt{m''_{N_0 \pi}^3 m'_{N_0}^3}} \langle N_0'' \pi'' | | K_\pi^\dagger | | N_0' \rangle^* \\ & \quad \times (m_N - m''_{N_0 \pi})^{-1} \Delta_{V V''} \frac{1}{\sqrt{m''_{N_0 \pi}^3 m_{N_0}^3}} \langle N_0'' \pi'' | | K_\pi^\dagger | | N_0 \rangle, \end{aligned} \quad (4.10)$$

and after elimination of the Delta functions we get the final result

$$\begin{aligned} & \langle V' N_0' | V_{\text{opt}} | V N_0 \rangle \\ &= \frac{\Delta_{VV'}}{m_{N_0}^3} \sum_{\pi''} \frac{D k''_{N_0}}{2 \omega''_\pi} \langle N_0'' \pi'' | | K_\pi^\dagger | | N_0' \rangle^* (m_N - m''_{N_0 \pi})^{-1} \langle N_0'' \pi'' | | K_\pi^\dagger | | N_0 \rangle \end{aligned} \quad (4.11)$$

where we have used $m_{N_0} = m'_{N_0}$ and $m \rightarrow m_N$ and the vertex matrix elements are determined by Eq. (4.7) or Eq. (4.8).

4.2 Constituent level

We now proceed analogously to Sec. 3.2 when calculating (hadronic) matrix elements of the optical potential on the constituent level. By equating the result to (4.11) we will then obtain a microscopic expression for the nucleon pseudoscalar (or pseudovector) current from which we will derive a microscopic expression for the strong form factor.

4.2.1 Basic setup

We model the nucleon the same way as we did in Chap. 3, i.e. we use a constituent quark model with u and d quarks of masses of approx. 0.26 GeV each. Confinement is enforced by an instantaneous interaction. Analogously to Sec. 4.1, a pion is now emitted by one quark and then absorbed by the same quark or another. In the rest frame of the incoming or outgoing nucleon (velocity states), the three-momentum that is transferred by the pion is the same on the nucleon level and on the quark level. Again we restrict ourselves to a nucleon (quark content uud or udd) in the intermediate state, even though propagation of a Δ baryon (quark content uuu , uud , udd or ddd for Δ^{++} , Δ^+ , Δ^0 and Δ^- respectively) or other nucleonic (mass) excitations are also thinkable (but less likely).

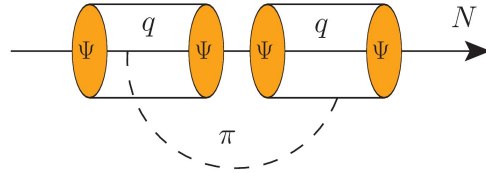


Figure 4.2: (One of nine) quark level diagram(s) for the calculation of the strong form factor of the “bare” nucleon. A pion is emitted by one of the three quarks, then a confined baryon state propagates, then the pion is absorbed again by a quark. The relation between the nucleon state and the three-quark state is described by the wave function Ψ .

4.2.2 Eigenvalue equation and Feshbach reduction

On quark level the coupled-channels eigenvalue equation reads

$$\begin{pmatrix} M_{3q}^{\text{conf}} & K_\pi \\ K_\pi^\dagger & M_{3q\pi}^{\text{conf}} \end{pmatrix} \begin{pmatrix} |\psi_{3q}\rangle \\ |\psi_{3q\pi}\rangle \end{pmatrix} = m \begin{pmatrix} |\psi_{3q}\rangle \\ |\psi_{3q\pi}\rangle \end{pmatrix}, \quad (4.12)$$

where the diagonal elements M_{3q}^{conf} and $M_{3q\pi}^{\text{conf}}$ include, beyond the relativistic energies of the three quarks and possibly the pion, also an instantaneous confinement potential

$$M_{3q(\pi)}^{\text{conf}} = M_{3q(\pi)} + V^{\text{conf}}. \quad (4.13)$$

Later on, we will need a complete set of velocity eigenstates of these mass operators. For $M_{3q(\pi)}$, these are just velocity states of free particles fulfilling the eigenvalue equation

$$M_{3q(\pi)}|V3q(\pi)\rangle = m_{3q(\pi)}|V3q(\pi)\rangle = \left(\sum_{i=1}^3 \omega_{q_i}(+\omega_\pi) \right) |V3q(\pi)\rangle. \quad (4.14)$$

For $M_{3q(\pi)}^{\text{conf}}$ one rather has states consisting of a (bare) baryon B_0 and possibly the pion:

$$M_{3q(\pi)}^{\text{conf}}|VB_0(\pi)\rangle = m_{B_0(\pi)}|VB_0(\pi)\rangle = (\omega_{B_0}(+\omega_\pi)) |VB_0(\pi)\rangle, \quad (4.15)$$

where $|B_0\rangle$ is an eigenstate of the pure confinement problem.

Reducing the problem to the 3-quark channel via a Feshbach reduction, we get

$$P_{3q}^{\text{conf}-1}|\psi_{3q}\rangle := (m_N - M_{3q}^{\text{conf}}) |\psi_{3q}\rangle = K_\pi P_{3q\pi}^{\text{conf}} K_\pi^\dagger |\psi_{3q}\rangle =: V_{\text{opt}} |\psi_{3q}\rangle, \quad (4.16)$$

where the optical potential V_{opt} now contains all the possibilities to exchange one pion between the quarks, even reabsorption by the same quark. Since we are mainly interested in the nucleon, we have already replaced the mass-eigenvalue m by the (physical) nucleon mass m_N . Here it should be emphasized that, due to the instantaneous confinement, the latter process does not renormalize the quark mass (since quarks do not propagate freely in our model). It is rather a contribution to the baryon-mass renormalization!

4.2.3 Vertex operators and completeness relations

We again need to calculate hadronic velocity-state matrix elements and use the hadronic propagator while keeping the quark-level vertex operators, as detailed in Sec. 3.2.3. Inserting the appropriate completeness relations and splitting the pion creation- and annihilation operators into sums of quark-pion vertex operators as

$$K_\pi^{(\dagger)}|V3q(\pi)\rangle = (K_{q_1\pi}^{(\dagger)} + K_{q_2\pi}^{(\dagger)} + K_{q_3\pi}^{(\dagger)})|V3q(\pi)\rangle, \quad (4.17)$$

the velocity-state matrix element of the optical potential between bare nucleons then corresponds to the following expression for 9 pion-loop diagrams:

$$\begin{aligned}
\langle V' N'_0 | V_{\text{opt}} | V N_0 \rangle &= \langle V' N'_0 | \underbrace{\mathbb{I}_{3q} K_{q_1 \pi} \mathbb{I}_{3q\pi} P_{N_0 \pi} \mathbb{I}_{N_0 \pi} \mathbb{I}_{3q\pi} K_{q_1 \pi}^\dagger \mathbb{I}_{3q}}_{V_{01}} | V N_0 \rangle \\
&+ \langle V' N'_0 | \mathbb{I}_{3q} K_{q_2 \pi} \mathbb{I}_{3q\pi} P_{N_0 \pi} \mathbb{I}_{N_0 \pi} \mathbb{I}_{3q\pi} K_{q_1 \pi}^\dagger \mathbb{I}_{3q} | V N_0 \rangle \\
&+ \langle V' N'_0 | \mathbb{I}_{3q} K_{q_3 \pi} \mathbb{I}_{3q\pi} P_{N_0 \pi} \mathbb{I}_{N_0 \pi} \mathbb{I}_{3q\pi} K_{q_1 \pi}^\dagger \mathbb{I}_{3q} | V N_0 \rangle \\
&+ \langle V' N'_0 | \mathbb{I}_{3q} K_{q_1 \pi} \mathbb{I}_{3q\pi} P_{N_0 \pi} \mathbb{I}_{N_0 \pi} \mathbb{I}_{3q\pi} K_{q_2 \pi}^\dagger \mathbb{I}_{3q} | V N_0 \rangle \\
&+ \langle V' N'_0 | \mathbb{I}_{3q} K_{q_2 \pi} \mathbb{I}_{3q\pi} P_{N_0 \pi} \mathbb{I}_{N_0 \pi} \mathbb{I}_{3q\pi} K_{q_2 \pi}^\dagger \mathbb{I}_{3q} | V N_0 \rangle \\
&+ \langle V' N'_0 | \mathbb{I}_{3q} K_{q_3 \pi} \mathbb{I}_{3q\pi} P_{N_0 \pi} \mathbb{I}_{N_0 \pi} \mathbb{I}_{3q\pi} K_{q_2 \pi}^\dagger \mathbb{I}_{3q} | V N_0 \rangle \\
&+ \langle V' N'_0 | \mathbb{I}_{3q} K_{q_1 \pi} \mathbb{I}_{3q\pi} P_{N_0 \pi} \mathbb{I}_{N_0 \pi} \mathbb{I}_{3q\pi} K_{q_3 \pi}^\dagger \mathbb{I}_{3q} | V N_0 \rangle \\
&+ \langle V' N'_0 | \mathbb{I}_{3q} K_{q_2 \pi} \mathbb{I}_{3q\pi} P_{N_0 \pi} \mathbb{I}_{N_0 \pi} \mathbb{I}_{3q\pi} K_{q_3 \pi}^\dagger \mathbb{I}_{3q} | V N_0 \rangle \\
&+ \langle V' N'_0 | \mathbb{I}_{3q} K_{q_3 \pi} \mathbb{I}_{3q\pi} P_{N_0 \pi} \mathbb{I}_{N_0 \pi} \mathbb{I}_{3q\pi} K_{q_3 \pi}^\dagger \mathbb{I}_{3q} | V N_0 \rangle \\
&= \sum_{i,j=1}^3 \langle V' N'_0 | \mathbb{I}_{3q} K_{q_i \pi} \mathbb{I}_{3q\pi} P_{N_0 \pi} \mathbb{I}_{N_0 \pi} \mathbb{I}_{3q\pi} K_{q_j \pi}^\dagger \mathbb{I}_{3q} | V N_0 \rangle. \tag{4.18}
\end{aligned}$$

Note that the propagator is a purely hadronic propagator. Due to instantaneous confinement, only hadrons are allowed to propagate in intermediate states.

The completeness relations again follow from Eq. (2.52) and read

$$\begin{aligned}
\mathbb{I}_{N_0 \pi} &= \sum_{\tau_\pi} \sum_{\mu_{q_1}} \int DV Dk_{N_0} \frac{m_{N_0 \pi}^3}{2 \omega_\pi} |V N_0 \pi\rangle \langle V N_0 \pi|, \\
\mathbb{I}_{3q} &= \sum_{\mu_{q_1}, \tau_{q_1}} \sum_{\mu_{q_2}} \int DV Dk_{q_2} Dk_{q_3} \frac{m_{3q}^3}{2 \omega_{q_1}} |V 3q\rangle \langle V 3q|, \\
\mathbb{I}_{3q\pi} &= \sum_{\mu_{q_1}, \tau_{q_1}} \sum_{\mu_{q_2}} \int DV Dk_{q_2} Dk_{q_3} Dk_\pi \frac{m_{3q\pi}^3}{2 \omega_{q_1}} |V 3q\pi\rangle \langle V 3q\pi|,
\end{aligned} \tag{4.19}$$

where the eigenvalues m_{\dots} of the free mass operators are defined via Eq. (2.46).

Inserting these expressions into Eq. (4.18), we obtain velocity-state matrix elements of the vertex operators on quark level on the one hand and, on the other hand, brackets of hadronic states with quark-level states which will lead to the three-quark wave function of the bare nucleon. These two entities will be treated in the next two sections in respective order.

4.2.4 Currents and spectator condition

We again concentrate on the calculation of the first line of Eq. (4.18), i.e. of $\langle V' N'_0 | V_{01} | V N_0 e \rangle$. The corresponding quark-level spectator condition reads

$$\langle V' 3q' \pi' | K_{q_1 \pi}^\dagger | V 3q \rangle = \Delta_{VV'} \Delta_{q_2 q'_2} \Delta_{q_3 q'_3} \frac{1}{\sqrt{m_{3q\pi}^3 m_{3q}^3}} \langle q'_1 \pi' | | K_{q_1 \pi}^\dagger | | q_1 \rangle. \tag{4.20}$$

There are now two possible choices for the quark–pion vertex $\langle q'_1 \pi' | K_{q_1 \pi}^\dagger | q_1 \rangle$ (cf. Sec. 2.5.3): We can use either pseudoscalar or pseudovector pion–quark coupling. The corresponding expressions are

$$\langle q'_1 \pi' | | K_{q_1 \pi}^\dagger | | q_1 \rangle_{\text{ps}} = -i g \bar{u}_{\mu'_{q_1}}(\vec{k}'_{q_1}) \gamma^5 u_{\mu_{q_1}}(\vec{k}_{q_1}) \cdot \mathcal{F}(\tau_{q_1}, \tau'_{q_1}, \tau_\pi)$$

and

$$\langle q'_1 \pi' | | K_{q_1 \pi}^\dagger | | q_1 \rangle_{\text{pv}} = +i \frac{f}{m_\pi} \bar{u}_{\mu'_{q_1}}(\vec{k}'_{q_1}) \gamma_\nu \gamma^5 u_{\mu_{q_1}}(\vec{k}_{q_1}) k_\pi^\nu \cdot \mathcal{F}(\tau_{q_1}, \tau'_{q_1}, \tau_\pi), \quad (4.21)$$

respectively, where g is the strong pseudoscalar pion–quark coupling constant, f the corresponding pseudovector coupling constant, and \mathcal{F} is the flavor function as treated in Sec. 2.5.3.

4.2.5 Wave functions

The 3-quark wave functions that arise from expressions of the form $\mathbb{I}_N \mathbb{I}_{3q}$, $\mathbb{I}_N \mathbb{I}_{3q\pi}$, etc. are derived in the same way as in Sec. 3.2.5. The result is

$$\begin{aligned} \langle V' 3q' | V N_0 \rangle &= \mathcal{N}_1 \Delta_{VV'} \langle 3q' | N_0 \rangle, \\ \langle V' 3q' \pi' | V N_0 \pi \rangle &= \mathcal{N}_2 \Delta_{VV'} \Delta_{\pi\pi'} \langle 3q' | N_0 \rangle. \end{aligned} \quad (4.22)$$

From the normalization condition

$$\sum_{\substack{\tilde{\mu}_{q_1}'' \tilde{\mu}_{q_2}'' \tilde{\mu}_{q_3}'' \\ \tau_{q_1}'' \tau_{q_2}'' \tau_{q_3}''}} \int d^3 \tilde{k}_{q_2}'' d^3 \tilde{k}_{q_3}'' \langle N' | 3q'' \rangle \langle 3q'' | N \rangle = \delta_{\mu_N \mu'_N} \delta_{\tau_N \tau'_N} \quad (4.23)$$

(momenta with a “tilde” defined as in Sec. 3.2.5) we obtain the normalization factors

$$\begin{aligned} \mathcal{N}_1 &= 4 \cdot (2\pi)^3 \frac{\sqrt{m_{N_0} \omega'_{q_1} \omega'_{q_2} \omega'_{q_3}}}{\sqrt{m_{N_0}^3 (\sum \omega'_{q_k})^3}}, \\ \mathcal{N}_2 &= 4 \cdot (2\pi)^3 \frac{\sqrt{\omega_{N_0} \tilde{\omega}'_{q_1} \tilde{\omega}'_{q_2} \tilde{\omega}'_{q_3} (\sum \omega'_{q_k})}}{\sqrt{(\sum \tilde{\omega}'_{q_k}) (\omega_{N_0} + \omega_\pi)^3 (\sum \omega'_{q_k} + \omega_\pi)^3}}. \end{aligned} \quad (4.24)$$

The derivation is quite analogous to the one in App. B.2.

4.2.6 Analytic calculation of the optical potential

We now continue our analytic calculations with the first term of the quark-level optical potential, V_{01} in Eq. (4.18). *In what follows, sums over spins and isospins of particles with redundant momenta are implied.* After inserting the eigenvalue of the propagator and some rearranging we obtain, via Eqs. (4.19),

$$\begin{aligned}
& \langle V' N_0' | V_{01} | V N_0 \rangle \\
&= \langle V' N_0' | \mathbb{I}_{3q} K_{q_1 \pi} \mathbb{I}_{3q \pi} P_{N_0 \pi} \mathbb{I}_{N_0 \pi} \mathbb{I}_{3q \pi} K_{q_1 \pi}^\dagger \mathbb{I}_{3q} | V N_0 \rangle \\
&= \sum_{\text{f}} DV^{(6)} Dk_{q_2}^{(6)} Dk_{q_3}^{(6)} \frac{\left(m_{3q}^{(6)}\right)^3}{2\omega_{q_1}^{(6)}} \sum_{\text{f}} DV^{(5)} Dk_{q_2}^{(5)} Dk_{q_3}^{(5)} Dk_\pi^{(5)} \frac{\left(m_{3q\pi}^{(5)}\right)^3}{2\omega_{q_1}^{(5)}} \\
&\quad \times \sum_{\text{f}} DV^{(4)} Dk_{N_0}^{(4)} \frac{\left(m_{N_0\pi}^{(4)}\right)^3}{2\omega_\pi^{(4)}} \left(m_N - m_{N_0\pi}^{(4)}\right)^{-1} \\
&\quad \times \sum_{\text{f}} DV''' Dk_{q_2}''' Dk_{q_3}''' Dk_\pi''' \frac{\left(m_{3q\pi}'''^{(3)}\right)^3}{2\omega_{q_1}'''^{(3)}} \sum_{\text{f}} DV'' Dk_{q_2}'' Dk_{q_3}'' \frac{\left(m_{3q}''^{(2)}\right)^3}{2\omega_{q_1}''^{(2)}} \\
&\quad \times \langle V' N_0' | V^{(6)} 3q^{(6)} \rangle \langle V^{(6)} 3q^{(6)} | K_{q_1 \pi} | V^{(5)} 3q^{(5)} \pi^{(5)} \rangle \langle V^{(5)} 3q^{(5)} \pi^{(5)} | V^{(4)} N_0^{(4)} \pi^{(4)} \rangle \\
&\quad \times \langle V^{(4)} N_0^{(4)} \pi^{(4)} | V''' 3q''' \pi''' \rangle \langle V''' 3q''' \pi''' | K_{q_1 \pi}^\dagger | V'' 3q'' \rangle \langle V'' 3q'' | V N_0 \rangle, \tag{4.25}
\end{aligned}$$

where $V^{(4)}$ again stands for V''' etc. and with the invariant masses m_{\dots} defined in Eq. (2.46).

Via the spectator condition (4.20) and the wave functions (4.22) (with the normalization factors (4.24)), the *last two lines* of (4.25) read

$$\begin{aligned}
& 4 \cdot (2\pi)^3 \frac{\sqrt{m_{N_0} \tilde{\omega}_{q_1}^{(6)} \tilde{\omega}_{q_2}^{(6)} \tilde{\omega}_{q_3}^{(6)}}}{\sqrt{m_{N_0}^3 \left(m_{3q}^{(6)}\right)^3}} \Delta_{V' V^{(6)}} \langle N_0' | 3q^{(6)} \rangle \\
& \times \Delta_{V^{(6)} V^{(5)}} \Delta_{q_2^{(6)} q_2^{(5)}} \Delta_{q_3^{(6)} q_3^{(5)}} \frac{1}{\sqrt{\left(m_{3q\pi}^{(5)}\right)^3 \left(m_{3q}^{(6)}\right)^3}} \langle q_1^{(5)} \pi^{(5)} | | K_{q_1 \pi}^\dagger | | q_1^{(6)} \rangle^* \\
& \times 4 \cdot (2\pi)^3 \frac{\sqrt{\omega_{N_0}^{(4)} \tilde{\omega}_{q_1}^{(5)} \tilde{\omega}_{q_2}^{(5)} \tilde{\omega}_{q_3}^{(5)} \left(\sum \omega_{q_k}^{(5)}\right)}}{\sqrt{\left(\sum \tilde{\omega}_{q_k}^{(5)}\right) \left(m_{N_0\pi}^{(4)}\right)^3 \left(m_{3q\pi}^{(5)}\right)^3}} \Delta_{V^{(4)} V^{(5)}} \Delta_{\pi^{(4)} \pi^{(5)}} \langle 3q^{(5)} | N_0^{(4)} \rangle \\
& \times 4 \cdot (2\pi)^3 \frac{\sqrt{\omega_{N_0}^{(4)} \tilde{\omega}_{q_1}''' \tilde{\omega}_{q_2}''' \tilde{\omega}_{q_3}''' \left(\sum \omega_{q_k}'''^{(3)}\right)}}{\sqrt{\left(\sum \tilde{\omega}_{q_k}'''^{(3)}\right) \left(m_{N_0\pi}^{(4)}\right)^3 \left(m_{3q\pi}'''^{(3)}\right)^3}} \Delta_{V^{(4)} V'''} \Delta_{\pi^{(4)} \pi'''} \langle N_0^{(4)} | 3q''' \rangle \\
& \times \Delta_{V''' V''} \Delta_{q_2''' q_2''} \Delta_{q_3''' q_3''} \frac{1}{\sqrt{\left(m_{3q\pi}'''^{(3)}\right)^3 \left(m_{3q}''^{(2)}\right)^3}} \langle q_1''' \pi''' | | K_{q_1 \pi}^\dagger | | q_1'' \rangle \\
& \times 4 \cdot (2\pi)^3 \frac{\sqrt{m_{N_0} \tilde{\omega}_{q_1}'' \tilde{\omega}_{q_2}'' \tilde{\omega}_{q_3}''}}{\sqrt{m_{N_0}^3 \left(m_{3q}''^{(2)}\right)^3}} \Delta_{V V''} \langle 3q'' | N_0 \rangle. \tag{4.26}
\end{aligned}$$

After cancelling the fractions and exploiting the Delta functions as well as the fact that in states without a pion, $\sum \omega_{q_k}^{(6)} = \sum \tilde{\omega}_{q_k}^{(6)} = m_{3q}^{(6)}$ resp. $\sum \omega_{q_k}'' = \sum \tilde{\omega}_{q_k}'' = m_{3q}''$, we

get

$$\begin{aligned}
& \langle V' N_0' | V_{01} | V N_0 \rangle \\
&= 16 \cdot (2\pi)^{12} \Delta_{VV'} \sum \frac{Dk_{q_2}^{(5)} Dk_{q_3}^{(5)}}{\omega_{q_1}^{(6)} \omega_{q_1}^{(5)}} \frac{Dk_{q_2}'' Dk_{q_3}''}{\omega_{q_1}''' \omega_{q_1}''} \frac{Dk_{N_0}^{(4)}}{2 \omega_{\pi}^{(4)}} \\
&\quad \times \frac{\sqrt{m_{N_0} \tilde{\omega}_{q_1}^{(6)} \tilde{\omega}_{q_2}^{(6)} \tilde{\omega}_{q_3}^{(6)}}}{\sqrt{m_{N_0}^3}} \langle N_0' | 3q^{(6)} \rangle \langle q_1^{(5)} \pi^{(4)} | | K_{q_1 \pi}^\dagger | | q_1^{(6)} \rangle^* \\
&\quad \times \frac{\sqrt{\omega_{N_0}^{(4)} \tilde{\omega}_{q_1}^{(5)} \tilde{\omega}_{q_2}^{(5)} \tilde{\omega}_{q_3}^{(5)} (\sum \omega_{q_k}^{(5)})}}{\sqrt{(\sum \tilde{\omega}_{q_k}^{(5)})}} \langle 3q^{(5)} | N_0^{(4)} \rangle \left(m_N - m_{N_0 \pi}^{(4)} \right)^{-1} \\
&\quad \times \frac{\sqrt{\omega_{N_0}^{(4)} \tilde{\omega}_{q_1}''' \tilde{\omega}_{q_2}''' \tilde{\omega}_{q_3}''' (\sum \omega_{q_k}''')}}{\sqrt{(\sum \tilde{\omega}_{q_k}''')}} \langle N_0^{(4)} | 3q''' \rangle \langle q_1''' \pi^{(4)} | | K_{q_1 \pi}^\dagger | | q_1'' \rangle \\
&\quad \times \frac{\sqrt{m_{N_0} \tilde{\omega}_{q_1}'' \tilde{\omega}_{q_2}'' \tilde{\omega}_{q_3}''}}{\sqrt{m_{N_0}^3}} \langle 3q'' | N_0 \rangle.
\end{aligned} \tag{4.27}$$

Here we have kept the intermediate velocity-state momenta of quark 1, k_{q_1}''' and $k_{q_1}^{(6)}$, as well as all 3 quark momenta in the “tilde” frame, \tilde{k}_i''' and $\tilde{k}_i^{(6)}$ (and all dependent quantities), for readability. The non-tilde three-momenta are obtained via the definition of the velocity state (2.46) in combination with the spectator conditions (4.20), whence $\vec{k}_{q_1}''' + \vec{k}_{q_2}'' + \vec{k}_{q_3}'' + \vec{k}_\pi^{(4)} = 0$, i.e. $\vec{k}_{q_1}''' = \vec{k}_{q_1}'' - \vec{k}_\pi^{(4)}$ (and vice versa for states with 5 and 6 primes). To obtain the momenta in the “tilde” frame, we use equation (3.35); note that the velocity (3.36) of the 3-quark subsystem depends on all three quark momenta!

Finally, after the index replacements $'' \rightarrow ()$ for the incoming quark state, $(6) \rightarrow '$ for the outgoing one, $''' \rightarrow ''$ and $(5) \rightarrow ''$ for intermediate quark states and $(4) \rightarrow ''$ for the intermediate hadronic nucleon state, we can rewrite this into an ex-

pression compatible with Eq. (4.11):

$$\begin{aligned}
 \langle V' N_0' | V_{01} | V N_0 \rangle &= \frac{\Delta_{VV'}}{m_{N_0}^3} \sum \frac{Dk''_{N_0}}{2\omega''_\pi} \\
 &\times \left(4 \cdot (2\pi)^6 \sum \frac{Dk'_{q_2} Dk'_{q_3}}{\omega''_{q_1} \omega''_{q_1}} \frac{\sqrt{\omega''_{N_0} \tilde{\omega}''_{q_1} \tilde{\omega}''_{q_2} \tilde{\omega}''_{q_3} (\sum \omega''_{q_k})}}{\sqrt{(\sum \tilde{\omega}''_{q_k})}} \langle N_0'' | 3q'' \rangle \right. \\
 &\quad \times \left. \langle q_1'' \pi'' | | K_{q_1 \pi}^\dagger | | q_1' \rangle \sqrt{m_{N_0} \tilde{\omega}'_{q_1} \tilde{\omega}'_{q_2} \tilde{\omega}'_{q_3}} \langle 3q' | N_0' \rangle \right)^* \\
 &\times (m_N - m''_{N_0 \pi})^{-1} \\
 &\times \left(4 \cdot (2\pi)^6 \sum \frac{Dk_{q_2} Dk_{q_3}}{\omega''_{q_1} \omega_{q_1}} \frac{\sqrt{\omega''_{N_0} \tilde{\omega}''_{q_1} \tilde{\omega}''_{q_2} \tilde{\omega}''_{q_3} (\sum \omega''_{q_k})}}{\sqrt{(\sum \tilde{\omega}''_{q_k})}} \langle N_0'' | 3q'' \rangle \right. \\
 &\quad \times \left. \langle q_1'' \pi'' | | K_{q_1 \pi}^\dagger | | q_1 \rangle \sqrt{m_{N_0} \tilde{\omega}_{q_1} \tilde{\omega}_{q_2} \tilde{\omega}_{q_3}} \langle 3q | N_0 \rangle \right), \tag{4.28}
 \end{aligned}$$

where for the vertex matrix elements we will use Eqs. (4.21).

For symmetry reasons (we will use the same 3-quark wave function as in Sec. 3.3.2), $V_{\text{opt}} = 9 V_{01}$ (cf Eq. (4.18)).

4.3 The microscopic expression for the pion–nucleon vertex

From comparing Eqs. (4.11) and (4.28) we get for the pion–nucleon vertex

$$\begin{aligned}
 &\langle N_0'' \pi'' | | K_{N_0 \pi}^\dagger | | N_0^{(\prime)} \rangle \\
 &= 12 \cdot (2\pi)^6 \sum_{\substack{\mu''_{q_1}, \tau''_{q_1} \\ \mu_{q_1}^{(\prime)}, \tau_{q_1}^{(\prime)}}} \sum \frac{Dk_{q_2}^{(\prime)} Dk_{q_3}^{(\prime)}}{\omega''_{q_1} \omega_{q_1}^{(\prime)}} \sqrt{m_{N_0} \tilde{\omega}_{q_1}^{(\prime)} \tilde{\omega}_{q_2}^{(\prime)} \tilde{\omega}_{q_3}^{(\prime)}} \frac{\sqrt{\omega''_{N_0} \tilde{\omega}''_{q_1} \tilde{\omega}''_{q_2} \tilde{\omega}''_{q_3} (\sum \omega''_{q_k})}}{\sqrt{(\sum \tilde{\omega}''_{q_k})}} \\
 &\quad \times \langle N_0'' | 3q'' \rangle \langle q_1'' \pi'' | | K_{q_1 \pi}^\dagger | | q_1^{(\prime)} \rangle \langle 3q^{(\prime)} | N_0^{(\prime)} \rangle \tag{4.29}
 \end{aligned}$$

from which we can immediately derive the nucleon pseudoscalar and pseudovector currents by comparing with Eqs. (4.7) and (4.8), respectively.

As already mentioned, we will use either pseudoscalar or pseudovector coupling for the quark–pion vertex, cf Eqs. (4.21). Also, we use the same 3-quark wave function as we already did in Sec. 3.3.2:

$$\langle \tilde{q}_1 \tilde{q}_2 \tilde{q}_3 | \tilde{N} \rangle = \Phi_X \Phi_{\text{FS}} \Phi_C \tag{4.30}$$

with the momentum part

$$\Phi_X = \frac{\mathcal{N}}{\left((\sum \tilde{\omega}_k)^2 + \beta^2 \right)^\gamma} \tag{4.31}$$

and the spin-flavor part

$$\Phi_{\text{FS}} = \frac{1}{\sqrt{2}} \sum_s \sum_{\substack{\tilde{\mu}_1, \tilde{\mu}_2, \tilde{\mu}_3, \tilde{\mu}_s \\ \tau_1, \tau_2, \tau_3, \tau_s}} C_{\frac{1}{2} \tilde{\mu}_2 \frac{1}{2} \tilde{\mu}_3}^{s \tilde{\mu}_s} C_{\frac{1}{2} \tau_2 \frac{1}{2} \tau_3}^{s \tau_s} C_{s \tilde{\mu}_s \frac{1}{2} \tilde{\mu}_1}^{\frac{1}{2} \tilde{\mu}_N} C_{s \tau_s \frac{1}{2} \tau_1}^{\frac{1}{2} \tau_N}. \quad (4.32)$$

Both parts of the wave function are again defined in the “tilde” frame, i.e. in the rest frame of the nucleon.

We use Wigner-D-functions to transform the wave function to the overall rest frame (of the $3q\pi$ system) in the same manner as in Eqs. (3.57). However, we make use of the fact that for the incoming and outgoing states $|VN^{(i)}\rangle$ resp. $|V3q^{(i)}\rangle$, the coordinates with and without a tilde are identical. For symmetry reasons it can be assumed that the pion couples to quark 1, which implies an overall factor of 3 which has already been taken into account in equation (4.29). For the first vertex (the one between incoming nucleon state and intermediate nucleon–pion state), we thus end up with

$$\begin{aligned}
& g_{N_0} J_{N_0}^{5[\sharp]}(\vec{k}_{N_0}, \mu_{N_0}; \vec{k}_{N_0}'', \mu_{N_0}'') \mathcal{F}(\tau_{N_0}, \tau_{N_0}'', \tau_\pi'') \\
&= \frac{3}{2} \sqrt{\omega_{N_0} \omega_{N_0}''} \sum \int d^3 \tilde{k}_2 d^3 \tilde{k}_3 \frac{1}{\omega_1''} \sqrt{\frac{\tilde{\omega}_1'' \tilde{\omega}_2'' \tilde{\omega}_3''}{\tilde{\omega}_1 \tilde{\omega}_2 \tilde{\omega}_3}} \sqrt{\frac{\sum \omega_k''}{\sum \tilde{\omega}_k''}} \\
& \times D_{\mu_1'' \tilde{\mu}_1''}^*(B(\vec{v}_{3q}''), \tilde{\vec{v}}_1) D_{\mu_2'' \tilde{\mu}_2''}^*(B(\vec{v}_{3q}''), \tilde{\vec{v}}_2) D_{\mu_3'' \tilde{\mu}_3''}^*(B(\vec{v}_{3q}''), \tilde{\vec{v}}_3) \\
& \times C_{\frac{1}{2} \tilde{\mu}_2'' \frac{1}{2} \tilde{\mu}_3''}^{s'' \tilde{\mu}_s''} C_{\frac{1}{2} \tau_2 \frac{1}{2} \tau_3}^{s'' \tau_s} C_{s'' \tilde{\mu}_s'' \frac{1}{2} \tilde{\mu}_1''}^{\frac{1}{2} \tilde{\mu}_N''} C_{s'' \tau_s \frac{1}{2} \tau_1''}^{\frac{1}{2} \tau_N''} \frac{\mathcal{N}}{\left((\sum \tilde{\omega}_k'')^2 + \beta^2\right)^\gamma} \\
& \times C_{\frac{1}{2} \mu_2 \frac{1}{2} \mu_3}^{s \mu_s} C_{\frac{1}{2} \tau_2 \frac{1}{2} \tau_3}^{s \tau_s} C_{s \mu_s \frac{1}{2} \mu_1}^{\frac{1}{2} \mu_N} C_{s \tau_s \frac{1}{2} \tau_1}^{\frac{1}{2} \tau_N} \frac{\mathcal{N}}{\left((\sum \tilde{\omega}_k)^2 + \beta^2\right)^\gamma} \\
& \times \bar{u}_{\mu_1''}(\vec{k}_1'') \left(g \left[-\frac{f}{m_\pi g} \gamma^\nu k_{\pi \nu}'' \right] \gamma^5 \right) u_{\mu_1}(\vec{k}_1) \mathcal{F}(\tau_1, \tau_1'', \tau_\pi''),
\end{aligned} \quad (4.33)$$

where we have defined for the pseudovector coupling

$$J^{5\sharp}(N_0, N_0'') := -\frac{f_{N_0}}{m_\pi g_{N_0}} J_\nu^5(N_0, N_0'') k_\pi^\nu \quad (4.34)$$

to treat the pseudoscalar (without square brackets) and pseudovector (with square brackets) case at the same time. Additionally, we have again replaced the quark indices q_i by i and used the shorthand notation (2.41). The spectator conditions (4.20) (valid in the non-“tilde” frame!) have already been taken into account. Keeping in mind as well the relations $\sum \mu_i = \mu_N$, $\sum \tilde{\mu}_i'' = \mu_N''$ (spins can be coupled as usual only in the “tilde” frame) and $\sum \tau_i = \tau_N$, $\sum \tau_i'' = \tau_N''$, the sum is over quark spins and isospins $\mu_2, \mu_3, \tau_2, \tau_3, \mu_1'', \tilde{\mu}_2'', \tilde{\mu}_3''$ ($= \pm \frac{1}{2}$) as well as over intermediate (iso)spins $s, s'' (= \{0, 1\})$ and their polarizations $\mu_s, \tilde{\mu}_s''$ and $\tau_s (= -s^{(i)} \dots s^{(i)})$. Eq. (4.33) relates also the pseudoscalar (pseudovector) pion–quark coupling g (f) with the corresponding coupling g_{N_0} (f_{N_0}) on hadron level.

It is easily checked that

$$\sum_{\{\tau_k\}, s, \tau_s, \tau_1''} C_{\frac{1}{2} \tau_2 \frac{1}{2} \tau_3}^{s'' \tau_s''} C_{s'' \tau_s'' \frac{1}{2} \tau_1''}^{\frac{1}{2} \tau_N''} C_{\frac{1}{2} \tau_2 \frac{1}{2} \tau_3}^{s \tau_s} C_{s \tau_s \frac{1}{2} \tau_1}^{\frac{1}{2} \tau_N} \mathcal{F}(\tau_1, \tau_1'', \tau_\pi'') = \mathcal{F}(\tau_N, \tau_N'', \tau_\pi''); \quad (4.35)$$

however, this expression cannot be isolated from the above equation. The reason is that s and s'' also occur in the spin sum.

4.4 Extraction of the form factor

4.4.1 Kinematics

In order to extract the strong form factor and the $\pi N_0 N_0$ coupling, we use the following kinematics: The frame of reference is the rest frame of the incoming (and outgoing) nucleon. The pion is emitted in the x^1 -direction with momentum k ; the nucleon picks up the reverse 3-momentum:

$$k_{N_0} = \begin{pmatrix} m_{N_0} \\ 0 \\ 0 \\ 0 \end{pmatrix}, \quad k_\pi = \begin{pmatrix} \sqrt{k^2 + m_\pi^2} \\ k \\ 0 \\ 0 \end{pmatrix},$$

$$\vec{k}_{N_0}'' = \vec{k}_{N_0} - \vec{k}_\pi \quad \Rightarrow \quad k_{N_0}'' = \begin{pmatrix} \sqrt{k^2 + m_{N_0}^2} \\ -k \\ 0 \\ 0 \end{pmatrix}, \quad (4.36)$$

$$\vec{k}_{N_0}' = \vec{k}_{N_0}'' + \vec{k}_\pi \quad \Rightarrow \quad k_{N_0}' = \begin{pmatrix} m_{N_0} \\ 0 \\ 0 \\ 0 \end{pmatrix} = k_{N_0}.$$

The negative 4-momentum transfer to the nucleon is then

$$Q^2 = -q^2 = - (k_{N_0} - k_{N_0}'')^2 = - \begin{pmatrix} m_{N_0} - \sqrt{k^2 + m_{N_0}^2} \\ k \\ 0 \\ 0 \end{pmatrix}^2$$

$$= -2 m_{N_0}^2 + 2 m_{N_0} \sqrt{k^2 + m_{N_0}^2}. \quad (4.37)$$

4.4.2 Pseudoscalar coupling

To extract the strong form factor for pseudoscalar $\pi N_0 N_0$ coupling, we do the following: According to Eq. (2.65),

$$g_{N_0} J_{N_0}^5(\vec{k}_{N_0}, \mu_{N_0}; \vec{k}_{N_0}'', \mu_{N_0}'') = g_{N_0} G_{\text{ps}}(Q^2) \bar{u}_{\mu_{N_0}''}(\vec{k}_{N_0}'') \gamma^5 u_{\mu_{N_0}}(\vec{k}_{N_0}). \quad (4.38)$$

We evaluate this expression using Mathematica®. In our kinematics, Eq. (4.36), this reads

$$\begin{aligned} J_{N_0}^5\left(-\frac{1}{2}, -\frac{1}{2}\right) &= J_{N_0}^5\left(\frac{1}{2}, \frac{1}{2}\right) = 0, \\ J_{N_0}^5\left(\frac{1}{2}, -\frac{1}{2}\right) &= J_{N_0}^5\left(-\frac{1}{2}, \frac{1}{2}\right) = Q \cdot G_{\text{ps}}(Q^2), \end{aligned} \quad (4.39)$$

where we observe that

$$J_{N_0}^{5*} = J_{N_0}^5. \quad (4.40)$$

We thus obtain the strong nucleon form factor via

$$G_{\text{ps}}(Q^2) = \frac{1}{Q} J_{N_0}^5\left(\frac{1}{2}, -\frac{1}{2}\right). \quad (4.41)$$

4.4.3 Pseudovector coupling

With $J^{5\sharp}(N_0, N_0')$ defined as in Eqs. (4.34) and (2.66), the pseudovector analog reads

$$g_{N_0} J_{N_0}^{5\sharp}(\vec{k}_{N_0}, \mu_{N_0}; \vec{k}_{N_0}'', \mu_{N_0}'') = -\frac{f_{N_0}}{m_\pi} G_{\text{pv}}(Q^2) \bar{u}_{\mu_{N_0}''}(\vec{k}_{N_0}'') \gamma^\nu \gamma^5 u_{\mu_{N_0}}(\vec{k}_{N_0}) k_{\pi\nu}, \quad (4.42)$$

which gives

$$\begin{aligned} J_{N_0}^{5\sharp}\left(-\frac{1}{2}, -\frac{1}{2}\right) &= J_{N_0}^{5\sharp}\left(\frac{1}{2}, \frac{1}{2}\right) = 0, \\ J_{N_0}^{5\sharp}\left(\frac{1}{2}, -\frac{1}{2}\right) &= J_{N_0}^{5\sharp}\left(-\frac{1}{2}, \frac{1}{2}\right) \\ &= +\frac{f_{N_0}}{g_{N_0} m_\pi} G_{\text{pv}}(Q^2) \frac{k \sqrt{2m_{N_0}} \left(m_{N_0} + \sqrt{k^2 + m_{N_0}^2} + \sqrt{k^2 + m_\pi^2}\right)}{\left(\sqrt{k^2 + m_{N_0}^2} + m_{N_0}\right)}, \end{aligned}$$

and thus

$$G_{\text{pv}}(Q^2) = +\frac{\left(\sqrt{k^2 + m_{N_0}^2} + m_{N_0}\right)}{k \sqrt{2m_{N_0}} \left(m_{N_0} + \sqrt{k^2 + m_{N_0}^2} + \sqrt{k^2 + m_\pi^2}\right)} g_{N_0} \frac{m_\pi}{f_{N_0}} J_{N_0}^{5\sharp}\left(\frac{1}{2}, -\frac{1}{2}\right) \quad (4.43)$$

We fix g_{N_0} and f_{N_0} such that $G_{\text{ps}}(0) = G_{\text{pv}}(0) = 1$.

4.5 Numerical implementation

For the major part, the numerical evaluation of the nucleon pseudoscalar current, Eq. (4.33), runs along the same lines as that of the electromagnetic current in Sec. 3.5. The differences are as follows:

4.5.1 Kinematic quantities

The initialization of the quark momenta in the incoming state reads

```

knaked [2] <<   sqrt(pow(k2,2) + pow(m,2)),
                    k2*sin(theta2)*cos(phi2),
                    k2*sin(theta2)*sin(phi2),
                    k2*cos(theta2);
// (knaked [3] analogously)

Vector3d k1naked3d = -knaked[2].segment<3>(1)-knaked[3].segment<3>(1);
knaked[1](0) = sqrt(pow(m,2)+k1naked3d.dot(k1naked3d));
knaked[1].segment<3>(1) = k1naked3d;

```

where m is the quark mass (globally defined) and k_2 , ϕ_2 , θ_2 the three integration variables for quark 2.

The 3-momentum transfer (now “ k ”) to quark 1 is the same as to the nucleon in (4.36), while via the spectator conditions (4.20), quarks 2 and 3 remain unaffected:

```

Vector4d knakedpr [4]; // in class declaration

for (i=1; i<=3; i++){ knakedpr[i] = knaked[i]; }

knakedpr[1](1) = knaked[1](1) - k;

knakedpr[1](0) =
sqrt(pow(m,2) + pow(knakedpr[1](1),2) + pow(knakedpr[1](2),2) + ... );

```

We then get the double-primed invariant mass of the 3-quark subsystem and the velocity (3.36) via

```

double mclpr =
sqrt(pow(knakedpr[1](0)+knakedpr[2](0)+knakedpr[3](0),2)-pow(k,2));
Vector4d vclpr; // in class declaration
vclpr << (sqrt(pow(k,2) + pow(mclpr,2))/mclpr) , -k/mclpr , 0 , 0;

```

The double-primed quark momenta in the original (“tilde”) frame are obtained via an inverse boost (2.36) with the double-primed velocity of the 3-quark subsystem:

```

for (i=1; i<=3; i++){ ktildrepr [i] = invboost(vclpr)*knakedpr[i]; }

```

4.5.2 Quark current and flavor function

Naturally, in the function for the current of quark 1, `Matrix2cd Mompart::quark1current ()`, we now need γ^5 for pseudoscalar and $k_\pi^\nu \gamma_\nu \gamma^5$ for

pseudovector coupling, i.e. instead of `dirac(nu)` in the middle line of `Matrix4cd middlematrix` we have `dirac(5)` and

```
-1/(2*m) * (dirac(0)*sqrt(pow(k,2)+pow(mpi,2))-dirac(1)*k) * dirac(5)
```

respectively, where `mpi` is the pion mass.

In addition to the spin-momentum part of the quark current, we also need the flavor function \mathcal{F} from Sec. 2.5.3. It reads

```
double flavorfunction(int tau, int taupr){
    double ff;
    if (tau == 1 && taupr == 1) ff = 1;
    else if (tau == 1 && taupr == -1) ff = sqrt(2);
    else if (tau == -1 && taupr == 1) ff = sqrt(2);
    else if (tau == -1 && taupr == -1) ff = -1;
    return ff; }
```

4.5.3 Integrand function

The factor which is made up of all the Clebsch-Gordan coefficients (initialized by external call `Clebschgordan cg`) reads

```
double cgfactor =
1/sqrt(2) *
cg.coeff(1,mu2tildepr,1,mu3tildepr,spr,mustildepr) *
cg.coeff(1,tau2,1,tau3,spr,taus) *
cg.coeff(spr,mustildepr,1,mu1tildepr,1,params->muNpr) *
cg.coeff(spr,taus,1,tau1pr,1,params->tauNpr) *
1/sqrt(2) *
cg.coeff(1,mu2,1,mu3,s,mus) *
cg.coeff(1,tau2,1,tau3,s,taus) *
cg.coeff(s,mus,1,mu1,1,params->muN)*
cg.coeff(s,taus,1,tau1,1,params->tauN);
```

The full integrand reads

```

intgr +=
prefactor *
cgfactor *
wigrotfactor1pr ((1-mu1tildepr)/2,(1-mu1pr)/2) *
wigrotfactor2pr ((1-mu2tildepr)/2,(1-mu2)/2) *
wigrotfactor3pr ((1-mu3tildepr)/2,(1-mu3)/2) *
spacepartpr *
spacepart *
quark1current ((1-mu1pr)/2,(1-mu1)/2) *
flavorfunction(tau1,tau1pr);

```

with a sum over spins and isospins μ_2 , μ_3 , τ_2 , τ_3 , μ_{1pr} , $\mu_{2tildepr}$, $\mu_{3tildepr}$ ($= \pm 1$), s , spr ($= 0, 2$) and μ_{s} , $\mu_{stildepr}$, τ_{us} ($= -s[pr] \dots s[pr]$). The dependent variables int , μ_1 , $\mu_{1tildepr}$, τ_1 , τ_{1pr} are set accordingly (see comment after Eq. (4.33)) including a check whether they are in the range ± 1 . Note that the strong quark coupling constant g has yet to be determined and has thus been set to 1.

After continuing with the rest of the procedure as outlined in Sec. 3.5, we obtain a result for the pseudoscalar current, $R(Q^2)$, which equals the nucleon pseudoscalar current divided by the strong quark coupling constant, $g \cdot R(Q^2) = g_{N_0} J_{N_0}^5(Q^2)$. Since the r.h.s. at $Q^2 = 0$ equals the nucleon strong coupling constant, g_{N_0} , we obtain the quark coupling constant via

$$g_{N_0} = g \cdot R(0), \quad (4.44)$$

i.e. the pseudoscalar current of the bare nucleon reads

$$g_{N_0} J_{N_0}^5(Q^2) = \frac{g_{N_0}}{R(0)} \cdot R(Q^2). \quad (4.45)$$

4.6 Results

The normalized form factor $G_{N_0}(Q^2)$ is well described by a fit of the form [MCP09]

$$G(Q^2) = \frac{1}{1 + \left(\frac{k}{\Lambda_1}\right)^2 + \left(\frac{k}{\Lambda_2}\right)^4}, \quad (4.46)$$

where k is the three-momentum of the pion (related to Q^2 via Eq. (4.37)). For comparison with predictions from other approaches we will neglect the pionic component of the nucleon as well as the renormalization of the nucleon mass due to pion loops. As a consequence, the physical nucleon N can be identified with the bare nucleon N_0 (which is a pure 3-quark bound state). Possible pionic effects are then hidden in the parametrization of the 3-quark bound-state wave function and the constituent quark masses. For these quantities we will use the same values as for the calculation of the electromagnetic form

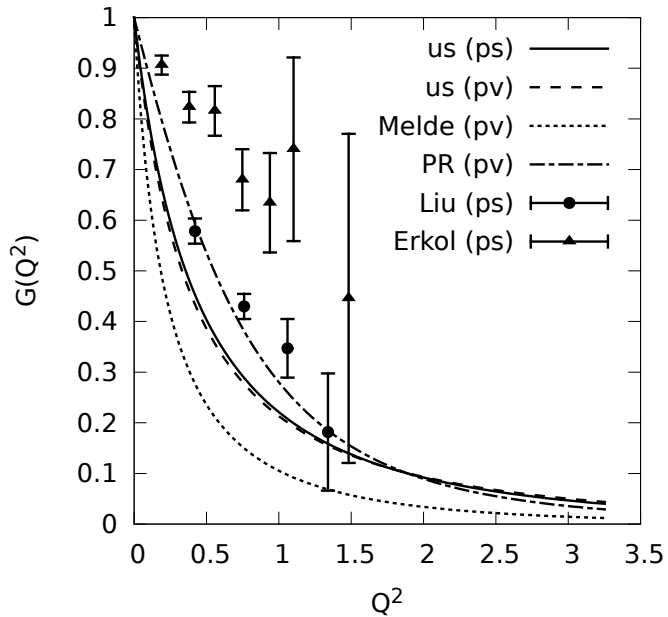


Figure 4.3: Strong πNN form factor: Comparison of our results (pseudoscalar and pseudovector coupling) with findings by Melde et al. [MCP09], Polinder and Rijken [PR05a, PR05b], and lattice results by Liu et al. [LDDW95] as well as Erkol et al. [EOT09].

factors in Chap. 3. A comparison of our results for pseudoscalar and pseudovector coupling with another constituent-quark-model calculation [MCP09] (pseudovector), with a hadronic pion-cloud model [PR05a, PR05b] (pseudovector) and with lattice predictions [LDDW95, EOT09] (pseudoscalar) is shown in Fig. 4.3. The normalized results, which are shown there, do not depend strongly on the choice of the coupling (pseudoscalar or pseudovector). Instead, there is a significant difference in the outcome for the strong quark-pion coupling constant.

For pseudoscalar coupling our results are well described by the fitting parameters $\Lambda_1 = 0.637$ and $\Lambda_2 = 1.46$. Taking the phenomenologically determined value for the πNN coupling constant $g_N = 13.1$ [Bug04], we obtain the quark pseudoscalar coupling constant $g = 3.55$ ($g^2/4\pi = 1.00$) by means of Eq. (4.44).

For pseudovector coupling we obtain $\Lambda_1 = 0.607$, $\Lambda_2 = 1.68$ and $g_{\text{pv}} := \frac{2m_q}{m_\pi} f = 2.85$ ($g_{\text{pv}}^2/4\pi = 0.65$). This coupling constant compares well with the one used in the Goldstone-Boson exchange relativistic constituent quark model by Glozman et al. ($g_{\text{pv}}^2/4\pi = 0.67$) [GPP⁺98].

Chapter 5

Overall Electromagnetic Form Factor

Having calculated the electromagnetic and the strong form factors of the bare nucleon, we now want to obtain the electromagnetic form factors of the nucleon including the pion-cloud effect. We restrict ourselves to a single pion that is emitted and reabsorbed by the nucleon. We will therefore treat the physical nucleon as a state consisting of a “bare” nucleon and a bare nucleon + pion component. This formalism calls for the mass of the “bare” nucleon, which differs from the physical one. Note that from now on, all calculations can and will be performed on the hadronic level, since the three-quark structure of the bare nucleon just enters the electromagnetic and strong couplings and vertex form factors, which have already been determined in the preceding sections. The formalism is treated in detail in what follows.

5.1 Basic setup

The starting point for our treatment of the electromagnetic nucleon form factors including the pion cloud is essentially the same as in Sec. 3.1. In order to properly describe the physical nucleon state, we consider it as a superposition of a bare nucleon state and a bare nucleon–pion state. The velocity states of Eq. (3.2) then become two-component state vectors

$$|VNe(\gamma)\rangle := |\widetilde{VNe}(\gamma)\rangle + |\widetilde{VN\pi e}(\gamma)\rangle. \quad (5.1)$$

The two components can be obtained by solving the eigenvalue problem for the matrix mass operator (cf. App. A):

$$M_{Ne(\gamma)} := \begin{pmatrix} M_{N_0 e(\gamma)} & K_\pi \\ K_\pi^\dagger & M_{N_0 \pi e(\gamma)} \end{pmatrix}. \quad (5.2)$$

The operators $M_{Ne(\gamma)}$ contain all interactions except photon exchange, that is, in our case, just the pion exchange. The diagonal elements of the matrices (5.2), in turn, are the

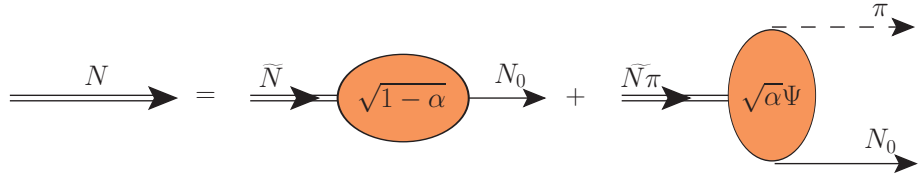


Figure 5.1: Physical nucleon N as a superposition of a bare nucleon component \tilde{N} and a bare nucleon + pion component $\tilde{N}\pi$. The \tilde{N} state consists of a single free nucleon N_0 with probability $(1 - \alpha)$. The $\tilde{N}\pi$ state is a distribution of free nucleon–pion states $N_0\pi$ which is described by the wave function Ψ and occurs with overall probability α .

free mass operators of the respective subsystems, that is, they only contain relativistic energies, whereas interactions with the pion are accounted for by the vertex operators $K_\pi^{(\dagger)}$. Note that, since we have $m_{N_0e} = \omega_{N_0} + \omega_e \neq m_{Ne} = \omega_N + \omega_e$ for the eigenvalues, also the masses of the physical and the bare nucleon are not equal (as long as $K_\pi^{(\dagger)}$ does not vanish):

$$m_N \neq m_{N_0} ! \quad (5.3)$$

We again work with velocity states also for the channels $|V\tilde{N}e(\gamma)\rangle$ and $|V\tilde{N}\pi e(\gamma)\rangle$. They are superpositions of corresponding *free* (i.e. orthogonal) states $|VN_0e(\gamma)\rangle$ and $|VN_0\pi e(\gamma)\rangle$, respectively, with the wave functions $\Psi_{N/N_0(\pi)}$ acting as coefficients. The latter are determined by solving the eigenvalue equation for the physical nucleon (cf. App. A). The normalization of the free states reads (cf. Eq. (2.50)):

$$\langle VN_0(\pi)e(\gamma) | V'N'_0(\pi')e'(\gamma') \rangle = \frac{2\omega_{N_0}}{m_{N_0(\pi)e(\gamma)}^3} \Delta_{VV'}(\Delta_{\pi\pi'}) \Delta_{ee'}(\Delta_{\gamma\gamma'}) \quad (5.4)$$

and the corresponding completeness relation (cf. Eq. (2.52)):

$$\mathbb{I}_{N_0(\pi)e(\gamma)} = \sum DV(Dk_\pi) Dk_e(Dk_\gamma) \frac{m_{N_0(\pi)e(\gamma)}^3}{2\omega_{N_0}} |VN_0(\pi)e(\gamma)\rangle\langle VN_0(\pi)e(\gamma)|, \quad (5.5)$$

where a sum over μ_{N_0} and τ_{N_0} is implied and the m_{\dots} are – as usual – the eigenvalues of the corresponding free mass operators, i.e. they contain no interactions.

5.2 The nucleon–pion wave function

In the following, we introduce the wave functions Ψ_{N/N_0} and $\Psi_{N/N_0\pi}$ in order to properly describe the bare nucleon and the bare nucleon + pion components in the physical nucleon, respectively. These are just appropriate projections onto free states, i.e.:

$$\begin{aligned} \langle V'N'_0e'(\gamma') | V\tilde{N}e(\gamma) \rangle &= \sqrt{1 - \alpha} \mathcal{N}_1 \Psi_{N/N'_0} \Delta_{V'V} \Delta_{e'e}(\Delta_{\gamma'\gamma}), \\ \langle V'N'_0\pi'e'(\gamma') | V\tilde{N}\pi e(\gamma) \rangle &= \sqrt{\alpha} \mathcal{N}_2 \Psi_{N/N'_0\pi'} \Delta_{V'V} \Delta_{e'e}(\Delta_{\gamma'\gamma}). \end{aligned} \quad (5.6)$$

The \mathcal{N}_i are normalization factors yet to be determined. The role of the coefficients $\sqrt{1 - \alpha}$ and $\sqrt{\alpha}$ will become clearer in a moment.

Using the relations above, the expansions of the nucleonic components in terms of free states then read

$$\begin{aligned}
 |V\tilde{N}e(\gamma)\rangle &= \mathbb{I}_{N_0e(\gamma)} |V\tilde{N}e(\gamma)\rangle \\
 &= \sum D V' D k'_e(D k'_\gamma) \frac{(m'_{N_0e(\gamma)})^3}{2\omega'_{N_0}} |V' N'_0 e'(\gamma')\rangle \langle V' N'_0 e'(\gamma') |V\tilde{N}e(\gamma)\rangle \\
 &= \sqrt{1-\alpha} \frac{(m'_{N_0e(\gamma)})^3}{2\omega'_{N_0}} \mathcal{N}_1 \Psi_{N/N'_0} |V N'_0 e(\gamma)\rangle
 \end{aligned} \tag{5.7}$$

and

$$\begin{aligned}
 |V\tilde{N}\pi e(\gamma)\rangle &= \mathbb{I}_{N_0\pi e(\gamma)} |\tilde{N}\pi e(\gamma)\rangle \\
 &= \sum D V' D k'_\pi D k'_e(D k'_\gamma) \frac{(m'_{N_0\pi e(\gamma)})^3}{2\omega'_{N_0}} |V' N'_0 \pi' e'(\gamma')\rangle \langle V' N'_0 \pi' e'(\gamma') |V\tilde{N}\pi e(\gamma)\rangle \\
 &= \sqrt{\alpha} \sum D k'_\pi \frac{(m'_{N_0\pi e(\gamma)})^3}{2\omega'_{N_0}} \mathcal{N}_2 \Psi_{N/N'_0\pi'} |V N'_0 \pi' e(\gamma)\rangle
 \end{aligned} \tag{5.8}$$

with a sum over μ'_{N_0} and τ'_{N_0} implied. Since a single bare nucleon necessarily has the same quantum numbers as the physical nucleon it relates to, the bare-nucleon-in-physical-nucleon wave function is simply a product of Kronecker deltas over spins and isospins:

$$\Psi_{N/N'_0} = \delta_{\mu_N \mu'_{N_0}} \delta_{\tau_N \tau'_{N_0}}. \tag{5.9}$$

Furthermore in the velocity-state representation, the three-momentum of both bare and physical nucleon is determined by the one of the electron:

$$\vec{k}_{N_0} = \vec{k}_N = -\vec{k}_e. \tag{5.10}$$

However, since $m_N \neq m_{N_0}$, this is not true for the four-momenta: $k_N \neq k_{N_0}$!

The normalization condition for the nucleon-pion wave function reads

$$\sum_{\mu''_{N_0} \tau''_{N_0} \tau''_\pi} \int d^3 \tilde{k}_\pi'' \Psi_{N/N'_0\pi''}^* \Psi_{N'/N''_0\pi''} = \delta_{\mu_N \mu'_{N_0}} \delta_{\tau_N \tau'_{N_0}}, \tag{5.11}$$

or, in our shorthand notation,

$$\sum_{\mu''_{N_0} \tau''_{N_0}} \sum_{\tau''_\pi} D \tilde{k}_\pi'' \tilde{\omega}_\pi'' \Psi_{N/N'_0\pi''}^* \Psi_{N'/N''_0\pi''} = \frac{\delta_{\mu_N \mu'_{N_0}} \delta_{\tau_N \tau'_{N_0}}}{2(2\pi)^3}. \tag{5.12}$$

The quantities with a “tilde” are defined in the center-of-momentum (c.o.m.) frame of the $N_0\pi$ subsystem which constitutes the physical nucleon, *not* the overall c.o.m. frame as usual (cf. Sec. 2.4.5), i.e.

$$\begin{aligned}
 \tilde{k}_{N_0} &= B^{-1}(\vec{v}_{N_0\pi}) k_{N_0}, & \tilde{k}_\pi &= B^{-1}(\vec{v}_{N_0\pi}) k_\pi, \\
 U_{B(\vec{v}_{N_0\pi})} |\tilde{k}_{N_0} \tilde{\mu}_{N_0}\rangle &= \sum_{\mu_{N_0}=\pm\frac{1}{2}} |k_{N_0} \mu_{N_0}\rangle D_{\mu_{N_0} \tilde{\mu}_{N_0}} (B(\vec{v}_{N_0\pi}), \frac{\tilde{k}_{N_0}}{m_{N_0}}),
 \end{aligned} \tag{5.13}$$

with

$$\begin{aligned}\vec{v}_{N_0\pi} &= \frac{\vec{k}_{N_0\pi}}{m_{N_0\pi}}, \\ \vec{k}_{N_0\pi} &= \vec{k}_{N_0} + \vec{k}_\pi = -\vec{k}_e = \vec{k}_N, \\ m_{N_0\pi} &= \tilde{\omega}_{N_0} + \tilde{\omega}_\pi = \sqrt{(\omega_{N_0} + \omega_\pi)^2 - \vec{k}_{N_0\pi}^2}.\end{aligned}\quad (5.14)$$

By $B(\vec{v})$ we mean a (canonical, i.e. rotationless) Lorentz boost with velocity \vec{v} . For the definition of the Wigner rotation R_W and its associated Wigner-D-function in Eq. (5.13), see Sec. 2.4.4. Note that the boost velocity $\vec{v}_{N_0\pi}$ is calculated from \vec{k}_N not by dividing by the physical nucleon mass m_N , but rather by the invariant mass $m_{N_0\pi}$! Applying the coordinate transformation from App. B.1,

$$Dk_\pi = D\tilde{k}_\pi \frac{\omega_{N_0}}{\tilde{\omega}_{N_0}} \frac{\tilde{\omega}_{N_0} + \tilde{\omega}_\pi}{\omega_{N_0} + \omega_\pi}, \quad (5.15)$$

we can also write

$$\sum_{\mu''_{N_0}} \sum_{\tau''_{N_0}} Dk_\pi'' \frac{\tilde{\omega}_{N_0}''}{\omega_{N_0}''} \frac{\omega_{N_0}'' + \omega_\pi''}{\tilde{\omega}_{N_0}'' + \tilde{\omega}_\pi''} \tilde{\omega}_\pi'' \Psi_{N/N_0''\pi''}^* \Psi_{N'/N_0''\pi''} \frac{\delta_{\mu_N\mu'_N} \delta_{\tau_N\tau'_N}}{2(2\pi)^3}. \quad (5.16)$$

Via Eq. (2.50) the normalization of the physical state and consequently, via Eq. (5.1), the substates should read

$$\begin{aligned}\langle VNe(\gamma) | V'N'e'(\gamma') \rangle &= \langle V\tilde{N}e(\gamma) | V'\tilde{N}'e'(\gamma') \rangle + \langle V\widetilde{N\pi}e(\gamma) | V'\widetilde{N'\pi'}e'(\gamma') \rangle \\ &= \frac{2\omega_N}{m_{Ne(\gamma)}^3} \Delta_{VV'} \Delta_{ee'} (\Delta_{\gamma\gamma'}) \delta_{\mu'_N\mu_N} \delta_{\tau'_N\tau_N}\end{aligned}\quad (5.17)$$

with the normalizations

$$\begin{aligned}\langle V\tilde{N}e(\gamma) | V'\tilde{N}'e'(\gamma') \rangle &= (1 - \alpha) \frac{2\omega_N}{m_{Ne(\gamma)}^3} \Delta_{VV'} \Delta_{ee'} (\Delta_{\gamma\gamma'}) \delta_{\mu'_N\mu_N} \delta_{\tau'_N\tau_N}, \\ \langle V\widetilde{N\pi}e(\gamma) | V'\widetilde{N'\pi'}e'(\gamma') \rangle &= \alpha \frac{2\omega_N}{m_{Ne(\gamma)}^3} \Delta_{VV'} \Delta_{ee'} (\Delta_{\gamma\gamma'}) \delta_{\mu'_N\mu_N} \delta_{\tau'_N\tau_N}\end{aligned}\quad (5.18)$$

for each component. This means that α is the probability for finding the nucleon–pion component in the physical nucleon. Likewise, the completeness relation for the physical nucleon state decomposes into

$$\begin{aligned}\mathbb{I}_{Ne(\gamma)} &= \sum_{\mu_N\tau_N} \sum_{\mu'_N\tau'_N} DV Dk_e (Dk_\gamma (-g^{\mu_\gamma\mu_\gamma})) \frac{m_{Ne(\gamma)}^3}{2\omega_N} |VNe(\gamma)\rangle\langle VNe(\gamma)| \\ &\stackrel{(5.1)}{=} \sum_{\mu_N\tau_N} \sum_{\mu'_N\tau'_N} DV Dk_e (Dk_\gamma (-g^{\mu_\gamma\mu_\gamma})) \frac{m_{Ne(\gamma)}^3}{2\omega_N} \\ &\quad \times \left(|V\tilde{N}e(\gamma)\rangle\langle V\tilde{N}e(\gamma)| + |V\widetilde{N\pi}e(\gamma)\rangle\langle V\widetilde{N\pi}e(\gamma)| \right. \\ &\quad \left. + |V\widetilde{N\pi}e(\gamma)\rangle\langle V\widetilde{N\pi}e(\gamma)| + |V\widetilde{N\pi}e(\gamma)\rangle\langle V\widetilde{N\pi}e(\gamma)| \right).\end{aligned}\quad (5.19)$$

The normalization factors \mathcal{N}_i in (5.7) and (5.8) are then obtained as follows:

\mathcal{N}_1 : Starting out from Eq. (5.7), we have

$$\begin{aligned} & \langle V \tilde{N} e(\gamma) | V' \tilde{N}' e'(\gamma') \rangle \\ &= (1 - \alpha) \mathcal{N}_1 \mathcal{N}'_1 \frac{(m_{N_0 e(\gamma)})^3}{2 \omega_{N_0}} \frac{(m'_{N_0 e(\gamma)})^3}{2 \omega'_{N_0}} \langle V N_0 e(\gamma) | V' N'_0 e'(\gamma') \rangle \\ &\stackrel{(5.4)}{=} (1 - \alpha) \mathcal{N}_1^2 \frac{(m_{N_0 e(\gamma)})^3}{2 \omega_{N_0}} \Delta_{VV'} \Delta_{ee'} (\Delta_{\gamma\gamma'}) . \end{aligned} \quad (5.20)$$

Equating this to (5.18), we see that

$$\mathcal{N}_1^2 = \frac{2 \omega_{N_0}}{(m_{N_0 e(\gamma)})^3} \frac{2 \omega_N}{m_{N e(\gamma)}^3} . \quad (5.21)$$

\mathcal{N}_2 : Starting out from Eq. (5.8), we have

$$\begin{aligned} & \langle V \tilde{N} \pi e(\gamma) | V' \tilde{N}' \pi' e'(\gamma') \rangle \\ &= \alpha \sum D k''_\pi D k'''_\pi \frac{(m''_{N_0 \pi e(\gamma)})^3}{2 \omega''_{N_0}} \frac{(m'''_{N_0 \pi e(\gamma)})^3}{2 \omega'''_{N_0}} \mathcal{N}_2 \mathcal{N}'_2 \Psi^*_{N/N'_0 \pi''} \Psi_{N'/N''_0 \pi'''} \\ &\quad \times \langle V N'_0 \pi'' e(\gamma) | V' N'''_0 \pi''' e'(\gamma') \rangle \\ &\stackrel{(5.4)}{=} \alpha \sum D k''_\pi \mathcal{N}_2 \mathcal{N}'_2 \frac{(m''_{N_0 \pi e(\gamma)})^3}{2 \omega''_{N_0}} \Psi^*_{N/N'_0 \pi''} \Psi_{N'/N''_0 \pi''} \Delta_{VV'} \Delta_{ee'} (\Delta_{\gamma\gamma'}) , \end{aligned} \quad (5.22)$$

with sums over μ''_{N_0} and τ''_{N_0} implied. Equating this to expression (5.18) we see that, under consideration of Eq. (5.16),

$$\mathcal{N}_2^2 = 2 (2\pi)^3 \frac{2 \omega_N}{m_{N e(\gamma)}^3} \frac{2 \omega''_{N_0}}{(m''_{N_0 \pi e(\gamma)})^3} \frac{\tilde{\omega}''_{N_0}}{\omega''_{N_0}} \frac{\tilde{\omega}''_\pi}{\tilde{\omega}''_{N_0} + \tilde{\omega}''_\pi} . \quad (5.23)$$

Thus, the expansion of the bare nucleon and bare nucleon + pion components in terms of free velocity states finally reads

$$\begin{aligned} |V \tilde{N} e(\gamma)\rangle &= \sqrt{1 - \alpha} \sqrt{\frac{(m_{N_0 e(\gamma)})^3}{\omega_{N_0}}} \sqrt{\frac{\omega_N}{m_{N e(\gamma)}^3}} |V N_0 e(\gamma)\rangle \\ |V \tilde{N} \pi e(\gamma)\rangle &= \sqrt{\alpha} \sqrt{2 (2\pi)^3} \sum_{\mu'_{N_0} \tau'_{N_0}} \sum D k'_\pi \\ &\quad \times \sqrt{\frac{(m'_{N_0 \pi e(\gamma)})^3}{\omega'_{N_0}}} \sqrt{\frac{\omega_N}{m_{N e(\gamma)}^3}} \sqrt{\frac{\tilde{\omega}'_{N_0}}{\omega'_{N_0}}} \sqrt{\frac{\tilde{\omega}'_\pi}{\tilde{\omega}'_{N_0} + \tilde{\omega}'_\pi}} \Psi_{N/N'_0 \pi'} |V N'_0 \pi' e(\gamma)\rangle . \end{aligned} \quad (5.24)$$

5.3 Eigenvalue equation and Feshbach reduction

We start with a coupled-channels approach exactly as in Sec. 3.1, Eq. (3.2):

$$\begin{pmatrix} M_{N e} & K_\gamma \\ K_\gamma^\dagger & M_{N e \gamma} \end{pmatrix} \begin{pmatrix} |V N e\rangle \\ |V N e \gamma\rangle \end{pmatrix} = \sqrt{s} \begin{pmatrix} |V N e\rangle \\ |V N e \gamma\rangle \end{pmatrix} , \quad (5.25)$$

where the diagonal elements M_{Ne} and $M_{Ne\gamma}$ are the mass operators for nucleon-electron and nucleon-electron-photon channels (without electromagnetic interactions), respectively, and the off-diagonal elements K_γ and K_γ^\dagger , linking the two channels, are the annihilation resp. creation operators of the photon. s is the Mandelstam variable for electron-nucleon scattering (i.e. the invariant mass squared of the whole system). A Feshbach reduction completely analogous to Sec. 3.1.2 yields

$$(\sqrt{s} - M_{Ne})|VNe\rangle =: P_{Ne}^{-1}|VNe\rangle = \underbrace{K_\gamma P_{Ne\gamma} K_\gamma^\dagger}_{V_{\text{opt}}}|VNe\rangle. \quad (5.26)$$

Via Eq. (5.1), the matrix elements of the optical potential V_{opt} can then be decomposed in terms of the nucleonic components:

$$\begin{aligned} & \langle V'N'e' | V_{\text{opt}} | VNe \rangle \\ &= \langle V'\tilde{N}'e' | K_\gamma P_{Ne\gamma} \mathbb{I}_{Ne\gamma} K_\gamma^\dagger | V\tilde{N}e \rangle \\ &+ \langle V'\tilde{N}'e' | K_\gamma P_{Ne\gamma} \mathbb{I}_{Ne\gamma} K_\gamma^\dagger | V\tilde{N}\pi e \rangle \\ &+ \langle V'\widetilde{N}'\pi'e' | K_\gamma P_{Ne\gamma} \mathbb{I}_{Ne\gamma} K_\gamma^\dagger | V\tilde{N}e \rangle \\ &+ \langle V'\widetilde{N}'\pi'e' | K_\gamma P_{Ne\gamma} \mathbb{I}_{Ne\gamma} K_\gamma^\dagger | V\widetilde{N}\pi e \rangle, \end{aligned} \quad (5.27)$$

where we have already inserted the unity operator, which is necessary so that the propagator can assume its eigenvalue.

Using the decomposition (5.19) for $\mathbb{I}_{Ne\gamma}$ and replacing the propagator by its eigenvalue, we get the following 4 expressions for the single matrix elements (between orthogonal states, i.e. the first line in Eq. (5.27) corresponds to $\langle V'\tilde{N}'e | V_{\text{opt}} | V\tilde{N}e \rangle$ etc.):

$$\begin{aligned} \langle V\widetilde{N}(\pi)e |' V_{\text{opt}} | V\widetilde{N}[\pi]e \rangle &= \sum_{\mu''_N \tau''_N} \sum_{\mu''_\gamma \tau''_\gamma} DV'' Dk''_e Dk''_\gamma \left(-g^{\mu''_\gamma \mu''_\gamma} \right) \\ &\times \langle V\widetilde{N}(\pi)e |' K_\gamma | V\widetilde{N}(\pi)e\gamma \rangle'' \frac{(m''_{Ne\gamma})^3}{2\omega''_N} \frac{1}{\sqrt{s} - m''_{Ne\gamma}} \langle V\widetilde{N}[\pi]e\gamma |'' K_\gamma^\dagger | V\widetilde{N}[\pi]e \rangle \end{aligned} \quad (5.28)$$

where either all the π 's in round brackets or all those in square brackets (or both) are included or omitted. *Here and from now on, we will use the shorthand notation $|VNe\rangle' := |V'N'e'\rangle$ etc. for primed states, wherever it seems necessary.* Note that

$$\langle V\tilde{N}e |' V_{\text{opt}} | V\widetilde{N}\pi e \rangle = \langle V\widetilde{N}\pi e | V_{\text{opt}}^\dagger | V\tilde{N}e \rangle'^*. \quad (5.29)$$

Using Eqs. (5.24), we obtain

$$\begin{aligned} \langle V\tilde{N}e |' V_{\text{opt}} | V\tilde{N}e \rangle &= \frac{1}{2} (1 - \alpha)^2 \sum_{\mu''_N \tau''_N} \sum_{\mu''_\gamma \tau''_\gamma} DV'' Dk''_e Dk''_\gamma \left(-g^{\mu''_\gamma \mu''_\gamma} \right) \\ &\times \sqrt{\frac{(m'_{N_0e})^3}{\omega'_{N_0}}} \sqrt{\frac{\omega'_N}{(m'_{Ne})^3}} \langle VN_0e |' K_\gamma | VN_0e\gamma \rangle'' \\ &\times \frac{(m''_{N_0e\gamma})^3}{\omega''_{N_0}} \frac{1}{\sqrt{s} - m''_{Ne\gamma}} \langle VN_0e\gamma |'' K_\gamma^\dagger | VN_0e \rangle \sqrt{\frac{(m_{N_0e})^3}{\omega_{N_0}}} \sqrt{\frac{\omega_N}{m_{Ne}^3}}, \end{aligned} \quad (5.30)$$

$$\begin{aligned}
\langle V\widetilde{N}e|'V_{\text{opt}}|V\widetilde{N\pi}e\rangle &= (2\pi)^3 \alpha (1-\alpha) \sum_{\mu''_N \tau''_N} \sum_{\mu''_N \tau''_N} DV'' Dk''_e Dk''_\gamma \left(-g^{\mu''_\gamma \mu''_\gamma} \right) \\
&\times \sqrt{\frac{(m'_{N_0 e})^3}{\omega'_{N_0}}} \sqrt{\frac{\omega'_N}{(m'_{N e})^3}} \langle V N_0 e|' K_\gamma |V N_0 e \gamma\rangle'' \sqrt{\frac{(m''_{N_0 e \gamma})^3}{\omega''_{N_0}}} \frac{1}{\sqrt{s} - m''_{N e \gamma}} \\
&\times \sum_{\mu'''_{N_0} \tau'''_{N_0}} \sum_{\mu'''_{N_0} \tau'''_{N_0}} Dk'''_\pi \sqrt{\frac{(m'''_{N_0 \pi e \gamma})^3}{\omega'''_{N_0}}} \frac{\tilde{\omega}'''_{N_0} \tilde{\omega}'''_\pi}{\omega'''_{N_0}} \sqrt{\frac{\omega'''_{N_0} + \omega'''_\pi}{\tilde{\omega}'''_{N_0} + \tilde{\omega}'''_\pi}} \Psi^*_{N''/N_0''' \pi'''} \langle V N_0 \pi e \gamma|''' K_\gamma^\dagger \\
&\times \sum_{\mu^{(4)}_{N_0} \tau^{(4)}_{N_0}} \sum_{\mu^{(4)}_{N_0} \tau^{(4)}_{N_0}} Dk^{(4)}_\pi |V N_0 \pi e\rangle^{(4)} \sqrt{\frac{(m^{(4)}_{N_0 \pi e \gamma})^3 \omega_N}{\omega^{(4)}_{N_0} m_{N e \gamma}^3}} \frac{\tilde{\omega}^{(4)}_{N_0} \tilde{\omega}^{(4)}_\pi}{\omega^{(4)}_{N_0}} \sqrt{\frac{\omega^{(4)}_{N_0} + \omega^{(4)}_\pi}{\tilde{\omega}^{(4)}_{N_0} + \tilde{\omega}^{(4)}_\pi}} \Psi_{N/N_0^{(4)} \pi^{(4)}} \\
\end{aligned} \tag{5.31}$$

and

$$\begin{aligned}
\langle V\widetilde{N\pi}e|'V_{\text{opt}}|V\widetilde{N\pi}e\rangle &= 2(2\pi)^6 \alpha^2 \sum_{\mu''_N \tau''_N} \sum_{\mu''_N \tau''_N} DV'' Dk''_e Dk''_\gamma \left(-g^{\mu''_\gamma \mu''_\gamma} \right) \\
&\times \sum_{\mu'''_{N_0} \tau'''_{N_0}} \sum_{\mu'''_{N_0} \tau'''_{N_0}} Dk'''_\pi \sqrt{\frac{(m'''_{N_0 \pi e})^3 \omega'_N}{\omega'''_{N_0} (m'_{N e})^3}} \frac{\tilde{\omega}'''_{N_0} \tilde{\omega}'''_\pi}{\omega'''_{N_0}} \sqrt{\frac{\omega'''_{N_0} + \omega'''_\pi}{\tilde{\omega}'''_{N_0} + \tilde{\omega}'''_\pi}} \Psi^*_{N'/N_0''' \pi'''} \langle V N_0 \pi e|''' K_\gamma \\
&\times \sum_{\mu^{(4)}_{N_0} \tau^{(4)}_{N_0}} \sum_{\mu^{(4)}_{N_0} \tau^{(4)}_{N_0}} Dk^{(4)}_\pi |V N_0 \pi e \gamma\rangle^{(4)} \sqrt{\frac{(m^{(4)}_{N_0 \pi e \gamma})^3}{\omega^{(4)}_{N_0}}} \frac{\tilde{\omega}^{(4)}_{N_0} \tilde{\omega}^{(4)}_\pi}{\omega^{(4)}_{N_0}} \sqrt{\frac{\omega^{(4)}_{N_0} + \omega^{(4)}_\pi}{\tilde{\omega}^{(4)}_{N_0} + \tilde{\omega}^{(4)}_\pi}} \Psi_{N''/N_0^{(4)} \pi^{(4)}} \\
&\times \frac{1}{\sqrt{s} - m''_{N e \gamma}} \\
&\times \sum_{\mu^{(5)}_{N_0} \tau^{(5)}_{N_0}} \sum_{\mu^{(5)}_{N_0} \tau^{(5)}_{N_0}} Dk^{(5)}_\pi \sqrt{\frac{(m^{(5)}_{N_0 \pi e \gamma})^3}{\omega^{(5)}_{N_0}}} \frac{\tilde{\omega}^{(5)}_{N_0} \tilde{\omega}^{(5)}_\pi}{\omega^{(5)}_{N_0}} \sqrt{\frac{\omega^{(5)}_{N_0} + \omega^{(5)}_\pi}{\tilde{\omega}^{(5)}_{N_0} + \tilde{\omega}^{(5)}_\pi}} \Psi^*_{N''/N_0^{(5)} \pi^{(5)}} \langle V N_0 \pi e \gamma|^{(5)} K_\gamma^\dagger \\
&\times \sum_{\mu^{(6)}_{N_0} \tau^{(6)}_{N_0}} \sum_{\mu^{(6)}_{N_0} \tau^{(6)}_{N_0}} Dk^{(6)}_\pi |V N_0 \pi e\rangle^{(6)} \sqrt{\frac{(m^{(6)}_{N_0 \pi e})^3 \omega_N}{\omega^{(6)}_{N_0} (m_{N e})^3}} \frac{\tilde{\omega}^{(6)}_{N_0} \tilde{\omega}^{(6)}_\pi}{\omega^{(6)}_{N_0}} \sqrt{\frac{\omega^{(6)}_{N_0} + \omega^{(6)}_\pi}{\tilde{\omega}^{(6)}_{N_0} + \tilde{\omega}^{(6)}_\pi}} \Psi_{N/N_0^{(6)} \pi^{(6)}} \\
\end{aligned} \tag{5.32}$$

5.4 Spectator conditions

Due to the structure of the interaction Lagrangian (2.55) we can now split the photon creation- and annihilation operators into sums of vertex operators as we already did in

Sec. 3.1.3:

$$\begin{aligned} K_\gamma^\dagger |N_0 e\rangle &= \left(K_{e\gamma}^\dagger + K_{N\gamma}^\dagger \right) |N_0 e\rangle, \\ K_\gamma^\dagger |N_0 \pi e\rangle &= \left(K_{e\gamma}^\dagger + K_{N\gamma}^\dagger + K_{\pi\gamma}^\dagger \right) |N_0 \pi e\rangle \end{aligned} \quad (5.33)$$

and vice versa for the annihilation operators.

Having done this, we can employ the following spectator conditions:

$$\begin{aligned} \langle V' N_0' e' \gamma' | K_{N_0\gamma}^\dagger | V N_0 e \rangle &= \Delta_{VV'} \Delta_{ee'} \frac{(-1)}{\sqrt{m_{N_0 e \gamma}^3 m_{N_0 e}^3}} \langle N_0' \gamma' | | K_{N_0\gamma}^\dagger | | N_0 \rangle, \\ \langle V' N_0' e' \gamma' | K_{e\gamma}^\dagger | V N_0 e \rangle &= \Delta_{VV'} \Delta_{N_0 N_0'} \frac{(-1)}{\sqrt{m_{N_0 e \gamma}^3 m_{N_0 e}^3}} \langle e' \gamma' | | K_{e\gamma}^\dagger | | e \rangle, \\ \langle V' N_0' \pi' e' \gamma' | K_{N_0\gamma}^\dagger | V N_0 \pi e \rangle &= \Delta_{VV'} \Delta_{\pi\pi'} \Delta_{ee'} \frac{(-1)}{\sqrt{m_{N_0 \pi e \gamma}^3 m_{N_0 \pi e}^3}} \langle N_0' \gamma' | | K_{N_0\gamma}^\dagger | | N_0 \rangle, \\ \langle V' N_0' \pi' e' \gamma' | K_{e\gamma}^\dagger | V N_0 \pi e \rangle &= \Delta_{VV'} \Delta_{N_0 N_0'} \Delta_{\pi\pi'} \frac{(-1)}{\sqrt{m_{N_0 \pi e \gamma}^3 m_{N_0 \pi e}^3}} \langle e' \gamma' | | K_{e\gamma}^\dagger | | e \rangle, \\ \langle V' N_0' \pi' e' \gamma' | K_{\pi\gamma}^\dagger | V N_0 \pi e \rangle &= \Delta_{VV'} \Delta_{N_0 N_0'} \Delta_{ee'} \frac{(-1)}{\sqrt{m_{N_0 \pi e \gamma}^3 m_{N_0 \pi e}^3}} \langle \pi' \gamma' | | K_{\pi\gamma}^\dagger | | \pi \rangle \end{aligned} \quad (5.34)$$

and vice versa for the annihilation operators. In addition, the electromagnetic interaction leaves the isospin of the nucleon or pion invariant, whence the vertex operator matrix elements read

$$\begin{aligned} \langle N_0' \gamma' | | K_{N_0\gamma}^\dagger | | N_0 \rangle &= \langle N_0 | | K_{N_0\gamma} | | N_0' \gamma' \rangle^* = |e| J_\nu(N_0, N_0') \epsilon^\nu(\gamma')^* \delta_{\tau_{N_0} \tau'_{N_0}}, \\ \langle e' \gamma' | | K_{e\gamma}^\dagger | | e \rangle &= \langle e | | K_{e\gamma} | | e' \gamma' \rangle^* = |e| J_\nu(e, e') \epsilon^\nu(\gamma')^*, \\ \langle \pi' \gamma' | | K_{\pi\gamma}^\dagger | | \pi \rangle &= \langle \pi | | K_{\pi\gamma} | | \pi' \gamma' \rangle^* = |e| J_\nu(\pi, \pi') \epsilon^\nu(\gamma')^* \delta_{\tau_\pi \tau'_{\pi'}} \end{aligned} \quad (5.35)$$

where we again use the shorthand notation (3.15), i.e. the $J^\nu(\dots)$ are the currents of the respective particles and $\epsilon^\nu(\gamma')$ is the photon polarization vector. Furthermore, we will use

$$J^\nu(X, X')^* = J^\nu(X', X). \quad (5.36)$$

(For a more detailed explanation we refer to Sec. 3.1.5, for details on the currents being inserted to Sec. 5.6.)

5.5 Diagrams

Using the splitting of the photon creation- and annihilation operators from Eq. (5.33), we are now ready to write down the time-ordered diagrams which correspond to the matrix elements of the optical potential, Eqs. (5.30) – (5.32). Furthermore, we will employ the spectator conditions (5.34). In the final step, we will obtain the three covariant diagrams pertaining to the problem at hand.

5.5.1 Time-ordered diagrams

Neglecting self-energy photon loops and photon exchange between pion and nucleon, we obtain the following expressions for time-ordered diagrams. Note that via Eqs. (5.9) and (5.10), we have $\vec{k}_N'' = \vec{k}_{N_0}''$, $\mu_N'' = \mu_{N_0}''$ and $\tau_N'' = \tau_{N_0}''$!

Nucleon component incoming and outgoing: For the following calculation it is more convenient to render the photon momentum instead of the nucleon momentum in Eq. (5.30) redundant, whence, via Eq. (2.52), we have to replace

$$\sum_{\mu_N'' \tau_N''} \sum \int \frac{Dk_\gamma''}{\omega_{N_0}''} \rightarrow \sum_{\mu_\gamma''} \sum \int \frac{Dk_{N_0}''}{\omega_\gamma''}, \quad (5.37)$$

so that for Eq. (5.30) we can write

$$\begin{aligned} & \langle V' \tilde{N}' e' | V_{\text{opt}} | V \tilde{N} e \rangle \\ &= (1 - \alpha)^2 \Delta_{VV'} \sqrt{\frac{\omega_N'}{(m'_{Ne})^3}} \frac{1}{\sqrt{\omega'_{N_0}}} \\ & \times \sum_{\mu_\gamma''} \sum \int Dk_e'' Dk_{N_0}'' \left(-g^{\mu_\gamma'' \mu_\gamma''} \right) \frac{1}{2\omega_\gamma''} \frac{1}{\sqrt{s} - m''_{Ne\gamma}} \frac{1}{\sqrt{\omega_{N_0}}} \sqrt{\frac{\omega_N}{m_{Ne}^3}} \\ & \times \left(\Delta_{e'e''} \langle N_0' | | K_{N_0\gamma} | | N_0'' \gamma'' \rangle \Delta_{N_0 N_0''} \langle e'' \gamma'' | | K_{e\gamma}^\dagger | | e \rangle \right. \\ & \quad \left. + \Delta_{N_0' N_0''} \langle e' | | K_{e\gamma} | | e'' \gamma'' \rangle \Delta_{ee''} \langle N_0'' \gamma'' | | K_{N_0\gamma}^\dagger | | N_0 \rangle \right). \end{aligned} \quad (5.38)$$

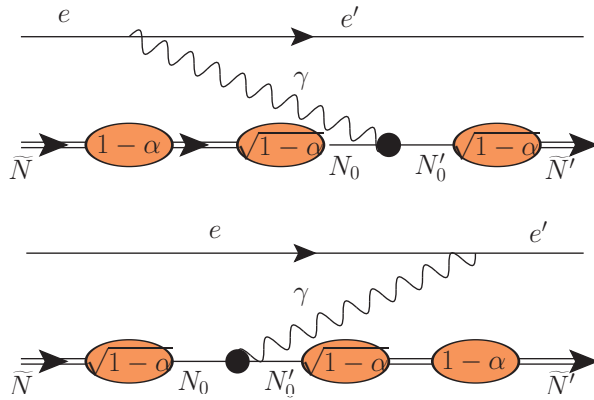


Figure 5.2: Time-ordered diagrams for bare nucleon component incoming and outgoing. Note that, in addition to the normalization factors $\sqrt{1 - \alpha}$ for incoming and outgoing wave functions, one has an additional factor $(1 - \alpha)$, which comes from insertion of the completeness relation (5.19).

Evaluating the Deltas and inserting the current expressions (5.35) for the vertex matrix elements, we obtain

$$\begin{aligned}
 & \langle V' \tilde{N}' e' | V_{\text{opt}} | V \tilde{N} e \rangle \\
 &= (1 - \alpha)^2 |e|^2 \frac{\Delta_{VV'}}{2 m_{N_e}^3} \sum_{\mu_\gamma} (-g^{\mu_\gamma \mu_\gamma}) \sqrt{\frac{\omega'_N}{\omega'_{N_0}}} \sqrt{\frac{\omega_N}{\omega_{N_0}}} \\
 & \quad \times \frac{1}{\omega_\gamma} \left(\frac{\epsilon^\lambda(\gamma) \epsilon^\nu(\gamma)}{\sqrt{s} - \omega_N - \omega'_e - \omega_\gamma} \Big|_{\vec{k}_\gamma = \vec{k}_e - \vec{k}'_e} + \frac{\epsilon^\lambda(\gamma) \epsilon^\nu(\gamma)}{\sqrt{s} - \omega'_N - \omega_e - \omega_\gamma} \Big|_{\vec{k}_\gamma = \vec{k}'_e - \vec{k}_e} \right) \\
 & \quad \times J_\lambda(N_0, N'_0) J_\nu(e, e') ,
 \end{aligned} \tag{5.39}$$

where we have performed the index replacement $\gamma'' \rightarrow \gamma$ and kept k_γ outside the brackets for readability. Inserting the completeness relation for photons, Eq. (2.11), we obtain

$$\begin{aligned}
 & \langle V' \tilde{N}' e' | V_{\text{opt}} | V \tilde{N} e \rangle = -(1 - \alpha)^2 |e|^2 \frac{\Delta_{VV'}}{2 m_{N_e}^3} \sqrt{\frac{\omega'_N}{\omega'_{N_0}}} \sqrt{\frac{\omega_N}{\omega_{N_0}}} \\
 & \quad \times \frac{1}{\omega_\gamma} \left(\frac{1}{\sqrt{s} - \omega_N - \omega'_e - \omega_\gamma} \Big|_{\vec{k}_\gamma = \vec{k}_e - \vec{k}'_e} + \frac{1}{\sqrt{s} - \omega'_N - \omega_e - \omega_\gamma} \Big|_{\vec{k}_\gamma = \vec{k}'_e - \vec{k}_e} \right) \\
 & \quad \times J^\nu(N_0, N'_0) J_\nu(e, e') .
 \end{aligned} \tag{5.40}$$

Nucleon+pion component incoming, nucleon component outgoing: For the following calculation we start out from Eq. (5.31) and again perform the splitting of the vertex operators (5.33). In order to exploit the spectator conditions (5.34), we will have to render the double-primed photon momentum instead of the double-primed nucleon momentum redundant in two terms (the ones involving the $\Delta_{N'_0 N''_0}$). Via Eq. (2.52) we

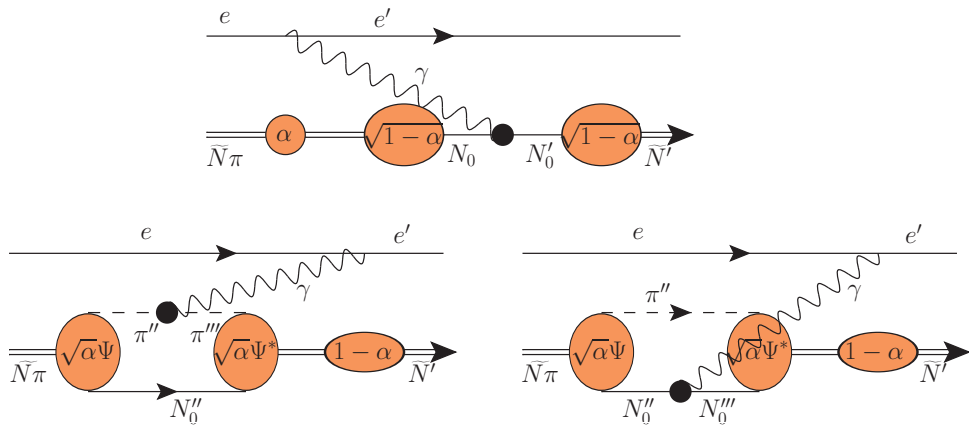


Figure 5.3: Time-ordered diagrams for bare nucleon+pion incoming and bare nucleon outgoing.

replace

$$\sum_{\mu''_N \tau''_N} \sum \int \frac{Dk''_\gamma}{\omega''_{N_0}} \rightarrow \sum_{\mu''_\gamma} \sum \int \frac{Dk''_{N_0}}{\omega''_\gamma}, \quad (5.41)$$

so that for Eq. (5.31) we can write

$$\begin{aligned} & \langle V' \tilde{N}' e' | V_{\text{opt}} | V \tilde{N} \pi e \rangle \\ &= \alpha (1 - \alpha) (2\pi)^3 \Delta_{VV'} \sqrt{\frac{\omega'_N}{(m'_{Ne})^3}} \frac{1}{\sqrt{\omega'_{N_0}}} \sum_{\mu''_N \tau''_N} \sum \int Dk''_e Dk''_\gamma (-g^{\mu''_\gamma \mu''_\gamma}) \frac{1}{\sqrt{\omega''_{N_0}}} \\ & \quad \times \frac{1}{\sqrt{s - m''_{Ne\gamma}}} \sum_{\mu'''_N \tau'''_N} \sum \int Dk'''_\pi \sqrt{\tilde{\omega}'''_{N_0} \tilde{\omega}'''_\pi} \frac{\sqrt{\omega'''_{N_0} + \omega'''_\pi}}{\sqrt{\tilde{\omega}'''_{N_0} + \tilde{\omega}'''_\pi}} \Psi^*_{N''/N_0''' \pi''' \omega'''_{N_0}} \frac{1}{\omega'''_{N_0}} \\ & \quad \times \sum_{\mu^{(4)}_{N_0} \tau^{(4)}_{N_0}} \sum \int Dk^{(4)}_\pi \frac{1}{\omega^{(4)}_{N_0}} \sqrt{\frac{\omega_N}{m_{Ne}^3}} \sqrt{\tilde{\omega}^{(4)}_{N_0} \tilde{\omega}^{(4)}_\pi} \frac{\sqrt{\omega^{(4)}_{N_0} + \omega^{(4)}_\pi}}{\sqrt{\tilde{\omega}^{(4)}_{N_0} + \tilde{\omega}^{(4)}_\pi}} \Psi_{N/N_0^{(4)} \pi^{(4)}} \\ & \quad \times \Delta_{e'e''} \langle N'_0 | | K_{N_0\gamma} | | N''_0 \gamma'' \rangle \Delta_{N'''_0 N_0^{(4)}} \Delta_{\pi''' \pi^{(4)}} \langle e'' \gamma'' | | K_{e\gamma}^\dagger | | e \rangle \\ &+ \alpha (1 - \alpha) (2\pi)^3 \Delta_{VV'} \sqrt{\frac{\omega'_N}{(m'_{Ne})^3}} \frac{1}{\sqrt{\omega'_{N_0}}} \sum_{\mu''_\gamma} \sum \int Dk''_e Dk''_{N_0} (-g^{\mu''_\gamma \mu''_\gamma}) \frac{\omega''_{N_0}}{\omega''_\gamma} \\ & \quad \times \frac{1}{\sqrt{\omega''_{N_0}}} \frac{1}{\sqrt{s - m''_{Ne\gamma}}} \sum_{\mu'''_N \tau'''_N} \sum \int Dk'''_\pi \sqrt{\tilde{\omega}'''_{N_0} \tilde{\omega}'''_\pi} \frac{\sqrt{\omega'''_{N_0} + \omega'''_\pi}}{\sqrt{\tilde{\omega}'''_{N_0} + \tilde{\omega}'''_\pi}} \Psi^*_{N''/N_0''' \pi''' \omega'''_{N_0}} \frac{1}{\omega'''_{N_0}} \\ & \quad \times \sum_{\mu^{(4)}_{N_0} \tau^{(4)}_{N_0}} \sum \int Dk^{(4)}_\pi \frac{1}{\omega^{(4)}_{N_0}} \sqrt{\frac{\omega_N}{m_{Ne}^3}} \sqrt{\tilde{\omega}^{(4)}_{N_0} \tilde{\omega}^{(4)}_\pi} \frac{\sqrt{\omega^{(4)}_{N_0} + \omega^{(4)}_\pi}}{\sqrt{\tilde{\omega}^{(4)}_{N_0} + \tilde{\omega}^{(4)}_\pi}} \Psi_{N/N_0^{(4)} \pi^{(4)}} \\ & \quad \times \left(\Delta_{N'_0 N''_0} \langle e' | | K_{e\gamma} | | e'' \gamma'' \rangle \Delta_{\pi''' \pi^{(4)}} \Delta_{e''e} \langle N'''_0 \gamma'' | | K_{N_0\gamma}^\dagger | | N_0^{(4)} \rangle \right. \\ & \quad \left. + \Delta_{N'_0 N''_0} \langle e' | | K_{e\gamma} | | e'' \gamma'' \rangle \Delta_{N'''_0 N_0^{(4)}} \Delta_{e''e} \langle \pi''' \gamma'' | | K_{\pi\gamma}^\dagger | | \pi^{(4)} \rangle \right). \end{aligned} \quad (5.42)$$

For the first term we then make use of the relations

$$\begin{aligned} & \vec{k}_{N_0}^{(4)} + \vec{k}_\pi^{(4)} + \vec{k}_e = 0, \\ & \vec{k}_{N_0}''' + \vec{k}_\pi''' + \vec{k}_e'' + \vec{k}_\gamma'' = 0, \\ & \Rightarrow \delta^3(\vec{k}_{N_0}''' - \vec{k}_{N_0}^{(4)}) \delta^3(\vec{k}_\pi''' - \vec{k}_\pi^{(4)}) = \delta^3(\vec{k}_\pi''' - \vec{k}_\pi^{(4)}) \delta^3(\vec{k}_e - \vec{k}_e'' - \vec{k}_\gamma''), \quad (5.43) \\ & \Rightarrow \frac{1}{\omega'''_{N_0}} \Delta_{N'''_0 N_0^{(4)}} \Delta_{\pi''' \pi^{(4)}} \Delta_{e''e''} = \frac{1}{\omega''_\gamma} \Delta_{\pi''' \pi^{(4)}} \Delta_{(e-e')\gamma''} \Delta_{e''e''} \delta_{\mu'''_N \mu^{(4)}_{N_0}} \delta_{\tau'''_N \tau^{(4)}_{N_0}}. \end{aligned}$$

For the third term we change the momentum to be integrated over (making the other the redundant one):

$$\sum_{\mu^{(4)}_{N_0} \tau^{(4)}_{N_0}} \sum \int \frac{Dk^{(4)}_\pi}{\omega^{(4)}_{N_0}} \dots = \sum_{\tau^{(4)}_\pi} \sum \int \frac{Dk^{(4)}_{N_0}}{\omega^{(4)}_\pi} \dots \quad (5.44)$$

Evaluating the Deltas and inserting the current expressions (5.35) for the vertex matrix elements together with the nucleon–pion wave-function normalization (5.16), the completeness relations for photon polarization vectors, Eq. (2.11) and the index identifications $\gamma'' \rightarrow \gamma$ and $(N_0/\pi)^{(4)} \rightarrow (N_0/\pi)''$ we then obtain

$$\begin{aligned}
& \langle V' \tilde{N}' e' | V_{\text{opt}} | \tilde{V} \tilde{N} \pi e \rangle \\
&= -\frac{1}{2} \alpha (1 - \alpha) |e|^2 \Delta_{VV'} \sqrt{\frac{\omega_N}{(m_{Ne})^3}} \sqrt{\frac{\omega'_N}{(m'_{Ne})^3}} \frac{1}{\omega_\gamma} \\
&\quad \times \frac{1}{\sqrt{\omega_{N_0} \omega'_{N_0}}} \frac{1}{\sqrt{s - \omega_N - \omega'_e - \omega_\gamma}} J_\nu(N_0, N'_0) J^\nu(e, e') \Big|_{\vec{k}_\gamma = \vec{k}_e - \vec{k}'_e} \\
&\quad - \alpha (1 - \alpha) |e|^2 \Delta_{VV'} \sqrt{\frac{\omega_N}{(m_{Ne})^3}} \sqrt{\frac{\omega'_N}{(m'_{Ne})^3}} \frac{1}{\omega_\gamma} \frac{1}{\sqrt{s - \omega'_N - \omega_e - \omega_\gamma}} \\
&\quad \times \frac{1}{2} \sum_{\mu''_{N_0} \tau''_{N_0} \tau''_\pi} \int \frac{d^3 k''_\pi}{\omega''_\pi \omega''_{N_0}} \sqrt{\tilde{\omega}''_{N_0} \tilde{\omega}''_\pi} \frac{\sqrt{\omega''_{N_0} + \omega''_\pi}}{\sqrt{\tilde{\omega}''_{N_0} + \tilde{\omega}''_\pi}} \Psi_{N/N''_0 \pi''} J_\nu(e, e') \\
&\quad \times \left(\sum_{\mu'''_{N_0}} \frac{1}{\omega'''_{N_0}} \sqrt{\tilde{\omega}'''_{N_0} \tilde{\omega}'''_\pi} \frac{\sqrt{\omega'''_{N_0} + \omega'''_\pi}}{\sqrt{\tilde{\omega}'''_{N_0} + \tilde{\omega}'''_\pi}} \Psi^*_{N'/N'''_0 \pi''} J^\nu(N''_0, N'''_0) \Big|_{\substack{\vec{k}'''_{N_0} = \vec{k}''_{N_0} - \vec{k}_\gamma \\ \vec{k}_\gamma = \vec{k}'_e - \vec{k}_e}} \right. \\
&\quad \left. + \frac{1}{\omega'''_\pi} \sqrt{\tilde{\omega}''_{N_0} \tilde{\omega}'''_\pi} \frac{\sqrt{\omega''_{N_0} + \omega'''_\pi}}{\sqrt{\tilde{\omega}''_{N_0} + \tilde{\omega}'''_\pi}} \Psi^*_{N'/N''_0 \pi'''} J^\nu(\pi'', \pi''') \Big|_{\substack{\vec{k}'''_\pi = \vec{k}''_\pi - \vec{k}_\gamma \\ \vec{k}_\gamma = \vec{k}'_e - \vec{k}_e}} \right). \tag{5.45}
\end{aligned}$$

Nucleon component incoming, Nucleon+pion component outgoing: Via Eq. (5.29) we have, analogously,

$$\begin{aligned}
 & \langle V' \widetilde{N' \pi'} e' | V_{\text{opt}} | V \bar{N} e \rangle \\
 &= -\frac{1}{2} \alpha (1-\alpha) |e|^2 \Delta_{VV'} \sqrt{\frac{\omega_N}{(m_{Ne})^3}} \sqrt{\frac{\omega'_N}{(m'_{Ne})^3}} \frac{1}{\omega_\gamma} \\
 & \quad \times \frac{1}{\sqrt{\omega_{N_0} \omega'_{N_0}}} \frac{1}{\sqrt{s - \omega'_N - \omega_e - \omega_\gamma}} J^\nu(N_0, N'_0) J_\nu(e, e') \Big|_{\vec{k}_\gamma = \vec{k}'_e - \vec{k}_e} \\
 &= -\alpha (1-\alpha) |e|^2 \Delta_{VV'} \sqrt{\frac{\omega_N}{(m_{Ne})^3}} \sqrt{\frac{\omega'_N}{(m'_{Ne})^3}} \frac{1}{\omega_\gamma} \frac{1}{\sqrt{s - \omega_N - \omega'_e - \omega_\gamma}} \\
 & \quad \times \frac{1}{2} \sum_{\mu''_{N_0} \tau''_{N_0} \tau''_\pi} \int \frac{d^3 k''_\pi}{\omega''_\pi \omega''_{N_0}} \sqrt{\tilde{\omega}''_{N_0} \tilde{\omega}''_\pi} \frac{\sqrt{\omega''_{N_0} + \omega''_\pi}}{\sqrt{\tilde{\omega}''_{N_0} + \tilde{\omega}''_\pi}} \Psi_{N/N''_0 \pi''} J^\nu(e, e') \\
 & \quad \times \left(\sum_{\mu'''_{N_0}} \frac{1}{\omega'''_{N_0}} \sqrt{\tilde{\omega}'''_{N_0} \tilde{\omega}'''_\pi} \frac{\sqrt{\omega'''_{N_0} + \omega'''_\pi}}{\sqrt{\tilde{\omega}'''_{N_0} + \tilde{\omega}'''_\pi}} \Psi^*_{N'/N'''_0 \pi''} J_\nu(N''_0, N'''_0) \Big|_{\substack{\vec{k}'''_{N_0} = \vec{k}''_{N_0} + \vec{k}_\gamma \\ \vec{k}_\gamma = \vec{k}_e - \vec{k}'_e}} \right. \\
 & \quad \left. + \frac{1}{\omega'''_\pi} \sqrt{\tilde{\omega}''_{N_0} \tilde{\omega}'''_\pi} \frac{\sqrt{\omega''_{N_0} + \omega'''_\pi}}{\sqrt{\tilde{\omega}''_{N_0} + \tilde{\omega}'''_\pi}} \Psi^*_{N'/N'''_0 \pi'''} J_\nu(\pi'', \pi''') \Big|_{\substack{\vec{k}'''_\pi = \vec{k}''_\pi + \vec{k}_\gamma \\ \vec{k}_\gamma = \vec{k}_e - \vec{k}'_e}} \right). \tag{5.46}
 \end{aligned}$$

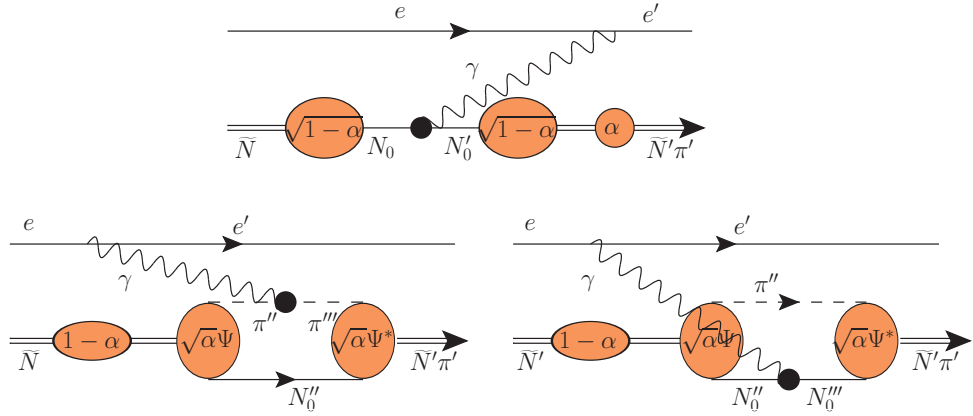


Figure 5.4: Time-ordered diagrams for bare nucleon incoming and bare nucleon+pion outgoing.

Nucleon+pion component incoming and outgoing: Upon inserting the splitting of the vertex operators and the spectator conditions from Sec. 5.4, Eq. (5.32) becomes

$$\begin{aligned}
\langle V' \widetilde{N' \pi'} e' | V_{\text{opt}} | V \widetilde{N \pi} e \rangle &= 2 (2\pi)^6 \alpha^2 \Delta_{VV'} \sqrt{\frac{\omega_N}{m_{N_e}^3}} \sqrt{\frac{\omega'_N}{(m'_{N_e})^3}} \\
&\times \sum_{\mu''_{N_0} \tau''_{N_0}} \sum_{\mu'''_{N_0} \tau'''_{N_0}} \frac{Dk'''_{\pi}}{\omega'''_{N_0}} \sqrt{\widetilde{\omega'''_{N_0}} \widetilde{\omega'''_{\pi}}} \sqrt{\frac{\omega'''_{N_0} + \omega'''_{\pi}}{\widetilde{\omega'''_{N_0}} + \widetilde{\omega'''_{\pi}}}} \Psi_{N'/N_0''' \pi'''}^* \\
&\times \sum_{\mu^{(4)}_{N_0} \tau^{(4)}_{N_0}} \sum_{\mu^{(4)}_{N_0} \tau^{(4)}_{N_0}} \frac{Dk^{(4)}_{\pi}}{\omega^{(4)}_{N_0}} \sqrt{\widetilde{\omega^{(4)}_{N_0}} \widetilde{\omega^{(4)}_{\pi}}} \sqrt{\frac{\omega^{(4)}_{N_0} + \omega^{(4)}_{\pi}}{\widetilde{\omega^{(4)}_{N_0}} + \widetilde{\omega^{(4)}_{\pi}}}} \\
&\times \sum_{\mu''_N \tau''_N} \sum_{\mu''_N \tau''_N} Dk''_e Dk''_{\gamma} \left(-g^{\mu''_e \mu''_{\gamma}} \right) \Psi_{N''/N_0^{(4)} \pi^{(4)}} \frac{1}{\sqrt{s - \omega''_N - \omega''_e - \omega''_{\gamma}}} \\
&\times \sum_{\mu^{(5)}_{N_0} \tau^{(5)}_{N_0}} \sum_{\mu^{(5)}_{N_0} \tau^{(5)}_{N_0}} \frac{Dk^{(5)}_{\pi}}{\omega^{(5)}_{N_0}} \sqrt{\widetilde{\omega^{(5)}_{N_0}} \widetilde{\omega^{(5)}_{\pi}}} \sqrt{\frac{\omega^{(5)}_{N_0} + \omega^{(5)}_{\pi}}{\widetilde{\omega^{(5)}_{N_0}} + \widetilde{\omega^{(5)}_{\pi}}}} \Psi_{N''/N_0^{(5)} \pi^{(5)}}^* \\
&\times \sum_{\mu^{(6)}_{N_0} \tau^{(6)}_{N_0}} \sum_{\mu^{(6)}_{N_0} \tau^{(6)}_{N_0}} \frac{Dk^{(6)}_{\pi}}{\omega^{(6)}_{N_0}} \sqrt{\widetilde{\omega^{(6)}_{N_0}} \widetilde{\omega^{(6)}_{\pi}}} \sqrt{\frac{\omega^{(6)}_{N_0} + \omega^{(6)}_{\pi}}{\widetilde{\omega^{(6)}_{N_0}} + \widetilde{\omega^{(6)}_{\pi}}}} \Psi_{N/N_0^{(6)} \pi^{(6)}} \\
&\times \left(\Delta_{\pi''' \pi^{(4)}} \Delta_{e' e''} \langle N_0''' | | K_{N_0 \gamma} | | N_0^{(4)} \gamma'' \rangle \Delta_{N_0^{(5)} N_0^{(6)}} \Delta_{\pi^{(5)} \pi^{(6)}} \langle e'' \gamma'' | | K_{e\gamma}^\dagger | | e \rangle \right. \\
&\quad + \Delta_{N_0''' N_0^{(4)}} \Delta_{e' e''} \langle \pi''' | | K_{\pi\gamma} | | \pi^{(4)} \gamma'' \rangle \Delta_{N_0^{(5)} N_0^{(6)}} \Delta_{\pi^{(5)} \pi^{(6)}} \langle e'' \gamma'' | | K_{e\gamma}^\dagger | | e \rangle \\
&\quad + \Delta_{N_0''' N_0^{(4)}} \Delta_{\pi''' \pi^{(4)}} \langle e' | | K_{e\gamma} | | e'' \gamma'' \rangle \Delta_{\pi^{(5)} \pi^{(6)}} \Delta_{e'' e} \langle N_0^{(5)} \gamma'' | | K_{N_0 \gamma}^\dagger | | N_0^{(6)} \rangle \\
&\quad \left. + \Delta_{N_0''' N_0^{(4)}} \Delta_{\pi''' \pi^{(4)}} \langle e' | | K_{e\gamma} | | e'' \gamma'' \rangle \Delta_{N_0^{(5)} N_0^{(6)}} \Delta_{e'' e} \langle \pi^{(5)} \gamma'' | | K_{\pi\gamma}^\dagger | | \pi^{(6)} \rangle \right). \tag{5.47}
\end{aligned}$$

To proceed, we make use of the following relations:

- For terms one and two (left side of Fig. 5.5),

$$\begin{aligned}
\vec{k}_{N_0}^{(5)} + \vec{k}_{\pi}^{(5)} + \vec{k}_e'' + \vec{k}_{\gamma}'' &= 0, \\
\vec{k}_{N_0}^{(6)} + \vec{k}_{\pi}^{(6)} + \vec{k}_e &= 0, \\
\Rightarrow \delta^3(\vec{k}_{N_0}^{(5)} - \vec{k}_{N_0}^{(6)}) \delta^3(\vec{k}_{\pi}^{(5)} - \vec{k}_{\pi}^{(6)}) &= \delta^3(\vec{k}_e'' + \vec{k}_{\gamma}'' - \vec{k}_e) \delta^3(\vec{k}_{\pi}^{(5)} - \vec{k}_{\pi}^{(6)}), \\
\Rightarrow \frac{1}{\omega^{(5)}_{N_0}} \Delta_{N_0^{(5)} N_0^{(6)}} \Delta_{\pi^{(5)} \pi^{(6)}} \Delta_{e' e''} &= \frac{1}{\omega''_{\gamma}} \Delta_{\gamma''(e-e')} \Delta_{\pi^{(5)} \pi^{(6)}} \Delta_{e'' e} \delta_{\mu_{N_0}^{(5)} \mu_{N_0}^{(6)}} \delta_{\tau_{N_0}^{(5)} \tau_{N_0}^{(6)}}, \tag{5.48}
\end{aligned}$$

along with the index identifications $\gamma'' \rightarrow \gamma$ and $(N_0/\pi)^{(4)} \rightarrow (N_0/\pi)''$.

- For term two, in addition,

$$\sum_{\mu^{(4)}_{N_0} \tau^{(4)}_{N_0}} \sum_{\tau^{(4)}_{\pi}} \frac{Dk^{(4)}_{\pi}}{\omega^{(4)}_{N_0}} \dots = \sum_{\tau^{(4)}_{\pi}} \sum_{\tau^{(4)}_{\pi}} \frac{Dk^{(4)}_{N_0}}{\omega^{(4)}_{\pi}} \dots \tag{5.49}$$

- For terms three and four (right side of Fig. 5.5),

$$\begin{aligned}
\vec{k}_{N_0}^{(4)} + \vec{k}_{\pi}^{(4)} + \vec{k}_e'' + \vec{k}_{\gamma}'' &= 0, \\
\vec{k}_{N_0}''' + \vec{k}_{\pi}''' + \vec{k}_e' &= 0, \\
\Rightarrow \delta^3(\vec{k}_{N_0}^{(4)} - \vec{k}_{N_0}''') \delta^3(\vec{k}_{\pi}^{(4)} - \vec{k}_{\pi}''') &= \delta^3(\vec{k}_e'' + \vec{k}_{\gamma}'' - \vec{k}_e') \delta^3(\vec{k}_{\pi}^{(4)} - \vec{k}_{\pi}''') , \\
\Rightarrow \frac{1}{\omega_{N_0}^{(4)}} \Delta_{N_0''' N_0^{(4)}} \Delta_{\pi''' \pi^{(4)}} \Delta_{e'' e} &= \frac{1}{\omega_{\gamma}''} \Delta_{\gamma''(e' - e)} \Delta_{\pi''' \pi^{(4)}} \Delta_{e'' e} \delta_{\mu_{N_0}''' \mu_{N_0}^{(4)}} \delta_{\tau_{N_0}''' \tau_{N_0}^{(4)}} ,
\end{aligned} \tag{5.50}$$

along with the index identifications $\gamma'' \rightarrow \gamma$, $(N_0/\pi)^{(5)} \rightarrow (N_0/\pi)'''$ and $(N_0/\pi)^{(6)} \rightarrow (N_0/\pi)''$.

- For term four, in addition,

$$\sum \frac{Dk_{\pi}^{(6)}}{\omega_{N_0}^{(5)}} \dots = \sum \frac{Dk_{N_0}^{(6)}}{\omega_{\pi}^{(6)}} \dots \tag{5.51}$$

Furthermore, employing the nucleon-pion wave-function normalization (5.16) and inserting the vertex matrix elements (5.35) along with the completeness relation for photons,

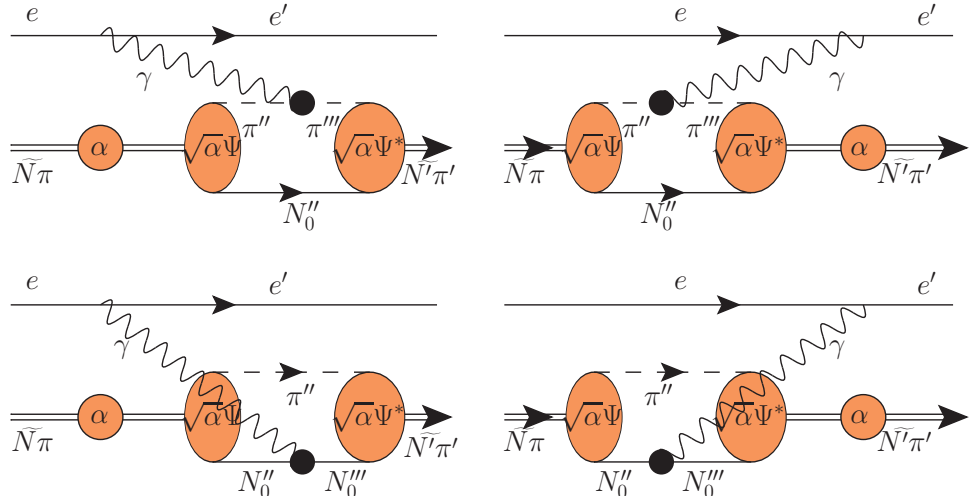


Figure 5.5: Time-ordered diagrams for bare nucleon+pion incoming and bare nucleon+pion outgoing.

Eq. (2.11), the result reads

$$\begin{aligned}
& \langle V' \widetilde{N' \pi'} e' | V_{\text{opt}} | V \widetilde{N \pi} e \rangle \\
&= -\alpha^2 |e|^2 \Delta_{VV'} \sqrt{\frac{\omega'_N}{(m'_{Ne})^3} \frac{\omega_N}{m_{Ne}^3}} \frac{1}{2\omega_\gamma} \sum_{\mu''_{N_0} \tau''_{N_0} \tau''_\pi} \int \frac{d^3 k''_\pi}{\omega''_{N_0} \omega''_\pi} \sqrt{\widetilde{\omega}''_{N_0} \widetilde{\omega}''_\pi} \sqrt{\frac{\omega''_{N_0} + \omega''_\pi}{\widetilde{\omega}''_{N_0} + \widetilde{\omega}''_\pi}} \\
&\quad \times \left(\sum_{\mu'''_{N_0}} \sqrt{\widetilde{\omega}'''_{N_0} \widetilde{\omega}'''_\pi} \sqrt{\frac{\omega'''_{N_0} + \omega''_\pi}{\widetilde{\omega}'''_{N_0} + \widetilde{\omega}'''_\pi}} \Psi^*_{N'/N'''_0 \pi''} \frac{1}{\omega'''_{N_0}} \Psi_{N/N''_0 \pi''} \frac{J^\nu(e, e') J_\nu(N''_0, N'''_0)}{\sqrt{s} - \omega_N - \omega'_e - \omega_\gamma} \right. \\
&\quad + \sqrt{\widetilde{\omega}''_{N_0} \widetilde{\omega}'''_\pi} \sqrt{\frac{\omega''_{N_0} + \omega'''_\pi}{\widetilde{\omega}''_{N_0} + \widetilde{\omega}'''_\pi}} \Psi^*_{N'/N''_0 \pi'''} \frac{1}{\omega'''_\pi} \Psi_{N/N''_0 \pi''} \frac{J^\nu(e, e') J_\nu(\pi'', \pi''')}{\sqrt{s} - \omega_N - \omega'_e - \omega_\gamma} \\
&\quad + \sum_{\mu'''_{N_0}} \sqrt{\widetilde{\omega}'''_{N_0} \widetilde{\omega}''_\pi} \sqrt{\frac{\omega'''_{N_0} + \omega''_\pi}{\widetilde{\omega}'''_{N_0} + \widetilde{\omega}''_\pi}} \Psi^*_{N'/N'''_0 \pi''} \frac{1}{\omega'''_{N_0}} \Psi_{N/N''_0 \pi''} \frac{J^\nu(e, e') J_\nu(N''_0, N'''_0)}{\sqrt{s} - \omega'_N - \omega_e - \omega_\gamma} \\
&\quad \left. + \sqrt{\widetilde{\omega}''_{N_0} \widetilde{\omega}'''_\pi} \sqrt{\frac{\omega''_{N_0} + \omega'''_\pi}{\widetilde{\omega}''_{N_0} + \widetilde{\omega}'''_\pi}} \Psi^*_{N'/N''_0 \pi'''} \frac{1}{\omega'''_\pi} \Psi_{N/N''_0 \pi''} \frac{J^\nu(e, e') J_\nu(\pi'', \pi''')}{\sqrt{s} - \omega'_N - \omega_e - \omega_\gamma} \right) \quad (5.52)
\end{aligned}$$

where we have kept ω_γ ($\vec{k}_\gamma = \vec{k}_e - \vec{k}'_e$ in the first two terms and $\vec{k}_\gamma = \vec{k}'_e - \vec{k}_e$ in the second two terms) and $\omega_{N'''_0/\pi''}$ ($\vec{k}'''_{N_0/\pi} = \vec{k}''_{N_0/\pi} + \vec{k}_\gamma$ in the first two terms and $\vec{k}'''_{N_0/\pi} = \vec{k}''_{N_0/\pi} - \vec{k}_\gamma$ in the second two terms) for readability.

5.5.2 Covariant diagrams

We observe that, except for the pion probability factor α resp. $(1 - \alpha)$, the following expressions are equal:

- Term 1 in (5.40) and term 1 in (5.45)
- Term 2 in (5.40) and term 1 in (5.46)
- Term 2 in (5.45) and term 3 in (5.52)
- Term 3 in (5.45) and term 4 in (5.52)
- Term 2 in (5.46) and term 1 in (5.52)
- Term 3 in (5.46) and term 2 in (5.52)

so that via Eq. (5.27), the result for the overall optical potential reads

$$\begin{aligned}
& \langle V' N' e' | V_{\text{opt}} | V N e \rangle \\
&= (1 - \alpha) |e|^2 \frac{\Delta_{VV'}}{m_{Ne}^3} \sqrt{\frac{\omega'_N \omega_N}{\omega'_{N_0} \omega_{N_0}}} \frac{1}{2\omega_\gamma} \left(\frac{J^\nu(N_0, N'_0) J_\nu(e, e')}{\sqrt{s} - \omega_N - \omega'_e - \omega_\gamma} + \frac{J^\nu(N_0, N'_0) J_\nu(e, e')}{\sqrt{s} - \omega'_N - \omega_e - \omega_\gamma} \right) \\
&+ \alpha |e|^2 \frac{\Delta_{VV'}}{m_{Ne}^3} \sqrt{\omega'_N \omega_N} \frac{1}{2\omega_\gamma} \sum_{\mu''_{N_0} \tau''_{N_0} \tau''_\pi} \int \frac{d^3 k''_\pi}{\omega''_{N_0} \omega''_\pi} \sqrt{\tilde{\omega}''_{N_0} \tilde{\omega}''_\pi} \sqrt{\frac{\omega''_{N_0} + \omega''_\pi}{\tilde{\omega}''_{N_0} + \tilde{\omega}''_\pi}} \\
&\times \left(\sum_{\mu'''_{N_0}} \sqrt{\tilde{\omega}'''_{N_0} \tilde{\omega}'''_\pi} \sqrt{\frac{\omega'''_{N_0} + \omega'''_\pi}{\tilde{\omega}'''_{N_0} + \tilde{\omega}'''_\pi}} \Psi^*_{N'/N''_0 \pi'''} \frac{1}{\omega'''_{N_0}} \Psi_{N/N''_0 \pi''} \frac{J^\nu(e, e') J_\nu(N''_0, N'''_0)}{\sqrt{s} - \omega_N - \omega'_e - \omega_\gamma} \right. \\
&+ \sqrt{\tilde{\omega}''_{N_0} \tilde{\omega}'''_\pi} \sqrt{\frac{\omega''_{N_0} + \omega'''_\pi}{\tilde{\omega}''_{N_0} + \tilde{\omega}'''_\pi}} \Psi^*_{N'/N''_0 \pi'''} \frac{1}{\omega'''_\pi} \Psi_{N/N''_0 \pi''} \frac{J^\nu(e, e') J_\nu(\pi'', \pi''')}{\sqrt{s} - \omega_N - \omega'_e - \omega_\gamma} \\
&+ \sum_{\mu'''_{N_0}} \sqrt{\tilde{\omega}'''_{N_0} \tilde{\omega}''_\pi} \sqrt{\frac{\omega'''_{N_0} + \omega''_\pi}{\tilde{\omega}'''_{N_0} + \tilde{\omega}''_\pi}} \Psi^*_{N'/N''_0 \pi'''} \frac{1}{\omega'''_{N_0}} \Psi_{N/N''_0 \pi''} \frac{J^\nu(e, e') J_\nu(N''_0, N'''_0)}{\sqrt{s} - \omega'_N - \omega_e - \omega_\gamma} \\
&\left. + \sqrt{\tilde{\omega}''_{N_0} \tilde{\omega}'''_\pi} \sqrt{\frac{\omega''_{N_0} + \omega'''_\pi}{\tilde{\omega}''_{N_0} + \tilde{\omega}'''_\pi}} \Psi^*_{N'/N''_0 \pi'''} \frac{1}{\omega'''_\pi} \Psi_{N/N''_0 \pi''} \frac{J^\nu(e, e') J_\nu(\pi'', \pi''')}{\sqrt{s} - \omega'_N - \omega_e - \omega_\gamma} \right) \quad (5.53)
\end{aligned}$$

where in terms 1 (first line, left), 3 and 4 (third and fourth line) we have $\vec{k}_\gamma = \vec{k}_e - \vec{k}'_e$ and $\vec{k}'''_{N_0/\pi} = \vec{k}''_{N_0/\pi} + \vec{k}_\gamma$ and in terms 2 (first line, right), 5 and 6 (fifth and sixth line) we have $\vec{k}_\gamma = \vec{k}'_e - \vec{k}_e$ and $\vec{k}'''_{N_0/\pi} = \vec{k}''_{N_0/\pi} - \vec{k}_\gamma$. Since in *all* terms, we have

$$\vec{k}'''_{N_0/\pi} = \vec{k}''_{N_0/\pi} + \vec{k}_e - \vec{k}'_e \quad (5.54)$$

and the only \vec{k}_γ -dependent quantity, ω_γ , is independent of its sign, we see that *except for the propagators* $\frac{1}{\sqrt{s} - \dots}$, terms 3 and 5 as well as terms 4 and 6 are each equal. Using App. B.3 for combination of the two time orderings, exactly as we did in Sec. 3.1.6, we

finally end up with

$$\begin{aligned}
 & \langle V' N' e' | V_{\text{opt}} | V N e \rangle \\
 &= (1 - \alpha) |e|^2 \frac{\Delta_{VV'}}{m_{Ne}^3} \sqrt{\frac{\omega'_N}{\omega'_{N_0}}} \sqrt{\frac{\omega_N}{\omega''_{N_0}}} \frac{1}{Q^2} J^\nu(N_0, N'_0) J_\nu(e, e') \\
 &+ \alpha |e|^2 \frac{\Delta_{VV'}}{m_{Ne}^3} \sqrt{\omega'_N \omega_N} \frac{1}{Q^2} \sum_{\mu''_{N_0} \tau''_{N_0} \tau''_\pi} \int \frac{d^3 k''_\pi}{\omega''_{N_0} \omega''_\pi} \sqrt{\tilde{\omega}''_{N_0} \tilde{\omega}''_\pi} \sqrt{\frac{\omega''_{N_0} + \omega''_\pi}{\tilde{\omega}''_{N_0} + \tilde{\omega}''_\pi}} \Psi_{N/N'_0 \pi''} \\
 &\times \left(\sum_{\mu'''_{N_0}} \sqrt{\tilde{\omega}'''_{N_0} \tilde{\omega}'''_\pi} \sqrt{\frac{\omega'''_{N_0} + \omega''_\pi}{\tilde{\omega}'''_{N_0} + \tilde{\omega}'''_\pi}} \Psi^*_{N'/N'_0 \pi'''} \frac{1}{\omega'''_{N_0}} J^\nu(e, e') J_\nu(N''_0, N'''_0) \right. \\
 &\quad \left. + \sqrt{\tilde{\omega}''_{N_0} \tilde{\omega}'''_\pi} \sqrt{\frac{\omega''_{N_0} + \omega''_\pi}{\tilde{\omega}''_{N_0} + \tilde{\omega}'''_\pi}} \Psi^*_{N'/N''_0 \pi'''} \frac{1}{\omega'''_\pi} J^\nu(e, e') J_\nu(\pi'', \pi''') \right)
 \end{aligned} \tag{5.55}$$

where $Q^2 = -q^2$ is the negative of the photon four-momentum transfer squared. Note that the three terms above correspond to a photon exchange of an electron with each of the three legs in Fig. 5.1: The first term (first line) corresponds to exchange of a photon with a “bare” nucleon (compare with Eq. (3.22) at the end of Sec. 3.1.6), the second term (second to last line) corresponds to photon exchange with the (bare) nucleon inside the pion loop, and the third term (last line) to photon exchange with the pion. The two possible time orderings have now been merged into a covariant photon propagator; the result being pictured in Fig. 5.6.

5.6 Calculation of nucleon current

In order to obtain an overall expression for the electromagnetic nucleon current including pion loop effects, we equate the result in Eq. (5.55) to the general expression for the invariant one-photon exchange amplitude on hadron level, Eq. (3.22). Furthermore, we transform the integration over the pion momenta from the velocity state (overall c.o.m. frame) to the c.o.m. frame of the nucleon–pion subsystem (coordinates with a “tilde”) in accordance with App. B.1: The transformation prescription reads

$$d^3 k''_\pi = \frac{\omega''_{N_0}}{\tilde{\omega}''_{N_0}} \frac{\omega''_\pi}{\tilde{\omega}''_\pi} \frac{\tilde{\omega}''_{N_0} + \tilde{\omega}''_\pi}{\omega''_{N_0} + \omega''_\pi} d^3 \tilde{k}''_\pi. \tag{5.56}$$

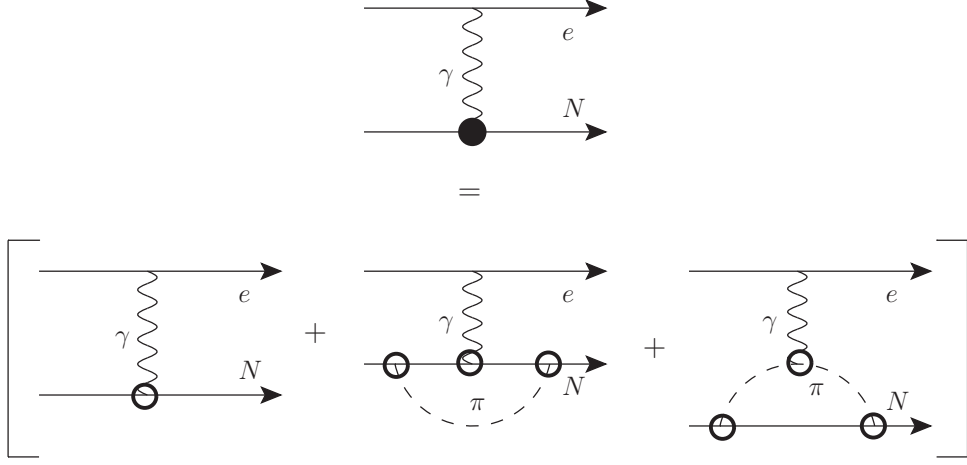


Figure 5.6: Covariant one-photon-exchange amplitude for electron scattering off a nucleon that consists of a bare nucleon and a bare nucleon+pion component. The black blob represents the overall photon-nucleon vertex, which consists of the three contributions shown in the second line. Open circles represent electromagnetic and strong form factors of a bare nucleon.

We then obtain the following expression for the overall nucleon current:

$$\begin{aligned}
 J^\nu(N, N') &= (1 - \alpha) \sqrt{\frac{\omega'_N}{\omega'_{N_0}}} \sqrt{\frac{\omega_N}{\omega_{N_0}}} J^\nu(N_0, N'_0) \\
 &+ \alpha \sqrt{\omega'_N \omega_N} \sum_{\mu''_{N_0} \tau''_{N_0} \tau''_\pi} \int \frac{d^3 \tilde{k}_\pi''}{\sqrt{\tilde{\omega}''_{N_0} \tilde{\omega}''_\pi}} \sqrt{\frac{\tilde{\omega}''_{N_0} + \tilde{\omega}''_\pi}{\omega''_{N_0} + \omega''_\pi}} \Psi_{N/N''_0 \pi''} \\
 &\times \left(\sum_{\mu'''_{N_0}} \sqrt{\tilde{\omega}'''_{N_0} \tilde{\omega}''_\pi} \sqrt{\frac{\omega'''_{N_0} + \omega''_\pi}{\tilde{\omega}'''_{N_0} + \tilde{\omega}''_\pi}} \Psi^*_{N'/N'''_0 \pi''} \frac{1}{\omega'''_{N_0}} J^\nu(N''_0, N'''_0) \right. \\
 &\left. + \sqrt{\tilde{\omega}''_{N_0} \tilde{\omega}'''_\pi} \sqrt{\frac{\omega''_{N_0} + \omega'''_\pi}{\tilde{\omega}''_{N_0} + \tilde{\omega}'''_\pi}} \Psi^*_{N'/N''_0 \pi'''} \frac{1}{\omega'''_\pi} J^\nu(\pi'', \pi''') \right). \tag{5.57}
 \end{aligned}$$

The nucleon-pion wave function becomes (in its own rest frame, cf. Eq. (A.12)), after insertion of the pseudoscalar $N_0\pi$ -vertex (4.7),

$$\tilde{\Psi}_{N/N''_0 \pi''} = \frac{-i g_{N_0} G(\tilde{Q}_\pi^2) \bar{u}_{\tilde{\mu}_{N_0}}(\tilde{k}_{N_0}'') \gamma^5 u_{\tilde{\mu}_{N_0}}(\tilde{k}_{N_0}) \mathcal{F}(\tau_{N_0}, \tau''_{N_0}, \tau''_\pi) \sqrt{1 - \alpha}}{2 \sqrt{2} (2\pi)^3 \sqrt{m_{N_0} \tilde{\omega}''_{N_0} \tilde{\omega}''_\pi} (m_N - \tilde{\omega}''_{N_0} - \tilde{\omega}''_\pi)} \frac{\sqrt{1 - \alpha}}{\sqrt{\alpha}}, \tag{5.58}$$

(analogously for triple-primed expressions), where $G(\tilde{Q}_\pi^2)$ is the strong nucleon form factor in dependence of the squared four-momentum transferred to the nucleon by the pion.

Since, due to the nature of the electromagnetic interaction, $\tau_{N_0} = \tau'_{N_0}$ and $\tau''_{N_0/\pi} = \tau'''_{N_0/\pi}$, the product of flavor functions in Eq. (5.57) becomes

$$\mathcal{F}^2(\tau''_\pi) := \mathcal{F}(\tau_{N_0}, \tau''_{N_0}, \tau''_\pi) \mathcal{F}(\tau_{N_0}, \tau''_{N_0}, \tau''_\pi) \quad (5.59)$$

and thus, via Eq. (2.69), takes on the values

$$\mathcal{F}^2(0) = \delta_{\tau_{N_0} \tau''_{N_0}} \quad \text{and} \quad \mathcal{F}^2(\pm 1) = 2 \left(1 - \delta_{\tau_{N_0} \tau''_{N_0}} \right) . \quad (5.60)$$

Due to the nature of its derivation, the wave function (5.58) is defined in the rest frame of the nucleon–pion subsystem (coordinates with a “tilde”). In order to obtain the wave function in the boosted system (overall rest frame), we proceed analogously to Sec. 3.3.2 using Eq. (5.13), whence

$$\begin{aligned} & \bar{u}_{\tilde{\mu}_{N_0}''}(\tilde{k}_{N_0}'') \gamma^5 u_{\tilde{\mu}_{N_0}}(\tilde{k}_{N_0}) \\ & \longrightarrow \sum_{\tilde{\mu}_{N_0}, \tilde{\mu}_{N_0}''} D_{\mu_{N_0}'' \tilde{\mu}_{N_0}''}(B(v_{N_0\pi}''), \frac{\tilde{k}_{N_0}}{m_{N_0}}) \bar{u}_{\tilde{\mu}_{N_0}''}(\tilde{k}_{N_0}'') \gamma^5 u_{\tilde{\mu}_{N_0}}(\tilde{k}_{N_0}) D_{\mu_{N_0} \tilde{\mu}_{N_0}}^*(B(v_{N_0}), \frac{\tilde{k}_{N_0}}{m_{N_0}}) \end{aligned} \quad (5.61)$$

(and likewise for triple-primed states), where $v_{N_0\pi}''$ is the relativistic velocity of the nucleon–pion subsystem with invariant mass $m_{N_0\pi}$, cf. Eqs. (5.13) and (5.14). Since in the incoming and outgoing states, where there is no pion present, we have a boost with $v_{N_0} = \frac{k_{N_0}}{m_{N_0}}$ and also, $\tilde{v}_{N_0} = 0$, we see that via Eq. (2.43), the second Wigner-D-function in Eq. (5.61) reduces to a Kronecker delta (compare to Eq. (3.56)!). The overall Wigner factor which then enters equation (5.57) is

$$D_{\mu_{N_0}'' \tilde{\mu}_{N_0}''}(B(v_{N_0\pi}''), \frac{\tilde{k}_{N_0}}{m_{N_0}}) D_{\mu_{N_0}''' \tilde{\mu}_{N_0}'''}^*(B(v_{N_0\pi}'''), \frac{\tilde{k}_{N_0}}{m_{N_0}}) \quad (5.62)$$

for the first part (nucleon struck) and

$$D_{\mu_{N_0}'' \tilde{\mu}_{N_0}''}(B(v_{N_0\pi}''), \frac{\tilde{k}_{N_0}}{m_{N_0}}) D_{\mu_{N_0}''' \tilde{\mu}_{N_0}'''}^*(B(v_{N_0\pi}'''), \frac{\tilde{k}_{N_0}}{m_{N_0}}) \quad (5.63)$$

for the second part (pion struck; note that due to the spectator conditions, $\mu_{N_0}''' = \mu_{N_0}''$!), with a sum over each spin polarization with a “tilde” implied.

The final result for the electromagnetic nucleon current reads

$$\begin{aligned}
& J^\nu(N, N') \\
&= (1 - \alpha) \sqrt{\frac{\omega'_N}{\omega'_{N_0}}} \sqrt{\frac{\omega_N}{\omega_{N_0}}} J^\nu(N_0, N'_0) \\
&+ (1 - \alpha) \sqrt{\omega'_N \omega_N} \sum_{\mu''_{N_0} \tau''_{N_0} \tau''_\pi \tilde{\mu}''_{N_0}} \mathcal{F}^2(\tau''_\pi) \int \frac{d^3 \tilde{k}''_\pi}{\sqrt{\tilde{\omega}''_{N_0} \tilde{\omega}''_\pi}} \sqrt{\frac{\tilde{\omega}''_{N_0} + \tilde{\omega}''_\pi}{\omega''_{N_0} + \omega''_\pi}} \\
&\times \frac{\left(g_{N_0} G(\tilde{Q}_\pi^2) \right)^2}{8(2\pi)^3} \frac{\bar{u}_{\tilde{\mu}'_{N_0}}(\tilde{k}''_{N_0}) \gamma^5 u_{\tilde{\mu}_{N_0}}(\tilde{k}_{N_0}) D_{\mu''_{N_0} \tilde{\mu}''_{N_0}}(B(v''_{N_0 \pi}), \frac{\tilde{k}_{N_0}}{m_{N_0}})}{\sqrt{m_{N_0} \tilde{\omega}''_{N_0} \tilde{\omega}''_\pi} (m_N - \tilde{\omega}''_{N_0} - \tilde{\omega}''_\pi)} \\
&\times \sum_{\tilde{\mu}'''_{N_0}} \sqrt{\tilde{\omega}'''_{N_0} \tilde{\omega}'''_\pi} \frac{\bar{u}_{\tilde{\mu}'_{N_0}}(\tilde{k}'_{N_0}) \gamma^5 u_{\tilde{\mu}'''_{N_0}}(\tilde{k}'''_{N_0})}{\sqrt{m_{N_0} \tilde{\omega}'''_{N_0} \tilde{\omega}'''_\pi} (m_N - \tilde{\omega}'''_{N_0} - \tilde{\omega}'''_\pi)} \\
&\times \left(\sum_{\mu'''_{N_0}} \sqrt{\frac{\omega'''_{N_0} + \omega''_\pi}{\tilde{\omega}'''_{N_0} + \tilde{\omega}'''_\pi}} \frac{1}{\omega'''_{N_0}} J^\nu(N''_0, N'''_0) D_{\mu'''_{N_0} \tilde{\mu}'''_{N_0}}^*(B(v'''_{N_0 \pi}), \frac{\tilde{k}'''_{N_0}}{m_{N_0}}) \right. \\
&\left. + \sqrt{\frac{\omega''_{N_0} + \omega'''_\pi}{\tilde{\omega}'''_{N_0} + \tilde{\omega}'''_\pi}} \frac{1}{\omega'''_\pi} J^\nu(\pi'', \pi''') D_{\mu''_{N_0} \tilde{\mu}'''_{N_0}}^*(B(v'''_{N_0 \pi}), \frac{\tilde{k}'''_{N_0}}{m_{N_0}}) \right)
\end{aligned} \tag{5.64}$$

where α is the pion loop probability, m_{N_0} the bare nucleon mass, g_{N_0} the bare strong nucleon-pion coupling constant, $G(\tilde{Q}_\pi^2)$ the strong form factor of the bare nucleon, $J^\nu(N''_0, N'''_0)$ the electromagnetic current of the bare nucleon in the intermediate state and $J^\nu(\pi'', \pi''')$ the corresponding electromagnetic pion current. The evaluation of these quantities using the results in App. A and Secs. 3.6 and 4.6 as well as in [Bie11] is explained in Sec. 5.7.

5.6.1 Kinematics

For the system containing the electron and the physical nucleon, we choose the same kinematics as in Sec. 3.4:

$$\begin{aligned}
k_N &= \begin{pmatrix} \sqrt{k^2 + m_N^2} \\ -\frac{Q}{2} \\ 0 \\ \sqrt{k^2 - \frac{Q^2}{4}} \end{pmatrix} \xrightarrow{k \rightarrow \infty} \begin{pmatrix} k \\ -\frac{Q}{2} \\ 0 \\ k \end{pmatrix}, \quad q = \begin{pmatrix} 0 \\ Q \\ 0 \\ 0 \end{pmatrix}, \\
k'_N &= k_N + q = \begin{pmatrix} \sqrt{k^2 + m_N^2} \\ \frac{Q}{2} \\ 0 \\ \sqrt{k^2 - \frac{Q^2}{4}} \end{pmatrix} \xrightarrow{k \rightarrow \infty} \begin{pmatrix} k \\ \frac{Q}{2} \\ 0 \\ k \end{pmatrix}.
\end{aligned} \tag{5.65}$$

For the pion momentum we make no assumptions. Since we will use spherical integration in the “tilde” frame, which is the rest frame of the physical nucleon, we use the parametrization

$$\begin{aligned}\tilde{k}_{N_0} &= \begin{pmatrix} m_{N_0} \\ 0 \\ 0 \\ 0 \end{pmatrix}, \quad \tilde{k}_\pi'' = \begin{pmatrix} \sqrt{\tilde{\kappa}^2 + m_\pi^2} \\ \tilde{\kappa} \sin \tilde{\theta} \cos \tilde{\phi} \\ \tilde{\kappa} \sin \tilde{\theta} \sin \tilde{\phi} \\ \tilde{\kappa} \cos \tilde{\theta} \end{pmatrix}, \\ \tilde{k}_{N_0}'' &= \tilde{k}_{N_0} - \tilde{k}_\pi'' \quad \Rightarrow \quad \tilde{k}_{N_0}'' = \begin{pmatrix} \sqrt{\tilde{\kappa}^2 + m_{N_0}^2} \\ -\tilde{\kappa} \sin \tilde{\theta} \cos \tilde{\phi} \\ -\tilde{\kappa} \sin \tilde{\theta} \sin \tilde{\phi} \\ -\tilde{\kappa} \cos \tilde{\theta} \end{pmatrix},\end{aligned}\tag{5.66}$$

with the integration measure

$$d^3\tilde{k}_\pi'' = \tilde{\kappa}^2 \sin \tilde{\theta} d\tilde{\kappa} d\tilde{\theta} d\tilde{\phi}.\tag{5.67}$$

The 4-momentum transfer for pion emission/absorption in the “tilde” frame thus reads

$$\begin{aligned}\tilde{Q}_\pi^2 &= -\tilde{q}_\pi^2 = -\left(\tilde{k}_{N_0} - \tilde{k}_{N_0}''\right)^2 = -\begin{pmatrix} m_{N_0} - \sqrt{\tilde{\kappa}^2 + m_{N_0}^2} \\ \tilde{\kappa} \sin \tilde{\theta} \cos \tilde{\phi} \\ \tilde{\kappa} \sin \tilde{\theta} \sin \tilde{\phi} \\ \tilde{\kappa} \cos \tilde{\theta} \end{pmatrix}^2 \\ &= -2m_{N_0}^2 + 2m_{N_0}\sqrt{\tilde{\kappa}^2 + m_{N_0}^2}.\end{aligned}\tag{5.68}$$

5.7 Numerical implementation

For the numerical treatment of the result (5.64) we use a similar procedure as in Secs. 3.5 and 4.5. However, we first have to clarify some points on the “bare” quantities we will use.

5.7.1 Form-factor input

Pion electromagnetic form factor: The electromagnetic current for a charged pion reads [EW88]

$$J^\nu(\pi^\pm, \pi^\pm') = \pm G_\pi^{\text{em}}(Q^2) (k_\pi^\nu + k_\pi'^\nu),\tag{5.69}$$

where $G_\pi(Q^2)$ is the electromagnetic pion form factor in dependence of four-momentum transfer squared. We take the result from [Bie11] and parametrize it, like the strong $\pi N_0 N_0$ form factor (cf. Eq. 4.46), in the form

$$G_\pi^{\text{em}}(Q^2) = \frac{1}{1 + \frac{Q^2}{\Lambda_1^2} + \left(\frac{Q^2}{\Lambda_2^2}\right)^2}\tag{5.70}$$

with $\Lambda_1^2 = 0.67$ and $\Lambda_2^2 = 1.59$.

Bare electromagnetic nucleon form factors: The electromagnetic current $J^\nu(N_0'', N_0''')$ in (5.64) is “bare”, i.e. it relates to a nucleon with bare mass m_{N_0} . We thus have to readjust the results of Chap. 3, which we obtained for the electromagnetic nucleon form factors leaving out the pion cloud.

Recall that these have been extracted from a microscopic expression for the physical nucleon current $J^\nu(N, N')$, Eq. (3.58), which uses the three-quark wave function obtained by Schlumpf [Schl92]. This wave function has been refitted by Pasquini and Boffi [PB07] to yield the best possible results for a problem (bare nucleon plus meson cloud) similar to the one we are dealing with here. We thus repeat the same procedure as described in Chap. 3, this time using the Pasquini–Boffi wave function, and use a parametrization of the result as described in Sec. 3.6 as input.

Note that in the main analytic result of Chap. 3, Eq. (3.58), the only dependence of the nucleon current on the nucleon mass is via the $\sqrt{\omega'_N \omega_N}$ factor (equals $k^2 + m_N^2$ in the kinematics (3.65)) in the first line. Since we use the infinite momentum frame with $k \rightarrow \infty$, it is irrelevant which nucleon mass is used in the currents. The (normalized) current of the bare nucleon and the three-quark-contribution to the physical nucleon current differ by just a factor $(1 - \alpha)$. Taking the physical nucleon mass in Eqs. (2.58) and (3.70) thus already gives the three-quark-contribution to the electromagnetic (Sachs) form factors of the physical nucleon. We finally use Eq. (2.57) in combination with (2.9) with bare nucleon masses m_{N_0} instead of physical ones, i.e. the replacement

$$F_2 = \frac{m_N}{k Q} J_{\frac{1}{2}, -\frac{1}{2}}^0 \quad \longrightarrow \quad \frac{m_{N_0}}{m_N} F_2 = \frac{m_{N_0}}{k Q} J_{\frac{1}{2}, -\frac{1}{2}}^0 \quad (5.71)$$

to obtain the bare nucleon current $J^\nu(N_0'', N_0''')$.

Bare nucleon–pion strong form factor: In what follows, we will restrict ourselves to pseudoscalar coupling. Since we start with a given 3-quark wave function of the bare nucleon instead of solving the pure confinement problem, we have to determine the bare nucleon mass m_0 . This cannot be done directly by solving the equation for nucleon-mass renormalization due to pion loops, since m_0 enters also the $\pi N_0 N_0$ coupling constant and the strong form factor, which are again needed to calculate the pion-loop kernel for the mass-renormalization equation. We thus employ a self-consistent iteration procedure which is sketched in Fig. 5.7:

First note that we can determine the quantities m_{N_0} and subsequently α from Eqs. (A.15) and (A.13). However, for this we need the *bare* nucleon–pion vertex, $\langle N'_0 \pi' || K_\pi^\dagger || N_0 \rangle = g_{N_0} J^5(N_0, N'_0)$. In principle, this vertex can be obtained from the result for the strong pseudoscalar current in Eq. (4.33). However, we know neither the bare nucleon mass m_{N_0} nor the bare nucleon–pion coupling constant g_{N_0} . We therefore do the following: First, we evaluate Eq. (4.33) for the physical nucleon mass, as has already been done in Chap. 4, this time with the already obtained quark coupling constant $g = 3.55$ (which we keep constant). We then obtain a new (“bare”) nucleon–pion coupling constant g_{N_0} and new parametrizations Λ_1, Λ_2 of the strong form factor which we

feed back into equation (A.15) to obtain a new nucleon mass m'_{N_0} which is fed back into Eqs. (4.33) (replacing m_N wherever needed), and so on. After 4 iterations the values of m'_{N_0} and g'_{N_0} converge with sufficient precision to give the desired values m_{N_0} and g_{N_0} for the bare nucleon. As a side product, we also obtain the pion loop probability α via Eq. (A.13). The results are shown in Tab. 5.1.

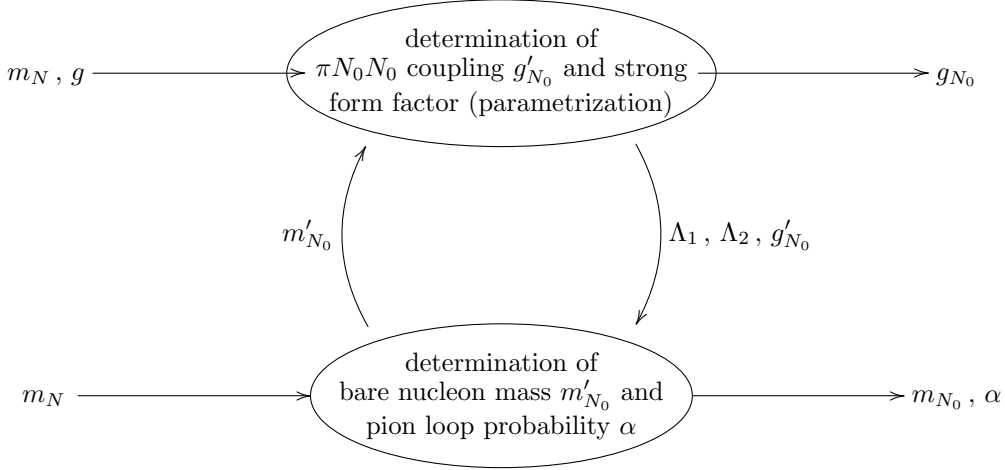


Figure 5.7: Flow chart for self-consistent calculation of $\pi N_0 N_0$ coupling, vertex form factor, bare nucleon mass and pion-loop probability α given the $3q$ wave function of the bare nucleon.

Run	g'_{N_0}	Λ_1	Λ_2	m'_{N_0}	α
1	13.00	0.648	1.65	1.08	0.12
2	14.87	0.634	1.51	1.10	0.13
3	15.16	0.631	1.51	1.11	0.14
4	15.30	0.631	1.48	1.11	0.14

Table 5.1: Iterations for the determination of the bare nucleon mass m_{N_0} , the bare nucleon–pion coupling constant g_{N_0} and the pion loop probability α .

5.7.2 Class structure in C++

Functions for Pauli and Dirac matrices, `Matrix2cd pauli (int i)` and `Matrix4cd dirac (int i)`, are defined globally. So are the fits for the pion electromagnetic form factor (5.70), `double pielmagff (double qsquared)` the proton and neutron electric and magnetic Sachs form factors (Eq. (3.72) and following table as well as Eq. (3.73)), `double pelfff (double qsquared)`, `double pmagff (double qsquared)`, `double nelfff (double qsquared)` and `double nmagff (double qsquared)`, as well as the strong nucleon–pion form factor (4.46):

```
double strongff (Vector4d kin,Vector4d kout){
double l1 = 0.554; double l2 = 0.823;
    // fit parameters
double Q2 = - pow((kin(0)-kout(0)),2) + pow((kin(1)-kout(1)),2)
    + pow((kin(2)-kout(2)),2) + pow((kin(3)-kout(3)),2);
    // momentum transfer squared
return 1/(1 + Q2/l1 + pow(Q2/l2,2)); }
```

Any quantities which depend on the momenta \tilde{k}_{N_0}'' , \tilde{k}_π'' of the nucleon and the pion in the intermediate state are again calculated in a class called `Mompart` which has a structure very similar to the one we used in Sec. 3.5.1. It is initialized again and again for each point of the Monte Carlo integration with the 3 independent momentum components of the pion, `double karray [3]` (spherical coordinates) and a pointer to parameters, `InputParams * params`, where the `struct InputParams` now contains parameters like the forward momentum of the nucleon (`double k`), the momentum transfer by the photon (`double Q`), the double value of the nucleon isospin and outgoing spin projections (`int tauN, muNpr`), double nucleon and pion isospins in the intermediate state (`int tauN02pr, taupi2pr`), which hadron in the intermediate state is to be struck by the photon (`char struckhadron`), the number of MC integration points (`size_t intpoints`) as well as the bare nucleon mass and the pion loop probability (`double mN0, alpha`).

The public functions of the `Mompart` class are: The Wigner rotations `Matrix2cd wigrotfactor2pr()` and `Matrix2cd wigrotfactor3prstar()`, the nucleon–pion wave functions `Matrix2cd NOpiwavefunction()` and `Matrix2cd NOpiwavefunctionprst()`, the electromagnetic currents of the nucleon and the pion in the intermediate state, `Matrix2cd nucleoncurrent()` and `double pioncurrent()`, as well as a prefactor `double prefactor()`. Note that all but the last two of these functions are complex 2×2 matrices in their spin polarization components.

The private functions are once again the Lorentz boost with 4-velocity `u` and its inverse in standard (2.35), (2.36) and $SL(2, \mathbb{C})$ (2.40) representations, `Matrix4d [inv]boost (Vector4d u)` and `Matrix2cd [inv]spinboost (Vector4d u)`. Also, the generic currents $\bar{u}_\mu(\vec{k}')\gamma^\nu u_\mu(\vec{k})$ and $\bar{u}_{\mu'}(\vec{k}')[\gamma^\nu, \gamma^\lambda] u_\mu(\vec{k})$ which are needed for constructing the electromagnetic nucleon current from the form factors, cf. Eq. (2.57): `Matrix2cd currentmatrix (Vector4d kin, Vector4d kout, int`

`mu`) and `Matrix2cd currentmatrix (Vector4d kin, Vector4d kout, int mu, int nu)` (overloaded function), as matrices in the spin polarizations; for details see Sec. 3.5.4. Note, however, that these are currents for the “bare” nucleon, i.e. in these definitions, the bare nucleon mass `mN0` is used.

In what follows, the class initialization and the more important or less obvious functions are discussed in detail.

5.7.3 Kinematic quantities

The initialization for the local variables reads

```
Mompart::Mompart (double karray[3] , InputParams * params):  
  
    kappatilde (karray[0]), thetatile (karray[1]),  
    phitilde (karray[2]), k (params->k), Q (params->Q),  
    struckhadron (params->struckhadron),  
    alpha(params->alpha), mN0(params->mN0),  
    tauN02pr (params->tauN02pr), taupi2pr (params->taupi2pr),  
    muNpr (params->muNpr), tauN (params->tauN)
```

We then (in the part written in curly brackets in the code) start out by initializing the 4-momenta of the nucleon and the pion in the “tilde” frame in spherical coordinates, Eq. (5.66):

```
Vector4d kN0tilde, kN0tilde2pr, kpitilde2pr; //in class declaration  
  
kN0tilde << mN0 , 0 , 0 , 0;  
  
kpitilde2pr << sqrt(pow(kappatilde,2) + pow(mpi,2)),  
            kappatilde*sin(thetatile)*cos(phitilde),  
            kappatilde*sin(thetatile)*sin(phitilde),  
            kappatilde*cos(thetatile);  
  
kN0tilde2pr << sqrt(pow(kappatilde,2) + pow(mN0,2)),  
            - kappatilde*sin(thetatile)*cos(phitilde),  
            - kappatilde*sin(thetatile)*sin(phitilde),  
            - kappatilde*cos(thetatile);
```

Following this, we introduce the invariant mass of the $N_0\pi$ subsystem and its velocity by means of Eq. (5.14) using the kinematics (5.65),

```
double mcl2pr; Vector4d vcl2pr; //in class declaration

mcl2pr = kN0tilde2pr(0)+kpitilde2pr(0);

vcl2pr << sqrt(pow(k,2)+pow(mcl2pr,2))/mcl2pr,
-Q/(2*mcl2pr),
0,
sqrt(pow(k,2)-pow(Q,2)/4)/mcl2pr;
```

Intermediate nucleon and pion momenta in the overall c.o.m. frame are obtained via a boost as defined in (2.35) with velocity `vcl2pr`:

```
Vector4d kN02pr, kpi2pr; //in class declaration
kN02pr = boost(vcl2pr)*kN0tilde2pr;
kpi2pr = boost(vcl2pr)*kpitilde2pr;
```

In the boosted frame the momentum transfer to the bare nucleon or the pion in the intermediate state (depending on the diagram) is the same as the one to the physical nucleon as a whole in (5.65). Via the spectator conditions (5.34) the other particle remains unaffected:

```
Vector4d kN03pr, kpi3pr; //in class declaration

if (struckhadron == 'N'){
kN03pr(1) = kN02pr(1) + Q;
kN03pr(2) = kN02pr(2);
kN03pr(3) = kN02pr(3);
kN03pr(0) = sqrt(pow(mN0,2)+pow(kN03pr(1),2)+pow(kN03pr(2),2)+...);
kpi3pr = kpi2pr;}

else if (struckhadron == 'pi'){
kpi3pr(1) = kpi2pr(1) + Q;
kpi3pr(2) = kpi2pr(2);
kpi3pr(3) = kpi2pr(3);
kpi3pr(0) = sqrt(pow(mpi,2)+pow(kpi3pr(1),2)+pow(kpi3pr(2),2)+...);
kN03pr = kN02pr;}
```

We then get the triple-primed invariant mass and velocity (5.14) for the $N_0\pi$ subsystem (in the kinematics (5.65)) via

```
double mcl3pr; Vector4d vcl3pr; //in class declaration

mcl3pr = sqrt(pow((kN03pr(0) + kpi3pr(0)),2) - pow(k,2));
vcl3pr << (sqrt(pow(k,2) + pow(mcl3pr,2))/mcl3pr) ,
    Q/(2*mcl3pr) ,
    0 ,
    (sqrt(pow(k,2) - pow(Q,2)/4)/mcl3pr);
```

and the triple-primed nucleon and pion momenta in the “tilde” frame via an inverse boost (2.36):

```
Vector4d kN0tilde3pr, kpitilde3pr; //in class declaration
kN0tilde3pr = invboost(vcl3pr)*kN03pr;
kpitilde3pr = invboost(vcl3pr)*kpi3pr;
```

This ends the initialization of the class `Mompart`. In what follows, we discuss its public functions.

5.7.4 Currents and wave functions from form factors

The following public function of the `Mompart` class yields the 0-component of the electromagnetic current of the intermediate, bare nucleon (double- and triple-primed states, momenta `kN02pr` and `kN03pr`) as a complex 2×2 matrix in spin polarization components `int muN02pr, muN03pr = -1,1`. First the local variables for the electric and magnetic Sachs form factors, `GE` and `GM`, for the kind of particle determined by `tauN02pr`, are set to the values given in Sec. 3.6, `double n/p/el/magff(pow(Q,2))` (see above). Since these fits describe form factors determined for a physical rather than bare nucleon, we then use the physical nucleon mass `mN` to determine the corresponding Dirac and Pauli form factors `double F1` and `double F2` via Eqs. (2.58) and additionally, `double F2` gets multiplied by a factor `mN0/mN` as explained in the second paragraph of Sec. 5.7.1. The zero component of the nucleon current is then obtained via Eq. (2.57) with bare nucleon masses `mN0` instead of physical ones.

```

Matrix2cd Mompart::nucleoncurrent (){

double GE, GM; // Sachs form factors

    if (tauN02pr == -1){ //neutron
GE = nelff(pow(Q,2)); GM = nmagff(pow(Q,2));}
    else if (tauN02pr == 1){ //proton
GE = pelff(pow(Q,2)); GM = pmagff(pow(Q,2));}

double F1 = (GE + pow(Q,2)/(4*pow(mN,2)) * GM)/
            ( 1 + pow(Q,2)/(4*pow(mN,2)) );
double F2 = mN0/mN * (GM-GE)/(1+pow(Q,2)/(4*pow(mN,2)));

Matrix2cd nuclcurrent = F1*currentmatrix(kN02pr,kN03pr,0);
for (int nu =1; nu<=3; nu++){
    nuclcurrent += F2 * (kN03pr-kN02pr)(nu)/(4*mN) *
    currentmatrix(kN02pr,kN03pr,0,nu); }
return nuclcurrent; }

```

The pion current (5.69) depends on the isospin of the pion. Its zero component (which is the only one we need) reads

```

double Mompart::pioncurrent (){ int e;
if (taupi2pr== -2) e=-1; else if (taupi2pr== 0) e=0; else e=1;
return e * pielmagff(Qpi23squared) * (kpi2pr+kpi3pr)(0); }

```

Note that we use both $kN03pr$ and $kpi3pr$ even though one of them (depending on the parameter `struckhadron`) is always equal to $kN02pr$ resp. $kpi2pr$. The nucleon–pion wave functions (5.58) (again implemented as complex 2×2 matrices in spin polarization components $\mu N0tilde$, $\mu N0tilde2pr$) read

```

Matrix2cd Mompart::N0piwavefunction () { return
sqrt((1-alpha)/alpha)*gN0*strongff(kN0tilde,kN0tilde2pr) *
currentmatrix(kN0tilde,kN0tilde2pr,5) /
(2*sqrt(2*pow(2*pi,3)) *
sqrt(mN0*kN0tilde2pr(0)*kpitilde2pr(0)) *
(mN-kN0tilde2pr(0)-kpitilde2pr(0))); }

```

and

```
Matrix2cd Mompart::N0piwavefunctionprst () { return
sqrt((1-alpha)/alpha)*gN0*strongff(kN0tilde,kN0tilde3pr) *
currentmatrix(kN0tilde3pr,kN0tilde,5) /
(2*sqrt(2*pow(2*pi,3)) *
sqrt(mN0*kN0tilde3pr(0)*kpitilde3pr(0)) *
(mN-kN0tilde3pr(0)-kpitilde3pr(0)); }
```

where `Matrix2cd currentmatrix` is defined analogously to Sec. 3.5.4 and the isospin dependence $\mathcal{F}^2(\tau_\pi'')$ has been left out for now.

5.7.5 Wigner rotations

The Wigner rotations (5.62) (and (5.63), but this case is included by construction) are implemented as follows:

```
Matrix2cd Mompart::wigrotfactor2pr () { return
invspinboost(kN02pr/mN0) *
spinboost(vcl2pr) *
spinboost(kN0tilde2pr/mN0); }
```

and

```
Matrix2cd Mompart::wigrotfactor3prstar () { return
invspinboost(kN0tilde3pr/mN0) *
invspinboost(vcl3pr) *
spinboost(kN03pr/mN0); }
```

The final public function of the `Mompart` class is the remaining prefactor `double Mompart::prefactor ()` which is trivial. This ends the description of the `Mompart` class.

5.7.6 Bare part

The $\nu = 0$ component of the bare nucleon current (first line) in Eq. (5.64) is obtained as a 2×2 matrix in spin polarizations μ'_N and μ_N (`muNpr` and `muN`) as follows: First, the extraction of Dirac and Pauli form factors $F1$ and $F2$ from Sec. 3.6 works exactly as in Sec. 5.7.4. Then, in the kinematics (5.65), we first calculate the forward momentum of the bare nucleon, $\vec{k}_0 := \frac{m_{N_0}}{m_N} \vec{k}$, then the prefactor, and finally, via Eq. (3.70) (replace physical by bare quantities), the bare nucleon current:

```
Matrix2d barepart (InputParams  inp){
Matrix2d nuclcurrent;
double k0 = inp.mN0/mN * inp.k;

double prefactor = (1-inp.alpha) * sqrt(pow(inp.k,2)+pow(mN,2)) /
                     sqrt(pow(k0,2)+pow(inp.mN0,2));
nuclcurrent (0,0) = 2*k0*F1;
nuclcurrent (1,0) = (k0*inp.Q/inp.mN0) * F2;
nuclcurrent (0,1) = -(k0*inp.Q/inp.mN0) * F2;
nuclcurrent (1,1) = 2*k0*F1;

return prefactor * nuclcurrent; }
```

5.7.7 Integration

The integrand in (5.64) reads

```
complex<double> integrand (double karray[3], InputParams*params){
Mompert mp (karray, params);
Matrix2cd intgrmatrix;

if (params->struckhadron=='N'){
    intgrmatrix = mp.prefactor () *
        (params->taupi2pr == 0 ? 1 : 2)*
            mp.N0piwavefunctionprst () *
            mp.wigrotfactor3prstar () *
            mp.nucleoncurrent ()*
            mp.wigrotfactor2pr () *
            mp.N0piwavefunction ();
}
else if (params->struckhadron=='p'){
    intgrmatrix = mp.prefactor () *
        (params->taupi2pr == 0 ? 1 : 2)*
            mp.N0piwavefunctionprst () *
            mp.wigrotfactor3prstar () *
            mp.pioncurrent () *
            mp.wigrotfactor2pr () *
            mp.N0piwavefunction ();
} else intgrmatrix << 0,0,0,0;

return intgrmatrix((1-params->muNpr)/2,(1-muN)/2); }
```

where instead of the sums over $\tilde{\mu}_{N_0}''$, μ_{N_0}'' , μ_{N_0}''' and $\tilde{\mu}_{N_0}'''$ in the first part resp. $\tilde{\mu}_{N_0}''$, μ_{N_0}'' and $\tilde{\mu}_{N_0}'''$ in the second part we use simple matrix multiplication. Summation over τ_{N_0}'' resp. τ_π'' is achieved at a higher level (via `params->taupi2pr`).

Integration is then performed exactly as in Sec. 3.5.6, except only in three dimensions, with `double kmax[] = {10,3.1416,6.2832}`. A simple main function writing the results for various values of the momentum transfer Q and both outgoing nucleon spin polarizations `muNpr` to an ASCII output file (CSV table) `out.csv` could look like this:

```

int main(){
    InputParams inpar;
    inpar.k = 1000000; // forward momentum of nucleon
    inpar.intpoints = 10000; // number of MC integration points
    inpar.tauN = 1 // for proton, -1 for neutron
    inpar.alpha = 0.10; inpar.mN0 = 1.00; // from iteration
    char part = 'b' // for bare part, 'N' for nucleon, 'p' for pion struck

    ofstream outfile; outfile.open("out.csv");
    outfile << "Q^2;;samespin;spinflip" << endl << endl;

    for (inpar.Q=0.0001; inpar.Q<2.0002; inpar.Q+=0.1){
        outfile << pow(inpar.Q,2) << ";;" ;
        for (inpar.muNpr=1; inpar.muNpr>=-1; inpar.muNpr-=2){
            double result = 0;

            if (part == 'b'){
                result = barepart(inpar)((1-inpar.muNpr)/2,(1-muN)/2); }
            else {inpar.struckhadron = part;

                if (part == 'p') {
                    inpar.tauN02pr = -inpar.tauN; //pi^0 loops give no contrib.
                    inpar.taupi2pr = inpar.tauN - inpar.tauN02pr;
                    result = integration(inpar);
                }
                else if (part == 'N') {
                    for (inpar.tauN02pr=-1; inpar.tauN02pr<=1; inpar.tauN02pr+=2){
                        inpar.taupi2pr = inpar.tauN - inpar.tauN02pr;
                        result += integration(inpar); }
                    } else return (0); } // end if-else

            outfile << result << ";" ; } // end for (inpar.muNpr)
            outfile << endl; } // end for (inpar.Q)
            outfile.close(); return (0); }

```

Depending on the setting for `char part`, the result yields either the bare part (first term) of the nucleon current (5.64), or the pion loop contribution for the struck nucleon (second term) or the struck pion (third term); the form factors are then obtained via Eq. (3.70) (using physical nucleon masses!) using a tool of choice.

5.8 Results

5.8.1 Summary of results

The main results of our calculations as well as a comparison with results by Pasquini and Boffi [PB07] and experimental values [PDG] are shown in Tab. 5.2 and in figures referenced therein. For results concerning the mean quadratic charge radius, which (in the relativistic case) is defined as

$$\langle r_{EN}^2 \rangle := -6 \frac{dG_E^N(Q^2)}{dQ^2} \Big|_{Q^2=0}, \quad (5.72)$$

see Tab. 5.3.

	loop N	loop π	loop	bare	sum	f.f.	Fig.
Q_p	0.05	0.09	0.14	0.86	1.0	G_E^p	5.8
μ_p	0.04	0.14	0.19	2.39	2.58	G_M^p	5.9
Q_n	0.0	G_E^n	5.10
μ_n	0.01	-0.14	-0.13	-1.45	-1.58	G_M^n	5.11
Q_p [PB07]	.	.	0.09	0.91	1.0	G_E^p	
μ_p [PB07]	0.18	.	0.35	2.52	2.87	G_M^p	
Q_n [PB07]	0.0	G_E^n	
μ_n [PB07]	-0.12	.	-0.29	-1.51	-1.80	G_M^n	
Q_p (Ch. 3)	1.0	G_E^p	3.6
μ_p (Ch. 3)	2.79	G_M^p	3.7
Q_n (Ch. 3)	0.0	G_E^n	3.5
μ_n (Ch. 3)	-1.69	G_M^n	3.8
Q_p [PDG]	1.0		
μ_p [PDG]	2.79		
Q_n [PDG]	0.0		
μ_n [PDG]	-1.91		

Table 5.2: Overview of results for the nucleon including the pion loop (this chapter), the front-form calculations by Pasquini and Boffi [PB07], the nucleon without pionic contribution (Chap. 3), as well as current (CODATA) experimental values [PDG]. For each category we list the contribution to the overall proton charge Q_p (in units of $|e|$), to the magnetic moment of the proton μ_p , the overall neutron charge Q_n (for completeness), as well as the contribution to the magnetic moment of the neutron μ_n .

Left to right: Contribution of the loop nucleon, of the loop pion, overall loop contribution, contribution of the bare nucleon, sum of all contributions, corresponding Sachs form factor with reference to figure where form factor is plotted.

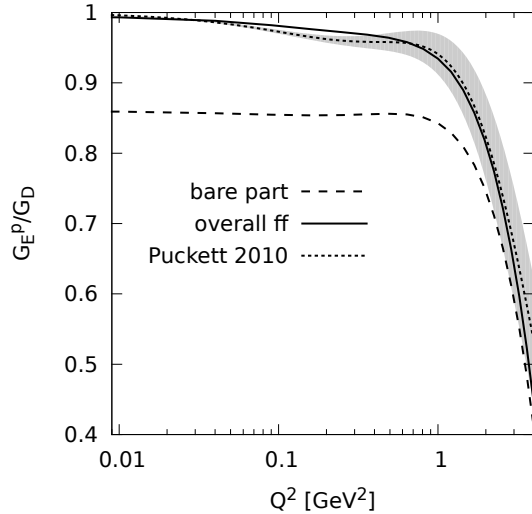


Figure 5.8: Our predictions for the electric proton form factor G_E^p normalized to the dipole form factor G_D , as a function of $Q^2 = -q^2$ on a logarithmic scale. Total result and contribution of the bare nucleon and the pion loops correspond to solid, dotted and dashed lines, respectively. Shaded area: fit of experimental data (including uncertainties) by Puckett [Puc10].

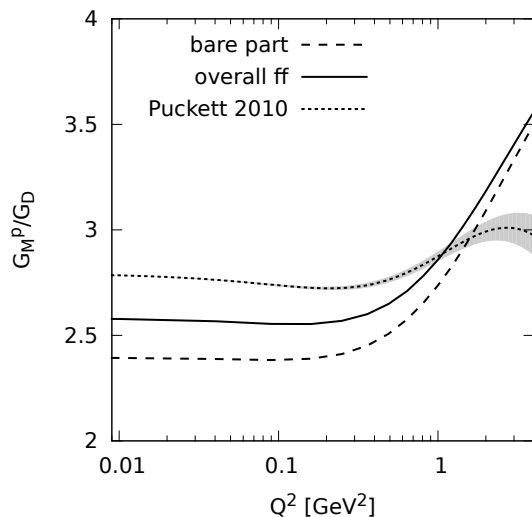


Figure 5.9: Our predictions for the magnetic proton form factor G_M^p normalized to the dipole form factor G_D , as a function of $Q^2 = -q^2$ on a logarithmic scale. Total result and contribution of the bare nucleon and the pion loops correspond to solid, dotted and dashed lines, respectively. Shaded area: fit of experimental data (including uncertainties) by Puckett [Puc10].

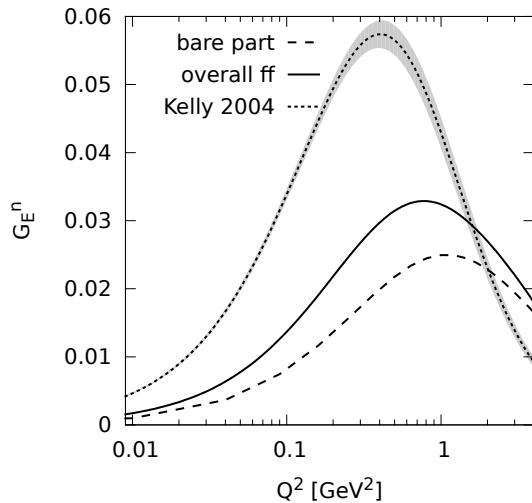


Figure 5.10: Our predictions for the electric neutron form factor G_E^n as a function of $Q^2 = -q^2$. Total result and contribution of the bare nucleon and the pion loops correspond to solid, dotted and dashed lines, respectively. Shaded area: fit of experimental data by Kelly [Kel04].

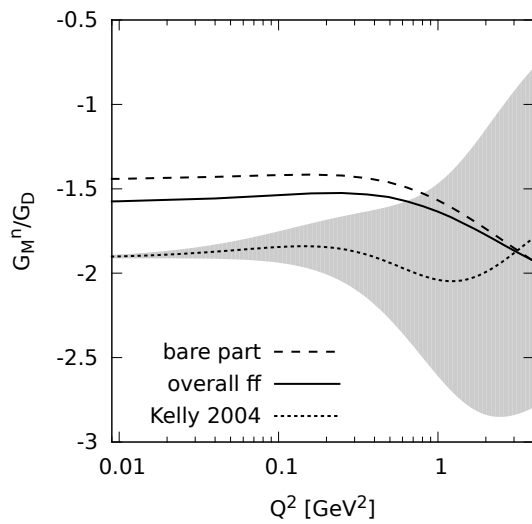


Figure 5.11: Our predictions for the magnetic neutron form factor G_M^n normalized to the dipole form factor G_D , as a function of $Q^2 = -q^2$ on a logarithmic scale. Total result and contribution of the bare nucleon and the pion loops correspond to solid, dotted and dashed lines, respectively. Shaded area: Fit of experimental data by Kelly [Kel04].

	$r_{E,p}$ (fm)	$r_{E,n}^2$ (fm 2)
bare part	0.77	-0.023
incl. π -loop	0.82	-0.050
bare nucleon (Ch. 3)	0.86	-0.026
bare part [PB07]	0.80	-0.010
incl. meson loop [PB07]	0.88	-0.063
exp. [PDG] ([ANS ⁺ 13])	0.88 (0.84)	-0.115

Table 5.3: Charge radii of the nucleon including the pion loop (contribution of the bare part and overall result) as well as of the bare nucleon, compared with results by Pasquini and Boffi ([PB07] using an $SU(6)$ -symmetric wave function with the momentum part (3.33)), and experimental values [PDG]. For the proton, the current value of measurements involving muonic hydrogen, giving rise to the so-called ‘‘proton radius puzzle’’, is included in brackets [ANS⁺13].

5.8.2 Discussion of results

We start the discussion of our results with the static properties of the nucleon. These are mainly the magnetic moment of the nucleon and its mean quadratic charge radius (5.72). In Tab. 5.2 our predictions for the nucleon magnetic moments are decomposed into the various contributions and compared with experimental results as well as the results of the front-form calculations of Ref. [PB07], from which we have taken our parametrisation of the three-quark wave function of the bare nucleon. What we observe already is that the relative size of the loop contribution is 7% of the total proton magnetic moment and 8.5% of the total neutron magnetic moment, the major part coming from the photon coupling to the pion. Our total result is smaller than the experimental one. It deviates by about 7% for the proton and 17% for the neutron. At this point, however, we want to emphasize that our main goal was not to reproduce the experimental data as good as possible by adapting the $3q$ -wave-function parameters and the πq -coupling. We rather aimed at an extension of the point-form approach so that pion-cloud effects can be appropriately described and we wanted to give a first estimate for the size of such effects.

When comparing our results with those of Ref. [PB07], one has to keep a few points in mind: Unlike the authors of [PB07], who took a phenomenological $\pi N_0 N_0$ form factor (of Gaussian form), we have calculated both electromagnetic form factors of the bare nucleon and the strong $\pi N_0 N_0$ vertex form factor with the same microscopic input, namely the $3q$ -bound-state wave function given in Eq. (3.54). With our value of the πq -coupling and this wave function, our valence-Fock-state probability becomes $(1 - \alpha) = 86\%$ (cf. Tab. 5.1), while Pasquini and Boffi obtained 91%. For the coupling of the pion to the physical nucleon we get

$$\frac{1}{4\pi} g_{\pi NN}^2 = (1 - \alpha)^2 \frac{1}{4\pi} g_{\pi N_0 N_0}^2 = 13.78,$$

a value similar to the one used in Ref. [PB07] (namely 13.6). A further difference is that

the authors of Ref. [PB07], in addition to πN , took into account also $N\rho$, $N\omega$, $\Delta\pi$ and $\Delta\rho$ intermediate states, with $\Delta\pi$ being the most important one. For all the intermediate states they, however, took the physical masses of the hadrons. To be consistent within our simple model we, on the other hand, use bare nucleon states with the corresponding bare masses within the pion loop. Taking into account the different probabilities for finding the bare nucleon in the physical nucleon, our results for the bare contribution to the magnetic moments appear to be consistent with those of Ref. [PB07].

The second interesting static quantity is the mean quadratic charge radius, cf. Eq. (5.72). In Tab. 5.3 we again compare our results with those of Ref. [PB07] as well as experiment. We find that in our results for the proton, the pion loop accounts for approx. 6% of the (linear) charge radius, while if we ignore the pion loop contribution, the proton appears about 5% larger. Also, our bare part of the proton radius is approx. 4% smaller than that found by Pasquini and Boffi, while our overall proton radius is about 7% smaller than theirs. Comparing with experiment, we see that our result for the nucleon ignoring the pion loop (0.86 fm) get very close to the CODATA value of 0.88 fm, while the result including the pion loop (0.82 fm) is closer to newer measurements using myonic hydrogen that yield a proton radius of 0.84 fm [ANS¹³]. This huge and as of today unexplained discrepancy in measurements is known as the proton radius puzzle.

For the neutron quadratic charge radius we obtain similar results as Pasquini and Boffi; however, the difference between the bare contribution (which in our case is almost the same as the result if we ignore any meson loops) and the overall result is much less pronounced in our case and also, we don't even reach 50% of the experimental value of -0.115 fm². Pasquini and Boffi managed to reproduce this value approximately only by including an s' -component in their wave function, however for comparability, we only included their results for a pure s -wave with $SU(6)$ -symmetry.

Our results for the nucleon electromagnetic form factors as functions of the (negative) four-momentum transfer squared are shown in Figs. 5.8–5.11 and compared with parametrizations of the experimental data. The form factors are normalized to the dipole form to make discrepancies with experiment and the experimental uncertainties more visible (except Fig. 5.10) and a logarithmic scale has been chosen for the abscissa to emphasize the region below 1 GeV.

We achieve reasonable agreement with experiment for the proton electric and magnetic form factor and the neutron magnetic form factor. The reproduction of the neutron electric form factor is less satisfactory, but as we have remarked already in Sec. 3.6, the absolute magnitude of this quantity is small and the actual size of the experimental error bars is larger than indicated by the shaded band. Also Pasquini and Boffi encountered the same problem; in order to better reproduce experimental results for the neutron electric form factor, they included an s' -component in their wave function, which we have not. The size of the pionic contribution to all the nucleon form factors is comparable to the one found in Refs. [PB07, CM12]. A significant effect of the non-valence $3q + \pi$ component on the form factors is only observed for momentum transfers $Q^2 \lesssim 0.5$ GeV².

Chapter 6

Summary and Outlook

Scattering experiments with electrons are an important method to determine the spatial distribution of electric charge and magnetic moment within a nucleon, i.e. proton or neutron. Relativistic constituent quark models are one of the most important means to provide a theoretical explanation of these distributions in terms of subnuclear degrees of freedom. They describe the nucleon as consisting of three valence (constituent) quarks. Such models are usually based on one of the three forms of relativistic dynamics found by Dirac. In this work we have taken the least utilized one, namely the point form, to treat electron–nucleon scattering in a relativistically invariant way. The main objective of this thesis was, however, not to redo such form factor calculations in point form, but rather to study the influence of non-valence contributions, which are modeled as pions that are emitted and reabsorbed by the constituent quarks, on the electromagnetic nucleon structure. To this end, we had to extend the relativistic multichannel formulation, which has already been applied successfully to calculating electroweak meson form factors within constituent quark models, to the case of baryons. A further necessary generalization of the formalism was the inclusion of pions as dynamical degrees of freedom, in addition to the constituent quarks, the electron, and the photon. Under the assumption of instantaneous confinement of the constituent quarks it turns out that the calculation of the pionic contributions can be reformulated as a purely hadronic problem in which the nucleon emits and reabsorbs the pion. The nucleonic substructure is then hidden in the strong coupling of the pion to a “bare” nucleon, i.e. an eigenstate of the pure confinement problem, and a corresponding vertex form factor, which can be calculated on quark level using the same kind of formalism as for the electromagnetic nucleon form factors within the pure constituent-quark model. The basic ingredients for calculating pion-loop effects are thus the electromagnetic and strong form factors of a bare nucleon.

In a first step, we have therefore calculated the electromagnetic nucleon form factors within the pure constituent-quark model assuming an instantaneous confinement potential between the quarks. This has been done by deriving the invariant one-photon-exchange amplitude within our relativistic multichannel approach, extracting the electromagnetic

nucleon current and analyzing its covariant structure. What enters the form factors essentially is the three-quark nucleon wave function. Instead of solving the three-quark mass eigenvalue equation with some confinement potential, we have rather taken an appropriate parametrization of this wave function. We have adopted an $SU(6)$ spin-flavor symmetric form with the momentum part chosen from Schlumpf [Schl94]. The relation of the boosted nucleon wave function to the wave function for the nucleon at rest is uniquely determined within our point-form approach. Thereby the Wigner rotations of the quarks' spin orientations play an important role. Already within this pure constituent-quark model, we were able to reproduce experimental results [Kel04, Puc10] as well as existing front-form calculations [Schl94, PB07] reasonably well. Only the – experimentally less precisely determined – electric Sachs form factor of the neutron obtained by us misses the peak value by about 50% (due to the restriction to a pure s-wave) and the peak is slightly shifted as compared to experiment, but the momentum-transfer dependence is roughly reproduced. The electric proton form factor fits experimental results very well for values of Q^2 up to about 3 GeV^2 . The magnetic form factors of proton and neutron fit quite well, especially below $Q^2 \approx 2 \text{ GeV}^2$. However, the absolute value of the neutron magnetic moment is underestimated by about 12%. Even over a larger range of Q^2 the momentum-transfer dependence of the form factors is reasonably well reproduced.

For the same wave-function model, using the same methods as above, we have then determined the strong coupling constants and form factors for the πNN -vertex for pseudoscalar as well as pseudovector coupling (Chap. 4). The normalized results for each form factor hardly differ from each other, and both compare well with results for a hadronic pion-cloud model [PR05a, PR05b], lattice results by Liu et al. [LDDW95], and another constituent-quark-model calculation by Melde et al. [MCP09]. For pseudovector coupling, the quark-pion coupling constant we determine from the phenomenologically known πNN coupling differs from the one used in the Goldstone-boson-exchange relativistic constituent quark model [GPP⁺98] by only 1.5%.

In order to determine the electromagnetic form factors of a physical nucleon, i.e. a bare nucleon that is surrounded by a pion cloud, we have finally treated the physical nucleon as a superposition of a bare nucleon component and a bare-nucleon-plus-pion component (Chap. 5). Using our results for the strong form factor, we have determined the probabilities of these components, the mass of the bare nucleon, and the nucleon-pion wave function. Together with our results for the electromagnetic and strong form factors of the bare nucleon, these quantities were then used to calculate the invariant one-photon-exchange amplitude for electron scattering off a physical nucleon. At this stage this becomes a purely hadronic problem with the quark substructure encoded in the strong and electromagnetic form factors of the bare nucleon. The final results resemble those of the pure constituent-quark model (Chap. 3). To compare with a similar front-form calculation we have only slightly readjusted the wave function parameters to the values chosen by Pasquini and Boffi [PB07]. One also has to take into account that the probability of finding the three-quark component in the physical nucleon is now less

than one, so that there is room left for the three-quark-pion component. Our results are comparable to experiment [Kel04, Puc10] as well as equivalent front-form calculations [PB07]. What has been achieved by including the pion cloud is:

- a slight improvement of the electric neutron form factor,
- a slight improvement of the electric proton form factor above momentum transfers squared of about $0.4\text{--}0.5 \text{ GeV}^2$, however slightly too high values between 0.04 GeV^2 and 0.4 GeV^2 ,
- an overall shift of the magnetic proton form factor, leading to a magnetic moment of the proton that is approx. 7.5% too low (as compared to experiment), and
- an overall shift of the magnetic neutron form factor, leading to a magnetic moment of the neutron about 17% smaller than the experimental value.

We obtain good results for the proton charge radius, about 2% below the CODATA value within the pure constituent-quark model and approx. 7% below for the proton including the pion cloud. However, the neutron charge radius squared is not even half the CODATA value due to the restriction of the three-quark wave function to an s-wave ground state, as already mentioned. Studying the contributions to the magnetic moments in detail we see that Pasquini and Boffi [PB07], who used a phenomenological ansatz for the π -baryon vertices, obtained a much smaller probability for finding mesons in the nucleon (9% instead of 14%), yet a much larger contribution of the meson loop (loop baryon + loop meson) to the magnetic moment, which renders their results much closer to experiment. The reason for this is probably that, while we restricted ourselves to studying just the pion loop with nucleon intermediate state, they in addition considered ρ and ω loops as well as an intermediate *Delta*. However, we want to point out that the aim of this work was mainly to establish the formalism and to estimate the role of pionic contributions to the electromagnetic nucleon structure.

In our simple model there is still room left for a better quantitative reproduction of the electromagnetic nucleon form factors. Altogether there are 4 parameters in the model: the constituent-quark mass, the πq coupling, and two parameters in the wave function. We believe that an appropriate readjustment of the parameters as well as the addition of an s' - component to the wave function, as has been done by Pasquini and Boffi [PB07], could already provide a considerable improvement of our form-factor predictions. Introducing an even more realistic wave function could further ameliorate our results. A physically more complete description of the nucleon structure may even require to introduce, in addition to the pion, other mesons in the cloud and, in particular, also Δ baryons within the meson loops. The same approach can then, of course, also be applied to describe the electromagnetic Δ and $N\Delta$ -transition form factors. In these cases the pionic contributions are expected to be much more important, since the Δ is a πN resonance.

Appendix A

The nucleon with pion cloud

In this appendix we summarize how a physical nucleon, consisting of a bare nucleon component and a bare nucleon+pion component, is described within our multichannel approach. We start by writing the physical nucleon state as a two-component vector, the components representing the contributions of the bare nucleon and the bare nucleon+pion states, respectively:

$$|VN\rangle := \begin{pmatrix} |V\tilde{N}\rangle \\ |V\tilde{N}\pi\rangle \end{pmatrix} \quad (\text{A.1})$$

with

$$\begin{aligned} |V\tilde{N}\rangle &= \sqrt{1-\alpha} \frac{m_{N_0}}{m_N} |VN_0\rangle, \\ |V\tilde{N}\pi\rangle &= \sqrt{\alpha} \sqrt{2(2\pi)^3} \sum Dk'_\pi \sqrt{\frac{(m'_{N_0\pi})^3}{\omega'_{N_0}}} \frac{\sqrt{\omega'_\pi}}{m_N} \Psi_{N/N'_0\pi'} |VN'_0\pi'\rangle \end{aligned} \quad (\text{A.2})$$

and the matrix mass operator

$$\hat{M}_N := \begin{pmatrix} M_{N_0} & K_\pi \\ K_\pi^\dagger & M_{N_0\pi} \end{pmatrix}. \quad (\text{A.3})$$

The kinematical factors in (A.2) are chosen such that α is the probability to find the bare nucleon+pion component in the physical nucleon. Correspondingly, $(1 - \alpha)$ is the probability to find the bare nucleon component in the physical nucleon. $\Psi_{N/N'_0\pi'}$ is the wave function of the bare nucleon+pion component. The normalization of the free states is

$$\begin{aligned} \langle VN_0 | V' N'_0 \rangle &= \frac{2}{m_{N_0}^2} \Delta_{VV'}, \\ \langle VN_0\pi | V' N'_0\pi' \rangle &= \frac{2\omega_{N_0}}{m_{N_0\pi}^3} \Delta_{VV'} \Delta_{\pi\pi'}. \end{aligned} \quad (\text{A.4})$$

The nucleon-pion vertex matrix element is, according to Eq. (4.6),

$$\langle V' N_0' \pi' | K_\pi^\dagger | V N_0 \rangle = \langle V N_0 | K_\pi | V' N_0' \pi' \rangle^* = \Delta_{VV'} \frac{1}{\sqrt{m_{N_0 \pi}^3 m_{N_0}^3}} \langle N_0' \pi' | K_\pi^\dagger | N_0 \rangle. \quad (\text{A.5})$$

The normalization condition for the nucleon-pion wave function reads

$$\sum D k_\pi'' \omega_\pi'' \Psi_{N/N_0'' \pi''}^* \Psi_{N'/N_0'' \pi''} = \frac{\delta_{NN'}}{2(2\pi)^3}. \quad (\text{A.6})$$

In order to extract the three unknown quantities, i.e. the probability α of the $\widetilde{N\pi}$ component, the nucleon-pion two-body wave function $\Psi_{N/N_0 \pi}$ and the bare nucleon mass m_{N_0} from this picture, we need a system of three independent equations involving these quantities. These equations are the following:

First equation: We calculate matrix elements of the mass operator \hat{M}_N (that describes the physical nucleon) between a free (“bare”) nucleon state and a physical nucleon state (A.1). We take the matrix form (A.3) of \hat{M}_N and equate the result with the corresponding matrix element of the mass operator’s eigenvalue m_N :

$$\begin{aligned} \langle V' N'_0 | \hat{M}_N | V N \rangle &:= \begin{pmatrix} \langle V' N'_0 | \\ 0 \end{pmatrix}^\top \begin{pmatrix} M_{N_0} & K_\pi \\ K_\pi^\dagger & M_{N_0 \pi} \end{pmatrix} \begin{pmatrix} |V \widetilde{N}\rangle \\ |V \widetilde{N\pi}\rangle \end{pmatrix} \\ &\stackrel{(\text{A.2})}{=} \sqrt{1-\alpha} \frac{m_{N_0}}{m_N} \langle V' N'_0 | M_{N_0} | V N_0 \rangle + \\ &\quad + \sqrt{\alpha} \sqrt{2(2\pi)^3} \sum D k_\pi'' \frac{\sqrt{(m_{N_0 \pi}'')^3}}{\sqrt{\omega_{N_0}''}} \frac{\sqrt{\omega_\pi''}}{m_N} \Psi_{N/N_0'' \pi''} \langle V' N'_0 | K_\pi | V N_0'' \pi'' \rangle \quad (\text{A.7}) \\ &\stackrel{(\text{A.4})}{=} \frac{2}{m_N} \sqrt{1-\alpha} \Delta_{VV'} \\ &\stackrel{(\text{A.5})}{=} \frac{\sqrt{2(2\pi)^3}}{m_N \sqrt{m_{N_0}^3}} \sqrt{\alpha} \sum D k_\pi'' \sqrt{\frac{\omega_\pi''}{\omega_{N_0}''}} \Psi_{N/N_0'' \pi''} \langle N'_0 | K_\pi | N_0'' \pi'' \rangle \Delta_{VV'}. \end{aligned}$$

(Recall that in the rest frame of the (bare) nucleon, $\omega_{N(0)} \equiv m_{N(0)}$!)

On the other hand, we have

$$\langle V' N'_0 | \hat{M}_N | V N \rangle \stackrel{(\text{A.2})}{=} m_N \frac{m_{N_0}}{m_N} \sqrt{1-\alpha} \langle V' N'_0 | V N_0 \rangle \stackrel{(\text{A.4})}{=} \frac{2}{m_{N_0}} \sqrt{1-\alpha} \Delta_{VV'}. \quad (\text{A.8})$$

Equating Eqs. (A.7) and (A.8), we obtain the result

$$(m_N - m_{N_0}) \frac{\sqrt{1-\alpha}}{\sqrt{\alpha}} = \sqrt{\frac{(2\pi)^3}{2m_{N_0}}} \sum D k_\pi'' \sqrt{\frac{\omega_\pi''}{\omega_{N_0}''}} \Psi_{N/N_0'' \pi''} \langle N'_0 | K_\pi | N_0'' \pi'' \rangle. \quad (\text{A.9})$$

Second equation: Analogously, we can calculate for a pion of given momentum k'_π

$$\begin{aligned}
\langle V' N'_0 \pi' | \hat{M}_N | V N \rangle &:= \begin{pmatrix} 0 \\ \langle V' N'_0 \pi' | \end{pmatrix}^\top \begin{pmatrix} M_{N_0} & K_\pi \\ K_\pi^\dagger & M_{N_0 \pi} \end{pmatrix} \\
\begin{pmatrix} |V \tilde{N}\rangle \\ |V \widetilde{N\pi}\rangle \end{pmatrix} &\stackrel{(A.2)}{=} \frac{m_{N_0}}{m_N} \sqrt{1-\alpha} \langle V' N'_0 \pi' | K_\pi^\dagger | V N_0 \rangle \\
&+ \sqrt{2(2\pi)^3} \sqrt{\alpha} \sum D k''_\pi \frac{\sqrt{(m''_{N_0 \pi})^3}}{\sqrt{\omega''_{N_0}}} \frac{\sqrt{\omega''_\pi}}{m_N} \Psi_{N/N'_0 \pi''} \langle V' N'_0 \pi' | M_{N_0 \pi} | V N_0'' \pi'' \rangle \\
&\stackrel{(A.4)}{=} \sqrt{1-\alpha} \frac{1}{m_N} \frac{1}{\sqrt{m_{N_0} (m'_{N_0 \pi})^3}} \langle N'_0 \pi' | K_\pi^\dagger | N_0 \rangle \Delta_{VV'} \\
&+ \sqrt{2(2\pi)^3} \sqrt{\alpha} \frac{2}{m_N} \frac{\sqrt{\omega'_{N_0} \omega'_\pi}}{\sqrt{m'_{N_0 \pi}}} \Psi_{N/N'_0 \pi'} \Delta_{VV'}.
\end{aligned} \tag{A.10}$$

On the other hand, we have

$$\begin{aligned}
\langle V' N'_0 \pi' | \hat{M}_N | V N \rangle &\stackrel{(A.2)}{=} m_N \sqrt{2(2\pi)^3} \sum D k''_\pi \frac{\sqrt{(m''_{N_0 \pi})^3 \omega''_\pi}}{\omega_N \sqrt{\omega''_{N_0}}} \sqrt{\alpha} \Psi_{N/N'_0 \pi''} \langle V' N'_0 \pi' | V N_0'' \pi'' \rangle \\
&\stackrel{(A.4)}{=} \sqrt{2(2\pi)^3} \frac{2 \sqrt{\omega'_{N_0} \omega'_\pi}}{\sqrt{(m'_{N_0 \pi})^3}} \sqrt{\alpha} \Psi_{N/N'_0 \pi'} \Delta_{VV'}
\end{aligned} \tag{A.11}$$

and equating (A.10) and (A.11), we obtain

$$\boxed{2 \sqrt{2(2\pi)^3} \Psi_{N/N'_0 \pi'} = \frac{1}{\sqrt{m_{N_0} \omega'_{N_0} \omega'_\pi}} \frac{\langle N'_0 \pi' | K_\pi^\dagger | N_0 \rangle \sqrt{1-\alpha}}{m_N - \omega'_{N_0} - \omega'_\pi} \frac{\sqrt{1-\alpha}}{\sqrt{\alpha}}}. \tag{A.12}$$

Determination of α : Applying the normalization condition (A.6) to Eq. (A.12), we get

$$\boxed{\frac{\alpha}{1-\alpha} = \frac{1}{4} \int D k''_\pi \frac{1}{m_{N_0} \omega''_{N_0}} \frac{|\langle N''_0 \pi'' | K_\pi^\dagger | N_0 \rangle|^2}{(m_N - \omega''_{N_0} - \omega''_\pi)^2}} \tag{A.13}$$

so we have obtained an explicit equation for α .

Eigenvalue equation for m_{N_0} : On the other hand, upon inserting (A.12) into (A.9) and using Eqs. (4.7) and (2.69), we obtain, for pseudoscalar coupling:

$$m_{N_0} (m_N - m_{N_0}) \delta_{\mu_{N_0} \mu'_{N_0}} \delta_{\tau_{N_0} \tau'_{N_0}} = g_{N_0}^2 \sum_{\mu''_{N_0}} \sum_{\tau''_{N_0}} Dk''_\pi \frac{J^{5*}(N''_0, N'_0) \mathcal{F}(\tau'_{N_0}, \tau''_{N_0}, \tau''_\pi) J^5(N_0, N''_0) \mathcal{F}(\tau_{N_0}, \tau''_{N_0}, \tau''_\pi)}{4 (m_N - \omega''_{N_0} - \omega''_\pi) \omega''_{N_0}}, \quad (\text{A.14})$$

i.e.

$$m_N - m_{N_0} = \frac{3}{4} \sum_{\mu''_{N_0}} \int Dk''_\pi \frac{g_{N_0}^2}{m_{N_0} \omega''_{N_0}} \frac{\left| J^5(\vec{k}_{N_0}, \frac{1}{2}, \vec{k}''_{N_0}, \mu''_{N_0}) \right|^2}{m_N - \omega''_{N_0} - \omega''_\pi}. \quad (\text{A.15})$$

This is the (non-linear) algebraic equation we use to determine the bare nucleon mass m_{N_0} , given the physical nucleon mass m_N by its experimental value. The final form of the mass-eigenvalue equation (A.15) is then obtained by using rotational invariance (also of $\sum_{\mu''_{N_0}} |J^5(\vec{k}_{N_0}, \frac{1}{2}, \vec{k}''_{N_0}, \mu''_{N_0})|$) to perform the angular integration (in spherical coordinates). This allows us to use the expression (4.39) for the pseudoscalar current J_N^5 (or (4.43) for the pseudovector current $J_N^{5\#}$). We then get:

$$m_N - m_{N_0} = \frac{3}{2} \int \frac{dk}{(2\pi)^2} \times \frac{k^4 g_{N_0}^2 G_{\text{ps}}(k)^2}{\sqrt{k^2 + m_\pi^2} \left(m_N - \sqrt{k^2 + m_{N_0}^2} - \sqrt{k^2 + m_\pi^2} \right) \left(k^2 + m_{N_0}^2 + m_{N_0} \sqrt{k^2 + m_{N_0}^2} \right)} \quad (\text{A.16})$$

for pseudoscalar $\pi N_0 N_0$ coupling or

$$m_N - m_{N_0} = \frac{3}{2} \int \frac{dk}{(2\pi)^2} k^4 f_{N_0}^2 G_{\text{pv}}(k)^2 \times \frac{\left(m_{N_0} + \sqrt{k^2 + m_{N_0}^2} + \sqrt{k^2 + m_\pi^2} \right)^2}{m_\pi^2 \sqrt{k^2 + m_\pi^2} \left(m_N - \sqrt{k^2 + m_{N_0}^2} - \sqrt{k^2 + m_\pi^2} \right) \left(k^2 + m_{N_0}^2 + m_{N_0} \sqrt{k^2 + m_{N_0}^2} \right)} \quad (\text{A.17})$$

for pseudovector $\pi N_0 N_0$ coupling, respectively, and likewise (middle bracket in the denominator gets squared) for Eq. (A.13).

It now remains to solve Eq. (A.15) numerically and use the result(s) in Eq. (A.13) and, consequently, in Eq. (A.12) to determine α and Ψ , respectively.

Appendix B

Calculational details

B.1 Transformation of integration measures

We start out with the integration measure of a general n -particle velocity state containing three quarks,

$$\int \prod_{i=1}^n \frac{d^3 p_i}{2 p_i^0} = \int \frac{d^3 V}{V^0} \prod_{i=1}^{n-1} \left(\frac{d^3 k_i}{2 \omega_i} \right) \frac{(\sum_{i=1}^n \omega_i)^3}{2 \omega_n} \quad (\text{B.1})$$

$$\equiv \int \frac{d^3 V}{V^0} \prod_{i=1}^n \left(\frac{d^3 k_i}{2 \omega_i} \right) \left(\sum_{i=1}^n \omega_i \right)^3 \delta^3 \left(\sum_{i=1}^n \vec{k}_i \right) \quad (\text{B.2})$$

$$\equiv \int \frac{d^3 V}{V^0} \prod_{i=1}^{n-3} \left(\frac{d^3 k_i}{2 \omega_i} \right) \frac{d^3 k_{q_2}}{2 \omega_{q_2}} \frac{d^3 k_{q_3}}{2 \omega_{q_3}} \frac{(\sum_{i=1}^n \omega_i)^3}{2 \omega_{q_1}}, \quad (\text{B.3})$$

assuming that the quarks are the last three particles and making the 3-momentum of quark no. 1 the redundant one. Starting out with expression (B.2), we insert an integration and a delta function over the overall four-momentum k_{3q} of the three quarks. Due to Lorentz invariance of the delta function and with

$$dk_{3q}^0 = \frac{\partial k_{3q}^0}{\partial m_{3q}} dm_{3q} = \frac{m_{3q}}{\omega_{3q}} dm_{3q}, \quad (\text{B.4})$$

the element being inserted reads

$$\int d^4 k_{3q} \delta^4 \left(k_{3q} - \sum_{i=1}^3 k_{q_i} \right) = \int dm_{3q} d^3 k_{3q} \frac{m_{3q}}{\omega_{3q}} \delta^4 \left(\begin{pmatrix} m_{3q} \\ \vec{0} \end{pmatrix} - \sum_{i=1}^3 \begin{pmatrix} \tilde{\omega}_{q_i} \\ \tilde{\vec{k}}_{q_i} \end{pmatrix} \right) \quad (\text{B.5})$$

$$= \int d^3 k_{3q} \frac{\sum_{i=1}^3 \tilde{\omega}_{q_i}}{\sum_{i=1}^3 \omega_{q_i}} \delta^3 \left(\sum_{i=1}^3 \tilde{\vec{k}}_{q_i} \right). \quad (\text{B.6})$$

We thus obtain

$$\int \prod_{i=1}^n \frac{d^3 p_i}{2 p_i^0} = \int \frac{d^3 V}{V^0} \prod_{i=1}^{n-3} \left(\frac{d^3 k_i}{2 \omega_i} \right) \left(\sum_{i=1}^n \omega_i \right)^3 \delta^3 \left(\sum_{i=1}^n \vec{k}_i \right) d^3 k_{3q} \frac{\sum_{i=1}^3 \tilde{\omega}_{q_i}}{\sum_{i=1}^3 \omega_{q_i}} \delta^3 \left(\sum_{i=1}^3 \tilde{\vec{k}}_{q_i} \right). \quad (\text{B.7})$$

Assuming that the quarks are the last three particles and using Lorentz invariance of the single-particle integration measures ($\frac{d^3 k_{qj}}{2\omega_{qj}} = \frac{d^3 \tilde{k}_{qj}}{2\tilde{\omega}_{qj}}$) and by use of (3.36), expression (B.7) becomes

$$\int \frac{d^3 V}{V^0} \prod_{i=1}^{n-3} \left(\frac{d^3 k_i}{2\omega_i} \right) \prod_{j=1}^3 \left(\frac{d^3 \tilde{k}_{qj}}{2\tilde{\omega}_{qj}} \right) \left(\sum_{i=1}^n \omega_i \right)^3 \delta^3 \left(\sum_{i=1}^{n-3} \vec{k}_i + \vec{k}_{3q} \right) d^3 k_{3q} \frac{\sum_{i=1}^3 \tilde{\omega}_{q_i}}{\sum_{i=1}^3 \omega_{q_i}} \delta^3 \left(\sum_{i=1}^3 \tilde{k}_{q_i} \right). \quad (\text{B.8})$$

Eliminating the delta functions (making the 3-momentum of quark no. 1 the redundant one), we get

$$\int \frac{d^3 V}{V^0} \prod_{i=1}^{n-3} \left(\frac{d^3 k_i}{2\omega_i} \right) \frac{d^3 \tilde{k}_{q_2}}{2\tilde{\omega}_{q_2}} \frac{d^3 \tilde{k}_{q_3}}{2\tilde{\omega}_{q_3}} \frac{\left(\sum_{i=1}^n \omega_i \right)^3}{2\tilde{\omega}_{q_1}} \frac{\sum_{i=1}^3 \tilde{\omega}_{q_i}}{\sum_{i=1}^3 \omega_{q_i}}. \quad (\text{B.9})$$

Comparing this with expression (B.3), the result is

$$d^3 V \dots d^3 k_{q_2} d^3 k_{q_3} = d^3 V \dots d^3 \tilde{k}_{q_2} d^3 \tilde{k}_{q_3} \frac{\omega_{q_1}}{\tilde{\omega}_{q_1}} \frac{\omega_{q_2}}{\tilde{\omega}_{q_2}} \frac{\omega_{q_3}}{\tilde{\omega}_{q_3}} \frac{\tilde{\omega}_{q_1} + \tilde{\omega}_{q_2} + \tilde{\omega}_{q_3}}{\omega_{q_1} + \omega_{q_2} + \omega_{q_3}} \quad (\text{B.10})$$

or, in our notation,

$$DV \dots Dk_{q_2} Dk_{q_3} = DV \dots D\tilde{k}_{q_2} D\tilde{k}_{q_3} \frac{\omega_{q_1}}{\tilde{\omega}_{q_1}} \frac{\tilde{\omega}_{q_1} + \tilde{\omega}_{q_2} + \tilde{\omega}_{q_3}}{\omega_{q_1} + \omega_{q_2} + \omega_{q_3}}. \quad (\text{B.11})$$

B.2 Normalization of the three-quark wave function

In order to find the normalization factors for the three-quark wave functions (3.33), we use the orthogonality relation (2.50) for hadronic velocity states and insert the quark-level completeness relations (3.30).

Nucleon–electron state: For the $N_0 e$ -state (with redundant nucleon 3-momentum), relation (2.50) reads

$$\langle V' N'_0 e' | V N_0 e \rangle = \frac{\Delta_{VV'} \Delta_{ee'} 2\omega_{N_0}}{(\omega_{N_0} + \omega_e)^3} \delta_{\mu_{N_0} \mu'_{N_0}} \delta_{\tau_{N_0} \tau'_{N_0}}, \quad (\text{B.12})$$

where we have now explicitly included the Kronecker deltas for the (iso-)spins of the particle with redundant momentum – the bare nucleon. Insertion of the quark-level unity element (3.30) yields

$$\begin{aligned} & \langle V' N'_0 e' | \mathbb{I}_{3qe} | V N_0 e \rangle \\ &= \sum_{q_1} DV'' Dk''_e Dk''_{q_2} Dk''_{q_3} \frac{m''_{3qe}}{2\omega''_{q_1}} \langle V' N'_0 e' | V'' 3q'' e'' \rangle \langle V'' 3q'' e'' | V N_0 e \rangle, \end{aligned} \quad (\text{B.13})$$

with a sum over μ''_{q_1} and τ''_{q_1} implied. After inserting our expression (3.33) for the three-quark wave function of the electron–nucleon system (now using more concise expressions

for the normalization factors representing the correct number of primes), we get

$$\begin{aligned} \langle V' N'_0 e' | \mathbb{I}_{3qe} | V N_0 e \rangle &= \sum D V'' D k''_e D k''_{q_2} D k''_{q_3} \frac{m''_3}{2 \omega''_{q_1}} \\ &\times \mathcal{N}_{N'_0 e' 3q''} \Delta_{V' V''} \Delta_{e' e''} \langle N'_0 | 3q'' \rangle \mathcal{N}_{N_0 e 3q''} \Delta_{V V''} \Delta_{e e''} \langle 3q'' | N_0 \rangle, \end{aligned} \quad (\text{B.14})$$

and after evaluating the Delta functions:

$$\begin{aligned} &\langle V' N'_0 e' | \mathbb{I}_{3qe} | V N_0 e \rangle \\ &= \sum D k''_{q_2} D k''_{q_3} \frac{m''_3}{2 \omega''_{q_1}} \mathcal{N}_{N'_0 e' 3q''} \mathcal{N}_{N_0 e 3q''} \Delta_{V V'} \Delta_{e e'} \langle N'_0 | 3q'' \rangle \langle 3q'' | N_0 \rangle, \end{aligned} \quad (\text{B.15})$$

and with (B.11):

$$\begin{aligned} &\langle V' N'_0 e' | \mathbb{I}_{3qe} | V N_0 e \rangle \\ &= \sum D \tilde{k}''_{q_2} D \tilde{k}''_{q_3} \frac{\tilde{\omega}''_{q_1} + \tilde{\omega}''_{q_2} + \tilde{\omega}''_{q_3}}{\omega''_{q_1} + \omega''_{q_2} + \omega''_{q_3}} \frac{m''_3}{2 \tilde{\omega}''_{q_1}} \mathcal{N}_{N'_0 e' 3q''} \mathcal{N}_{N_0 e 3q''} \Delta_{V V'} \Delta_{e e'} \langle N'_0 | 3q'' \rangle \langle 3q'' | N_0 \rangle. \end{aligned} \quad (\text{B.16})$$

We demand that $\langle V' N'_0 e' | \mathbb{I}_{3qe} | V N_0 e \rangle = \langle V' N'_0 e' | V N_0 e \rangle$ and thus equality of expressions (B.12) and (B.16). Applying the normalization condition (3.34), which in our short-hand notation can be written

$$4 \cdot (2\pi)^6 \sum D \tilde{k}''_{q_2} D \tilde{k}''_{q_3} \tilde{\omega}''_{q_2} \tilde{\omega}''_{q_3} \langle N'_0 | 3q'' \rangle \langle 3q'' | N_0 \rangle = \delta_{\mu_{N_0} \mu'_{N_0}} \delta_{\tau_{N_0} \tau'_{N_0}}, \quad (\text{B.17})$$

we see that a sufficient condition for the equality of Eqs. (B.12) and (B.16) is

$$\mathcal{N}_{N_0 e 3q'} = 4 \cdot (2\pi)^3 \frac{\sqrt{\omega_{N_0} \tilde{\omega}'_{q_1} \tilde{\omega}'_{q_2} \tilde{\omega}'_{q_3} (\sum \omega'_{q_i})}}{\sqrt{(\sum \tilde{\omega}'_{q_i}) (\omega_{N_0} + \omega_e)^3 (\sum \omega'_{q_i} + \omega_e)^3}}. \quad (\text{B.18})$$

Nucleon-electron-photon state: Analogously, when a photon is present, we have the orthogonality relation

$$\langle V' N'_0 e' \gamma' | V N_0 e \gamma \rangle = \frac{\Delta_{V V'} \Delta_{e e'} \Delta_{\gamma \gamma'} 2 \omega_{N_0}}{m_{N_0 e \gamma}^3}. \quad (\text{B.19})$$

Insertion of the quark-level completeness relation (3.30) yields

$$\begin{aligned} \langle V' N'_0 e' \gamma' | \mathbb{I}_{3qe\gamma} | V N_0 e \gamma \rangle &= \sum D V'' D k''_e D k''_{\gamma} D k''_{q_2} D k''_{q_3} \\ &\times \frac{m''_3}{2 \omega''_{q_1}} \left(-g^{\mu''_e \mu''_{\gamma}} \right) \langle V' N'_0 e' \gamma' | V'' 3q'' e'' \gamma'' \rangle \langle V'' 3q'' e'' \gamma'' | V N_0 e \gamma \rangle. \end{aligned} \quad (\text{B.20})$$

After inserting expression (3.33), we get

$$\begin{aligned} \langle V' N'_0 e' \gamma' | \mathbb{I}_{3qe\gamma} | V N_0 e \gamma \rangle &= \sum D V'' D k''_e D k''_{\gamma} D k''_{q_2} D k''_{q_3} \frac{m''_3}{2 \omega''_{q_1}} \left(-g^{\mu''_e \mu''_{\gamma}} \right) \\ &\times \mathcal{N}_{N'_0 e' \gamma' 3q''} \Delta_{V' V''} \Delta_{e' e''} \Delta_{\gamma' \gamma''} \langle N'_0 | 3q'' \rangle \mathcal{N}_{N_0 e \gamma 3q''} \Delta_{V V''} \Delta_{e e''} \Delta_{\gamma \gamma''} \langle 3q'' | N_0 \rangle \end{aligned} \quad (\text{B.21})$$

and after evaluating the Delta functions:

$$\begin{aligned} & \langle V' N'_0 e' \gamma' | \mathbb{I}_{3qe\gamma} | V N_0 e \gamma \rangle \\ &= \int Dk''_{q_2} Dk''_{q_3} \frac{m''^3_{3qe\gamma}}{2\omega''_{q_1}} \mathcal{N}_{N'_0 e' \gamma' 3q''} \mathcal{N}_{N_0 e \gamma 3q''} \Delta_{VV'} \Delta_{ee'} \Delta_{\gamma\gamma'} \langle N'_0 | 3q'' \rangle \langle 3q'' | N_0 \rangle \end{aligned} \quad (\text{B.22})$$

and with (B.11):

$$\begin{aligned} & \langle V' N'_0 e' \gamma' | \mathbb{I}_{3qe\gamma} | V N_0 e \gamma \rangle \\ &= \int D\tilde{k}''_{q_2} D\tilde{k}''_{q_3} \frac{\tilde{\omega}''_{q_1} + \tilde{\omega}''_{q_2} + \tilde{\omega}''_{q_3}}{\omega''_{q_1} + \omega''_{q_2} + \omega''_{q_3}} \frac{m''^3_{3qe\gamma}}{2\tilde{\omega}''_{q_1}} \mathcal{N}_{N_0 e \gamma 3q''}^2 \Delta_{VV'} \Delta_{ee'} \Delta_{\gamma\gamma'} \langle N'_0 | 3q'' \rangle \langle 3q'' | N_0 \rangle. \end{aligned} \quad (\text{B.23})$$

Demanding (B.19) = (B.23) and the norm (3.34), the result is

$$\mathcal{N}_{N_0 e \gamma 3q'} = 4(2\pi)^3 \frac{\sqrt{\omega_{N_0} \tilde{\omega}'_{q_1} \tilde{\omega}'_{q_2} \tilde{\omega}'_{q_3} (\sum \omega'_{q_i})}}{\sqrt{(\sum \tilde{\omega}'_{q_i}) (\omega_{N_0} + \omega_e + \omega_\gamma)^3 (\sum \omega'_{q_i} + \omega_e + \omega_\gamma)^3}} \quad (\text{B.24})$$

B.3 Combination of time orderings

This section treats the combination of the two time-orderings of the $Ne\gamma$ -propagator in Secs. 3.1.6 and 3.2.6.

We proceed as in [Bie11] and use energy and momentum conservation in the one-photon exchange amplitude, which implies $\sqrt{s} = m_{Ne} = \omega_N^{(\prime)} + \omega_e^{(\prime)}$ (hence $\omega'_N - \omega_N = \omega_e - \omega'_e$) and $\omega_\gamma = |\vec{k}_\gamma| = |\vec{k}_e - \vec{k}'_e|$, to obtain

$$\begin{aligned} \Pi_{Ne\gamma} &:= \frac{1}{\sqrt{s} - \omega'_N - \omega_e - \omega_\gamma} + \frac{1}{\sqrt{s} - \omega_N - \omega'_e - \omega_\gamma} \\ &= \frac{1}{\omega_N - \omega'_N - |\vec{k}_\gamma|} + \frac{1}{\omega_e - \omega'_e - |\vec{k}_\gamma|} \\ &= \frac{1}{\omega'_e - \omega_e - |\vec{k}_e - \vec{k}'_e|} + \frac{1}{\omega_e - \omega'_e - |\vec{k}_e - \vec{k}'_e|}. \end{aligned} \quad (\text{B.25})$$

Reducing this to the common denominator, we obtain

$$\Pi_{Ne\gamma} = \frac{-2|\vec{k}_e - \vec{k}'_e|}{-(\omega_e - \omega'_e)^2 + (\vec{k}_e - \vec{k}'_e)^2} = \frac{-2\omega_\gamma}{Q^2}, \quad (\text{B.26})$$

where we have introduced the photon four-momentum transfer

$$q := \left(\frac{\omega'_N - \omega_N}{\vec{k}'_N - \vec{k}_N} \right) \equiv \left(\frac{\omega_e - \omega'_e}{\vec{k}_e - \vec{k}'_e} \right) \quad \text{and} \quad Q^2 := -q^2. \quad (\text{B.27})$$

List of Figures

3.1	One-photon-exchange amplitude $\mathcal{M}_{1\gamma}$ for electron–nucleon scattering	22
3.2	Time-ordered diagrams contributing to $\mathcal{M}_{1\gamma}$	23
3.3	Quark-level diagram contributing to $\mathcal{M}_{1\gamma}$	27
3.4	Electromagnetic Sachs form factors of the nucleon (without pion cloud) . .	48
3.5	Electric neutron form factor (without pion cloud)	50
3.6	Electric proton form factor (without pion cloud)	50
3.7	Magnetic proton form factor (without pion cloud)	51
3.8	Magnetic neutron form factor (without pion cloud)	51
4.1	Pion-loop contribution to the nucleon mass	52
4.2	Pion-loop contribution to the nucleon mass on quark level	55
4.3	Strong πNN form factor	68
5.1	Physical nucleon as a superposition of N_0 and $N_0\pi$ component	70
5.2	Electron–nucleon scattering: Bare nucleon incoming and outgoing	77
5.3	Electron–nucleon scattering: Bare nucleon+pion incoming and bare nucleon outgoing	78
5.4	Electron–nucleon scattering: Bare nucleon incoming and bare nucleon+pion outgoing	81
5.5	Electron–nucleon scattering: Bare nucleon+pion incoming and outgoing .	83
5.6	Covariant one-photon-exchange amplitude for electron–nucleon scattering	87
5.7	Flow chart for calculation of bare nucleon parameters	92
5.8	Electric proton form factor	103
5.9	Magnetic proton form factor	103
5.10	Electric neutron form factor	104
5.11	Magnetic neutron form factor	104

List of Tables

3.1	Parameters for the Schlumpf wave function	36
3.2	Parametrization of bare form factors	49
5.1	Iterations for the determination of bare nucleon parameters	92
5.2	Overview of results for electromagnetic nuclear properties	102
5.3	Charge radii of the nucleon	105

Acknowledgements

I would like to thank my advisor Wolfgang Schweiger for his great support, patience and guidance throughout the rather non-linear course of this work. I thank the University of Graz, especially the organizers of the doctoral program “Hadrons in Vacuum, Nuclei and Stars” and everybody taking part for creating a wonderful environment to work in and for making me part of it. Thanks also to William Klink for being the referee to this work. Thanks to my parents for enabling me to even get started with this doctorate. Finally, I want to thank my wife, Nayla, for her endless patience and support and for always motivating me to keep going through all this time, and Nayla, Cilia and Fabia for bearing with me. You are the best family one could wish for!

Financial Support: This thesis was financially supported by the University of Graz and the Austrian Science Fund FWF under Grant No. DK W1203-N16 (Doctoral Program “Hadrons in Vacuum, Nuclei and Stars”).

Bibliography

- [ANS⁺13] A. Antognini, et al. Proton structure from the measurement of 2s-2p transition frequencies of muonic hydrogen. *Science*, 339(6118):417–420, 2013.
- [BT53] B. Bakamjian and L. H. Thomas. Relativistic Particle Dynamics. II. *Phys. Rev.*, 92:1300–1310, 1953.
- [Bie11] E. P. Biernat. *Electromagnetic Properties of Few-Body Systems Within a Point-Form Approach*. PhD thesis, Univ. Graz, 2011.
- [BS14] E. P. Biernat and W. Schweiger. Electromagnetic rho-meson form factors in point-form relativistic quantum mechanics. *Phys. Rev.*, C89(5):055205, 2014.
- [BSFK09] E. P. Biernat, W. Schweiger, K. Fuchsberger, and W. H. Klink. Electromagnetic meson form factor from a relativistic coupled-channels approach. *Phys. Rev. C* 79:055203, 2009.
- [Bug04] D. Bugg. The pion nucleon coupling constant. *The European Physical Journal C - Particles and Fields*, 33(4):505–509, 2004.
- [CDKM98] J. Carbonell, B. Desplanques, V. Karmanov, and J. Mathiot. Explicitly covariant light front dynamics and relativistic few body systems. *Phys. Rept.*, 300:215–347, 1998.
- [CM12] I. C. Cloët and G. A. Miller. Nucleon form factors and spin content in a quark-diquark model with a pion cloud. *Phys. Rev. C*, 86:015208, 2012.
- [Dir49] P. A. M. Dirac. Forms of Relativistic Dynamics. *Rev. Mod. Phys.*, 21:392–399, 1949.
- [DCC⁺66] J. R. Dunning, K. W. Chen, et al. Quasi-Elastic Electron-Deuteron Scattering and Neutron Form Factors. *Phys. Rev.*, 141:1286–1297, 1966.
- [EW88] T. Ericson and W. Weise. *Pions and Nuclei*, volume 74 of *International Series of Monographs on Physics*. Oxford Science Publications, 1988.
- [EOT09] G. Erkol, M. Oka, and T. T. Takahashi. Pseudoscalar-meson-octet-baryon coupling constants in two-flavor lattice QCD. *Phys. Rev. D*, 79:074509, Apr 2009.

- [Fes58] H. Feshbach. Unified theory of nuclear reactions. *Annals of Physics*, 5(4):357–390, 1958.
- [Fes62] H. Feshbach. A unified theory of nuclear reactions II. *Annals of Physics*, 19(2):287–313, 1962.
- [Fuc07] K. Fuchsberger. *Electromagnetic meson form factors within a relativistic coupled-channel approach*. Master’s thesis, Univ. Graz, 2007.
- [GKM⁺71] S. Galster, et al. Elastic electron - deuteron scattering and the electric neutron form-factor at four momentum transfers $5 \text{ fm}^{-2} < q^2 < 14 \text{ fm}^{-2}$. *Nucl. Phys.*, B32:221–237, 1971.
- [GPP⁺98] L. Y. Glozman, Z. Papp, W. Plessas, K. Varga, and R. F. Wagenbrunn. Effective Q-Q interactions in constituent quark models. *Phys. Rev.*, C57:3406–3413, 1998.
- [GR96] L. Y. Glozman and D. O. Riska. The spectrum of the nucleons and the strange hyperons and chiral dynamics. *Phys. Rept.*, 268(4):263–303, 1996.
- [GR13] M. Gómez Rocha. *Electroweak hadron structure within a relativistic point-form approach*. PhD thesis, Univ. Graz, 2013. (arXiv:hep-ph 1306.1248).
- [GRS12] M. Gómez Rocha and W. Schweiger. Electroweak form factors of heavy-light mesons: A relativistic point-form approach. *Phys. Rev. D*, 86:053010, 2012.
- [GSS02] W. Greiner, S. Schramm, and E. Stein. *Quantum Chromodynamics*. Physics and astronomy online library. Springer, 2002.
- [IZ80] C. Itzykson and J. B. Zuber. *Quantum Field Theory*. McGraw-Hill, 1980. New York, USA: McGraw-Hill (1980) (International Series In Pure and Applied Physics).
- [KM96] V. Karmanov and J.-F. Mathiot. On the calculation of the nucleon electromagnetic form factors in light-front dynamics. *Nucl. Phys. A*, 602:388–404, 1996.
- [KP91] B. Keister and W. Polyzou. Relativistic Hamiltonian dynamics in nuclear and particle physics. *Adv. Nucl. Phys.*, 20:225–479, 1991.
- [Kel04] J. J. Kelly. Simple parametrization of nucleon form factors. *Phys. Rev. C*, 70:068202, 2004.
- [Kli98a] W. H. Klink. Point form relativistic quantum mechanics and electromagnetic form factors. *Phys. Rev. C*, 58:3587–3604, 1998.
- [Kli98b] W. H. Klink. Relativistic simultaneously coupled multiparticle states. *Phys. Rev. C*, 58:3617–3626, 1998.
- [Kli03] W. H. Klink. Point Form Electrodynamics and the Gupta-Bleuler Formalism. *Nucl. Phys.*, A716:158–168, 2003.

- [Kra01] A. Krassnigg. *A Relativistic Point-Form Approach to Quark-Antiquark Systems*. PhD thesis, Univ. Graz, 2001.
- [LDDW95] K.-F. Liu, S.-J. Dong, T. Draper, and W. Wilcox. π NN and Pseudoscalar Form Factors from Lattice QCD. *Phys. Rev. Lett.*, 74:2172–2175, 1995.
- [MBC⁺07] T. Melde, K. Berger, L. Canton, W. Plessas, and R. F. Wagenbrunn. Electromagnetic nucleon form factors in instant and point form. *Phys. Rev. D*, 76:074020, 2007.
- [MCP09] T. Melde, L. Canton, and W. Plessas. Structure of Meson-Baryon Interaction Vertices. *Phys. Rev. Lett.*, 102:132002, 2009.
- [MCPW05] T. Melde, L. Canton, W. Plessas, and R. Wagenbrunn. Spectator-model operators in point-form relativistic quantum mechanics. *Eur. Phys. J.*, A25:97–105, 2005.
- [PDG] K. A. Olive et al. Review of Particle Physics. *Chin. Phys.*, C38:090001, 2014.
- [NIST] F. W. J. Olver, D. W. Lozier, R. F. Boisvert, and C. W. Clark. *NIST Handbook of Mathematical Functions*. Cambridge University Press, New York, NY, 2010.
- [PB07] B. Pasquini and S. Boffi. Electroweak structure of the nucleon, meson cloud and light-cone wavefunctions. *Phys. Rev.*, D76:074011, 2007.
- [PS95] M. Peskin and D. Schroeder. *An Introduction To Quantum Field Theory*. Advanced Book Program. Westview Press, 1995.
- [PR05a] H. Polinder and T. Rijken. Soft-core meson-baryon interactions. I. One-hadron-exchange potentials. *Phys. Rev.*, C72:065210, 2005.
- [PR05b] H. Polinder and T. Rijken. Soft-core meson-baryon interactions. II. π N and K N scattering. *Phys. Rev.*, C72:065211, 2005.
- [Puc10] A. Puckett. Final Results of the GEp-III Experiment and the Status of the Proton Form Factors. *Exclusive Reactions at High Momentum Transfer IV*, 23:222–229, 2010.
- [Pun⁺15] V. Punjabi, C. F. Perdrisat, M. K. Jones, E. J. Brash, and C. E. Carlson. The Structure of the Nucleon: Elastic Electromagnetic Form Factors. *Eur. Phys. J.*, A51:79, 2015.
- [Schl92] F. Schlumpf. *Relativistic Constituent Quark Model for Baryons*. PhD thesis, Univ. Zürich, 1992.
- [Schl94] F. Schlumpf. Nucleon form factors in a relativistic quark model. *J. Phys. G: Nuclear and Particle Physics*, 20(1):237, 1994.

- [Sen06] B. Sengl. *Mesonic Baryon Resonance Decays in Relativistic Constituent Quark Models*. PhD thesis, Univ. Graz, 2006.
- [SU00] R. Sexl and H. Urbantke. *Relativity, Groups, Particles: Special Relativity and Relativistic Symmetry in Field and Particle Physics*. Springer Physics. Springer, 2000.
- [Tha92] B. Thaller. *The Dirac Equation*. Texts and Monographs in Physics. Springer, 1992.
- [Wag98] R. F. Wagenbrunn. *Chiral Constituent-Quark Model for Light and Strange Baryons*. PhD thesis, Univ. Graz, 1998.
- [WB⁺01] R. F. Wagenbrunn, S. Boffi, W. Klink, W. Plessas, and M. Radici. Covariant nucleon electromagnetic form-factors from the Goldstone boson exchange quark model. *Phys. Lett.*, B511:33–39, 2001.